AFML-TR-68-49

THE HYDROTHERMAL GROWTH OF LARGE RUBY CRYSTALS

Richard C. Puttbach
Roger F. Belt
Roch R. Monchamp

TECHNICAL REPORT AFML-TR-68-49

July 1968

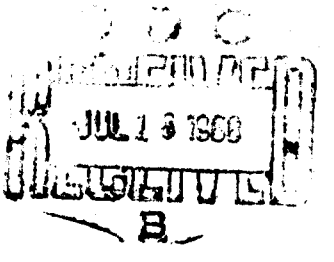

Air Force Materials Laboratory
Air Force Systems Command
Wright-Patterson Air Force Base, Ohio

NOTICES

When Government drawings, specifications, or other data are used for any purpose other than in connection with a definitely related Government procurement operation, the United States Government thereby incurs no responsibility nor any obligation whatsoever; and the fact that the Government may have formulated, furnished, or in any way supplied the said drawings, specifications, or other data, is not to be regarded by implication or otherwise as in any manner licensing the holder or any other person or corporation, or conveying any rights or permission to manufacture, use, or sell any patented invention that may in any way be related thereto.

Qualified requesters may obtain copies from Defense Documentation Center, Cameron Station, Alexandria, Virginia, 22314. Orders will be expedited if placed through the Librarian or other persons designated to request documents from DDC.

Copies of this report should not be returned unless return is required by security considerations, contractual obligations, or notice on a specific document.

DDC release to CFSTI is NOT authorized.

This document is subject to special export controls and each transmittal to foreign governments or foreign nationals may be made only with prior approval of the Manufacturing Technology Division (MAT), Air Force Materials Laboratory, Wright-Patterson Air Force Base, Ohio. The distribution of this report is limited because it contains technology identifiable with items on the strategic embargo lists excluded from export or re-export under U.S. Control Act of 1948 (63 STAT. 7) as amended (50 U.S.C. Appnl 2020-2031), as implemented by AFR 400-10, AFR 310-2, and AFSCR 80-20.

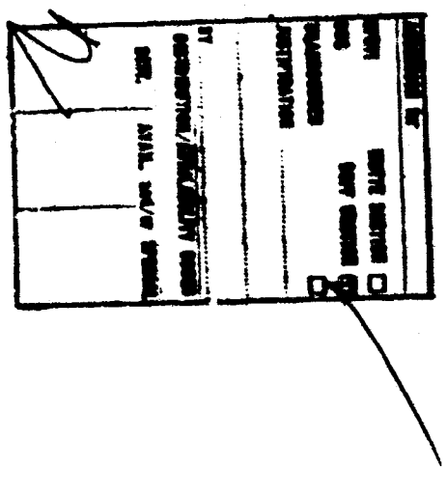

AFML-TR-68-49

HYDROTHERMAL GROWTH OF LARGE RUBY CRYSTALS

Richard C. Puttbach
Roger F. Belt
Roch R. Monchamp

Manufacturing Technology Division
Air Force Materials Laboratory
Directorate of Laboratories
Air Force Systems Command
Wright-Patterson Air Force Base, Ohio

FOREWORD

This Final Technical Report covers all work performed under Contract AF33(615)-3160 from 2 June 1965 through 31 December 1966.

The Contract with Airtron, a Division of Litton Industries, Morris Plains, New Jersey, was initiated under Manufacturing Methods Project No. 8-132, "The Hydrothermal Growth of Large Ruby Crystals". Phase I of this project was performed during 1 January 1963 to 15 April 1965 under Contract AF33(657)-10508 with the final report published as AFML-TR-65-369. The present report deals with Phase II of the project. It was accomplished under the direction of Mr. Robert C. Bratt of the Electronics Branch (MATE), Manufacturing Technology Division, Air Force Materials Laboratory, Wright-Patterson Air Force Base, Ohio.

Dr. Roch R. Monchamp was the Project Director. The report was prepared by Richard C. Puttbach, Project Engineer and Dr. Roger F. Belt, X-ray Crystallographer. Others involved in the project were: Dr. J. W. Nielsen, Manager, Solid State Laboratory; and Peter Wegesser, Stephen Munson, William Dorman and John Moss, Technicians. This report has been given Airtron report number R11-535.

This project has been accomplished as a part of the Air Force Manufacturing Methods Program, the primary objective of which is to develop, on a timely basis, manufacturing processes, techniques and equipment for use in economical production of USAF materials and components. The project encompasses the following technical areas:

Hydrothermal growth of large ruby crystals, high temperature-high pressure growth of large crystals, ruby crystal quality, autoclave design and construction.

Suggestions concerning additional Manufacturing Methods development required on this or other subjects will be appreciated.

This technical report has been reviewed and is approved.

JULES I. WITTEBORT
Chief, Electronics Branch
Manufacturing Technology Division

ABSTRACT

Techniques for the growth of pink ruby by the hydrothermal method have been studied. The principal objectives of this project were to grow crystals measuring several cm, to control optical properties and internal quality, and to provide manufacturing data for laser crystal production. A comprehensive investigation was performed on autoclave design, fabrication, and operation. The nutrient preparation, actual crystal growth, and physical examination of quality were also studied in detail.

Autoclaves of 1.5-3.0" internal diameter were designed and fabricated for ruby growth. These autoclaves performed as well or better than commercially available ones. Special sealing problems, operational procedures and can extraction methods were investigated. The maximum temperature of operation approach 55°C with pressures up to 3×10^4 psi. Growth periods as long as 36 days were attempted. The most common solvent was K_2CO_3. Significant advances in autoclave technology were made.

The nutrient for crystal growth was generally scrap flame fusion ruby. An arc fused Al_2O_3 or sintered pellets of Al_2O_3 with added Cr_2O_3 was under development. The residual problems were proper purity and adequate densification. These can be overcome by exacting preparative methods and were mostly a matter of economical availability.

Crystals of ruby were grown as large as 2 x 8 x 10 cm. During this time the growth rate along the c-axis averaged about 1 - 20 mils/day. Many of the crystals grown hydrothermally contained visible flaws called veils. The principal causes of veils were thought to be associated with high growth rates, temperature or pressure fluctuations, and possibly chemical or physical impurities and defects.

The quality of seed crystals and hydrothermally grown clear ruby crystals was determined with x-ray procedures. Residual misorientations approached 10" of arc, and the dislocation density was less than $10^3/cm^2$. Few dislocations propagated from the seed crystals. Veils were connected with severely strained areas of crystal and high dislocation densities. Small amounts of hydrated alumina were found in the hydrothermally grown ruby. Growth conditions directly influenced the dislocation content and the nature of the chemical impurities.

TABLE OF CONTENTS

TABLE OF CONTENTS (CONT'D)

TABLE OF CONTENTS (CONT'D.)

LIST OF ILLUSTRATIONS

LIST OF ILLUSTRATIONS (CONT'D)

LIST OF ILLUSTRATIONS (CONT'D.)

LIST OF TABLES

LIST OF TABLES (CONT'D)

1.0 INTRODUCTION

A two-phase program on the hydrothermal growth of large ruby crystals for lasers and other purposes has been conducted by Airtron Division of Litton Industries. Phase I has been previously described and completed[1]. This report deals exclusively with Phase II. The objectives of Phase II were the development of manufacturing processes, techniques, and equipment for the economical production of ruby crystals. Laboratory, analytical and engineering studies were performed in fulfilling Phase II. The principal technical areas included hydrothermal growth of large ruby crystals, high temperature-high pressure crystal growth techniques, autoclave design and fabrication and crystal quality.

At the conclusion of Phase I of this program (Contract AF33(657)-10508), the following problems were experimentally found to be most important. They required specific solutions in order to grow crystals of large size and high quality which would meet current ruby laser crystal requirements.

1.1 Crystal Quality

The major quality problem was veiling and cracking. Although crystals were grown of sufficient size and quality so that rods up to one inch long and 1/8 inch diameter could be cut from a crystal, these rods were cut from selected regions and circumvented veiled or cracked regions. For the production of larger rods it was necessary to eliminate the veils. Veiling in crystals has usually been associated with too fast a growth rate, seed quality, or impurities. Therefore, the solution to this problem was thought to reside in a modification of the crystal growth parameters.

The parameters affecting the growth rate include the solvent and its concentration, the crystallization temperature, the temperature difference between dissolution and growth, temperature of the nutrient, seed source and orientation, and working pressure.

During Phase I of the program, it was discovered that the quality of the seed crystal had a marked influence on the quality of the grown crystal. Early in that part of the program, 60° flame fusion rods were used as seeds, and the crystal growth in every case was highly veiled and cracked. Crystal plates grown from molten PbF_2 were then used and the extent of cracking and veiling was found to be reduced extensively. It has been demonstrated[2] that such molten salt ruby crystals are of a very high quality. A comparative study showed that the veiling and cracking decreased as the seed quality increased in the following order: 1) 0° flame fusion, 2) 60° flame

fusion and 3) <0001> or 0° molten salt plates. Further investigations were required to determine what characteristic of the seed was actually involved in improving the quality, e.g., dislocation content, strain, and mosaic structure.

Another suspected cause of veiling was impurity contamination. Elimination of the impurity influence on veiling has been accomplished in certain crystals, e.g., KDP and ADP which are also grown from aqueous solution. Heretofore, this problem had not been investigated but as higher quality crystals were required all facets of the problem had to be considered. A flexible program for Phase II was conducted using experience from Phase I and observations made during the course of the program. This program was directed towards the solution of the impurity influence.

1.1.1 Chromium Banding

In most crystal growing processes in which a dopant is to be incorporated into the crystal, there arises the problem of uniform dopant concentration throughout the crystal. During Phase I, it was found that a uniform chromium concentration was not obtained. There was little or no chromium in the first layer to grow next to the seed. The chromium concentration increased with the amount of growth and was greatest at the surface. At times there were light and dark bands of chromium well removed from the seed.

The proposed work to solve this problem was as follows:
(1) Minimize temperature fluctuations to reduce chromium banding,
(2) Add extra chromium to the solvent to decrease the chromium deficient layer next to the seed.

1.2 Nutrient

Phase I required the production of small quantities of ruby crystal and allowed the use of scrap flame fusion ruby as a source of nutrient. Since it was scrap, the availability of this material was limited by the production and yield of the flame fusion process. For the production of large quantities of ruby required in Phase III, it was essential that an alternate form of nutrient material be found during Phase II. The requisites for this nutrient were high purity, physical stability in the growth environment, reasonable production cost, and nutrient production capability commensurate with crystal production requirements.

One method considered was a sintered homogeneous mixture of aluminum oxide and chromium oxide powders. This mixture was pressed

INTRODUCTION (Continued)

into an appropriate form and then sintered under conditions which yielded a dense solid. Another method was to fuse alumina and chromia powders in an electric arc. The fused mass was then crushed in a press and sized for nutrient.

The desired chemical and physical properties of the nutrient are (1) high chemical purity, (2) size and shape of piece to allow both adequate solvent circulation and sufficient surface area, and (3) proper bonding of the particles so that the piece does not disintegrate into a powder and settle out as a sludge in the bottom of the nutrient chamber.

1.3 Scale-Up

The work in Phase I was carried out in small Waspalloy vessels whose internal cavity was 1.5 inches diameter by 15 inches long. The wall thickness was 2.25 inches. In order to scale up the process for Phase II it was necessary to use larger vessels with cavities 3 inches diameter by up to 52 inches long and wall thicknesses of 1.5 inches.

Because of the differences in wall thickness, total length, and cavity volume between the vessels used for Phase I and Phase II, it was necessary to adjust the measured growth parameters to effect a satisfactory scale-up. In addition to dimensional differences, the larger autoclaves for Phase II were constructed of A-286 alloy which has different pressure and temperature ratings. The Waspalloy vessels were rated for 40,000 psi and 700°C whereas the A-286 were rated for 30,000 psi and 590°C. Therefore, it was necessary to consider these differences. Of particular note was the temperature at the bottom of the vessel under operating conditions. With the conditions for growth in Phase I, the bottom of the vessel was near 650°C or well above the A-286 ratings. Some modification of power input was required to accommodate the A-286 ratings.

The solutions to these problems were viewed as most important in order for the hydrothermal process to prove itself capable of producing high quality ruby to fit laser applications. The present devices utilize rods approximately 2 to 3 inches long by about 1/4 inch in diameter. The goals of this contract were to solve the problems stated above, and produce crystals large enough to yield 3 inch long x 1/4 inch diameter rods. The schedule for the accomplishments of the contract was translated into a Management Control Plan Flow Chart shown in Figure 1.

MANAGEMENT CONTROL PLAN

HYDROTHERMAL GROWTH OF LARGE RUBY CRYSTALS - PHASE II

Figure 1.

2.0 SUMMARY

A developmental program has been performed by Airtron, a Division of Litton Industries, for the Air Force Materials Laboratory, Wright-Patterson Air Force Base, Ohio, encompassing the hydrothermal growth of large ruby crystals, high temperature-high pressure growth of large crystals, ruby crystal quality analysis, and autoclave design and construction. The program ran from June 1965 through March 1967 under Contract AF33(615)-3160.

2.1 Autoclave Equipment

Stress-corrosion cracking was found to shorten the lifetime of an autoclave considerably. Modifications in the autoclave design were made which eliminated regions of stress that are susceptible to stress-corrosion cracking. The vessel length was increased so that the seal area of the vessel would be cooler. The bottom of the cavity was finished in a hemisphere rather than a conical section to remove concentrated stress. The bottom thickness was increased to conform with the wall thickness. This added strength to the bottom and hottest part of the vessel.

2.2 Crystal Nutrient Material

Two methods of nutrient preparation were investigated. Arc fusion and ceramic sintering were both used to prepare a lump-type nutrient. However, both methods produced an impure product. The amount of growth obtained using these nutrients varied from a slight to none. With similar conditions and flame fusion scrap, the crystals grew larger and produced a higher quality growth.

2.3 Molten Salt Crystal Growth

A series of molten salt crystal growth runs with PbF_2 were made in 8-inch diameter x 8-inch high platinum cans. These runs resulted in many seed plates with large {0001} faces. The major portion of the crystals were 1 to 1-1/2 inches across. Plates up to 3 inches across were obtained and used as seeds in the hydrothermal system. All crystals grew as thin plates in the basal plane. Additions of lanthanum or high chromium ion concentrations were not successful in modifying the crystal habit.

2.4 Large Crystal Growth

Experiments were conducted in Airtron's large autoclaves using programmed warm-ups, low temperature gradients, and lithium carbonate and lithium nitrite as additives. These conditions were not effective in reducing or eliminating veiled and cracked growth. A

Summary (Continued)

1.5-inch run was made using sapphire molten salt seed plates and scrap flame fusion sapphire for nutrient to attempt to relate chromium fluctuations to the veiling. The crystals were veiled as much as in ruby, and it was concluded that chromium, or concentration changes in chromium, were not responsible for the origin of veils and cracks.

The reason for the cracking and veiling is not known at present; however, it is clear that flawing is augmented under conditions which lead to a high growth rate. Upon closer examination of all the growth run condition data, it has been found that the runs in which the high growth rates were obtained were those in which the longer autoclaves were used.

Two chromic oxide additions were made in order to reduce the width of the sapphire band at the seed. In both cases the sapphire band was almost eliminated.

2.5 Autoclave Specialized Treatment

Gold electroplating of the interior surface of an autoclave was attempted in order to produce an inert coating. A vessel which had been specially plated was tested under crystal growth conditions. Most of the gold was gone after the test except for a trace in the cooler section of the vessel. No trace of the gold could be found in the external fill or on the silver can. Possibly the gold had diffused into the vessel while it was under hydrothermal operating conditions.

2.6 Internal - External Temperatures

An investigation to relate internal and external temperature measurements was performed during this program. A specially prepared thermocouple was placed through a hole in the top of a dummy silver can. A thermocouple was also located on the external surface of the vessel at the same level. An average difference of 26°C was noted between measurements of the two couples with the internal temperature being higher. Also of significance was a very rapid temperature fluctuation within the fluid. A temperature change of 5 - 10°C was estimated and occurred in as short a period as 5 seconds. Temperatures were measured inside and outside the autoclave at a height equal to the top of the silver can during two ruby runs. It was found that the external temperature was about 30°C larger than the internal temperature.

Summary (Continued)

2.7 Crystal Quality Studies

X-ray topography of hydrothermally grown ruby has directly revealed internal defects such as dislocations, inclusions, and highly strained areas. The examination of different quality seed material has shown that few defects are propagated from the seed crystal. Hence the principal cause of most defects lies in the hydrothermal growth conditions and the lack of fine controls.

The dislocation density of hydrothermally grown ruby crystals may range from 10^2 - $10^4/cm^2$. X-ray topography and x-ray linewidths have both proved that high quality crystals can be obtained. These are at least comparable to ruby crystals grown by alternate methods. Two problems remain which may directly influence quality. The first is the formation of visible cracks on some crystals. The second is the incorporation of small amounts (<1000 ppm) of hydrated species. The two problems may be related and solved by modifying conditions of hydrothermal growth.

3.0 HYDROTHERMAL CRYSTAL GROWTH FACILITY

In order to fulfill the requirements of Phase II of the subject contract, Airtron, a Division of Litton Industries, has utilized a laboratory designed and assembled for hydrothermal growth of large ruby crystals. The laboratory contains a 20-foot long x 4-foot deep x 4-foot wide pit to hold the autoclaves and furnaces needed in crystal growth operations. There are six furnaces, four large ones for the A-286 alloy autoclaves, and two smaller ones for the Waspalloy autoclaves. All of the equipment was procured under Air Force Facilities Contract AF33(657)-10507, and was utilized in the performance of Phase I, Contract AF33(657)-10508. A floor plan of the laboratory is shown in Figure 2.

Among the commercially available items in the laboratory are the following:

1. A Tem-Pres HR-1B hydrothermal unit, comprising four small furnaces and autoclaves, used to carry out solubility determination and crystal growth experiments (Figure 3).

2. Six hydrothermal crystal growth autoclaves - two Waspalloy vessels with cavities measuring 1.5 inches x 15 inches in length; two A-286 alloy vessels 3 inches x 44 inches long, and two A-286 alloy vessels 3 inches x 52 inches long (Figure 4).

3. Silver containers or cans to hold the basic solutions used in ruby and sapphire crystal growth which prevent corrosion of the autoclave metals under hydrothermal conditions (Figures 5 and 6).

4. Hydrothermal furnaces with clam shell type heater sections (Figure 7).

5. Temperature controllers and programmers.

Special items were developed and fabricated by Airtron during the performance of the Phase I program to utilize the commercial equipment effectively and efficiently. These included autoclave opener tools which permitted opening of an autoclave after a high pressure or temperature had created a binding force. Large silver cans were constructed to compensate for variable volume and pressures developed during operating conditions. Special can extractors were designed for removing cans from autoclaves. Autoclave seal area lapping and polishing tools were also made for better long term seals.

All of the commercial items listed in 1-5 above and also the special tools have been described thoroughly in the final report[1] of Phase I. During the period of Phase II, the same equipment was utilized. However some additional autoclaves, silver containers, and tools were necessary. A detailed description of these is given in Section 4.0.

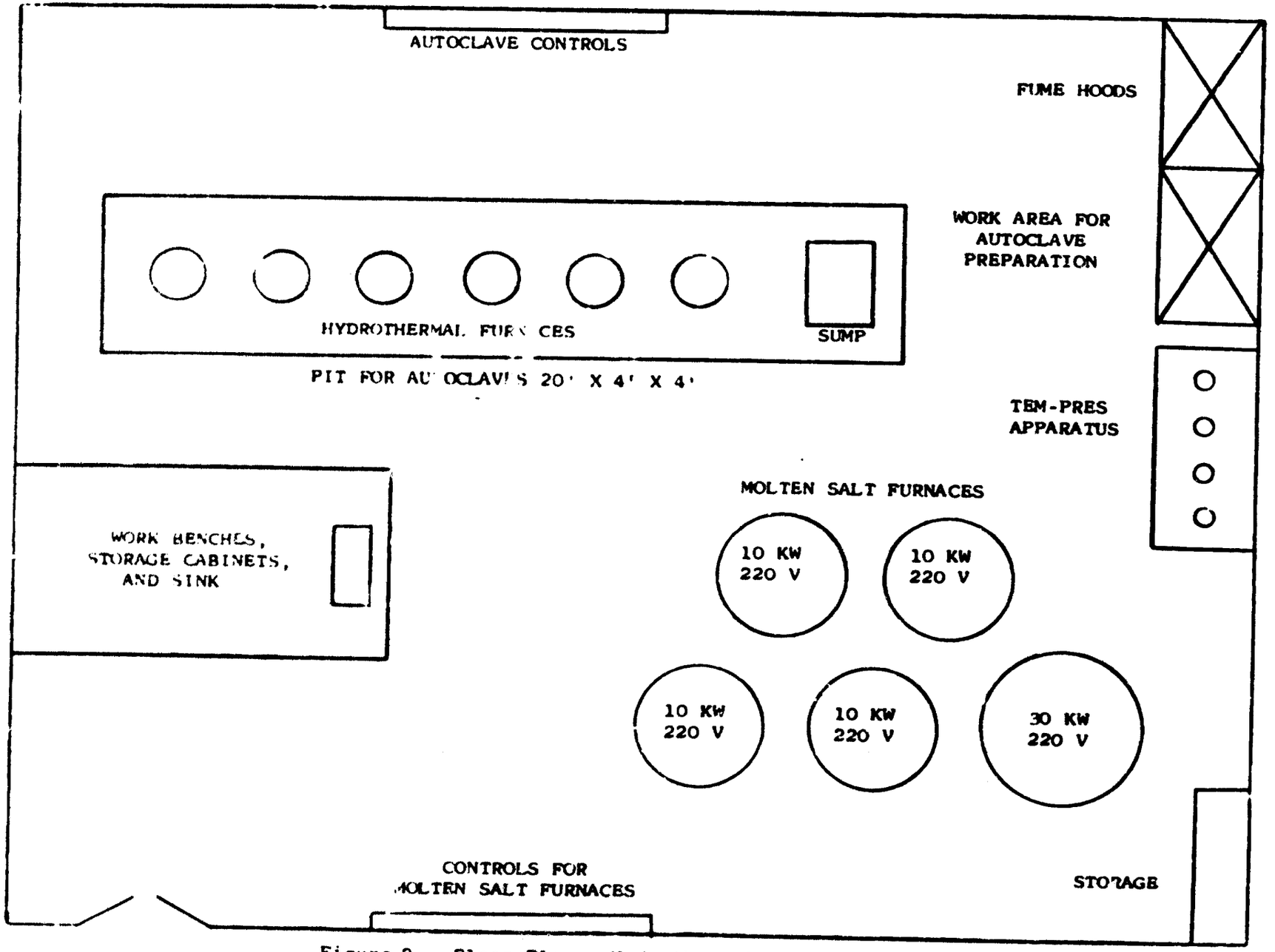

Figure 2. Floor Plan - Hydrothermal Laboratory

Figure 3. Tem-Pres Apparatus

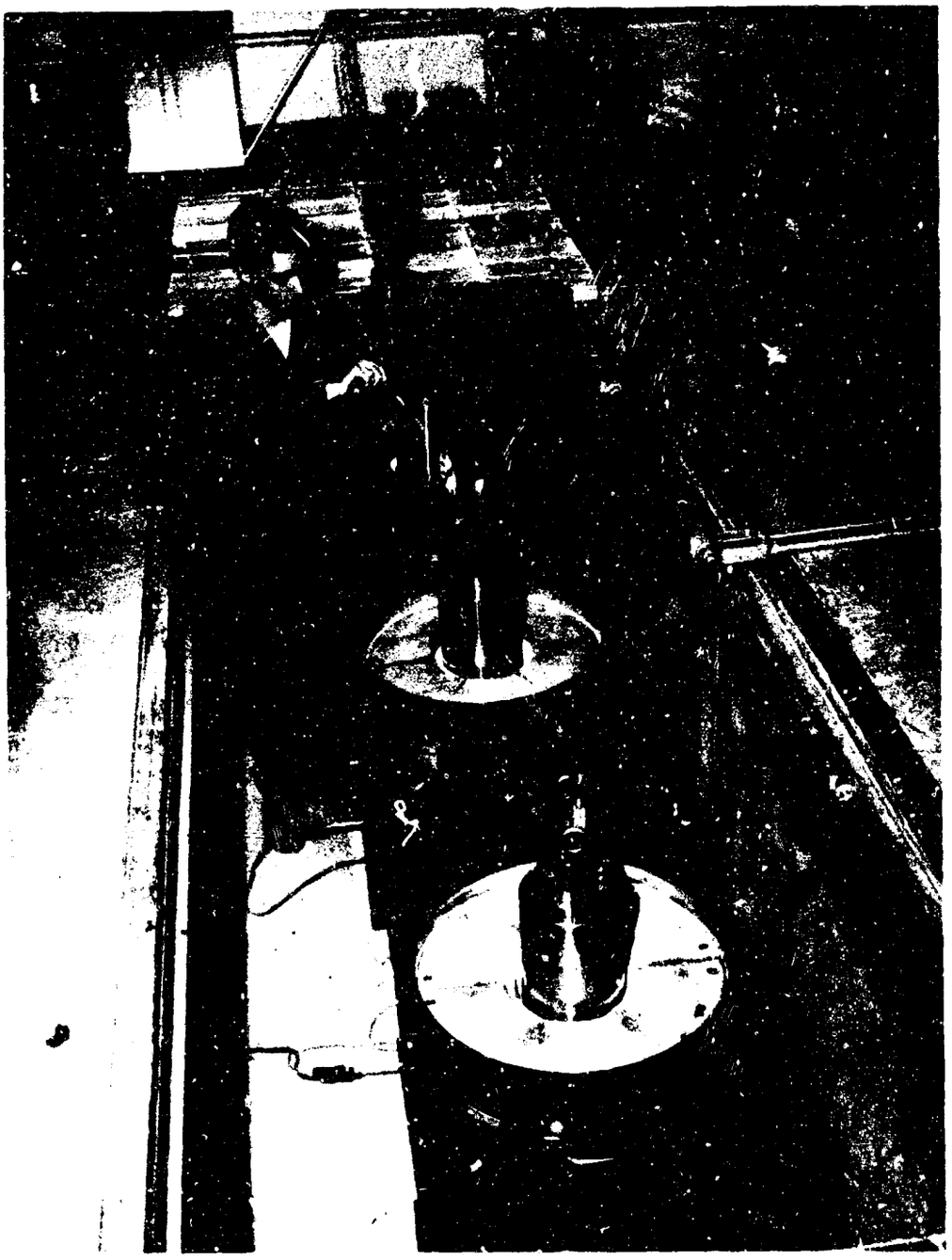

Figure 4. Furnaces and Autoclaves

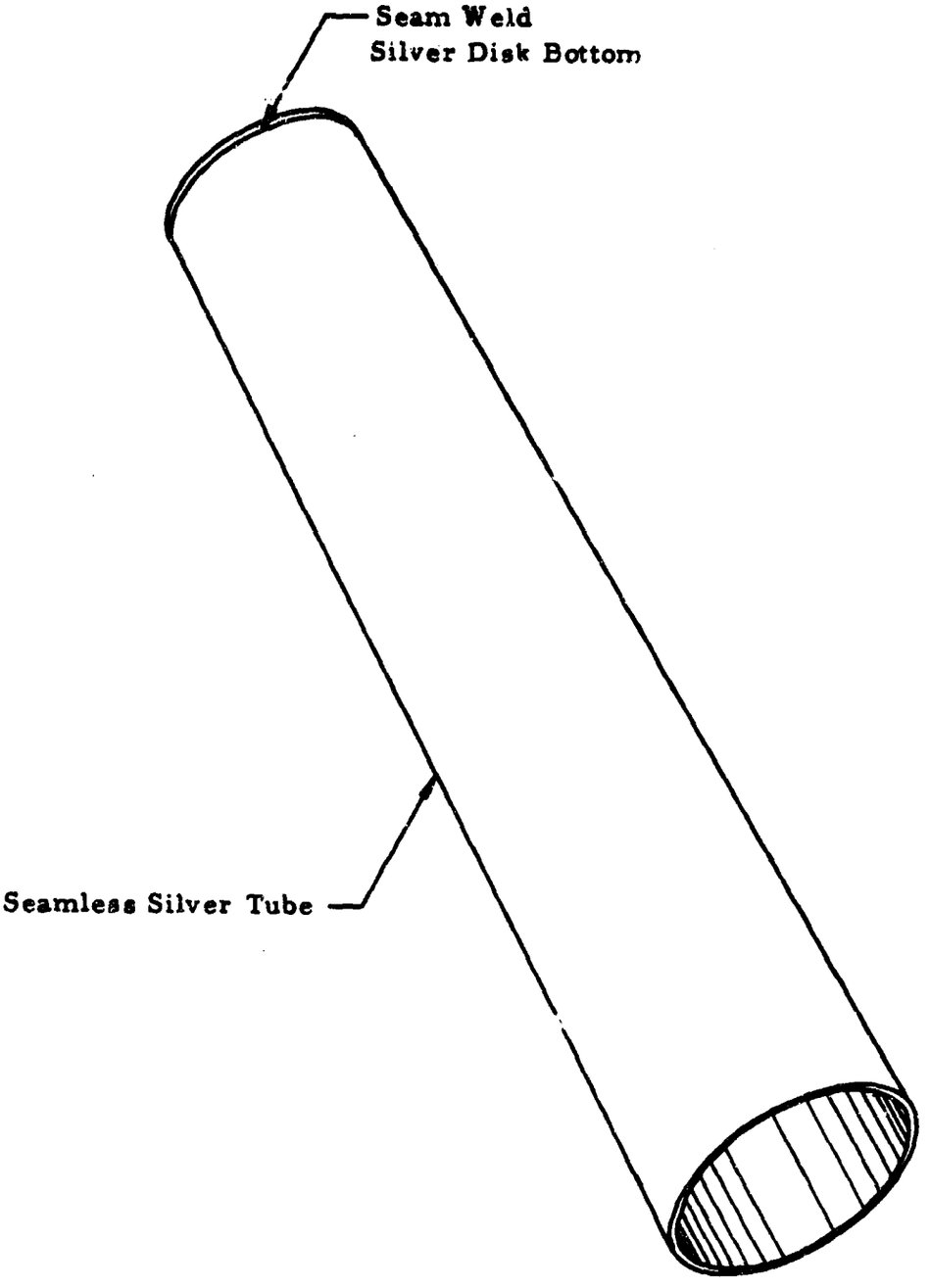

Figure 5. Silver Can Design

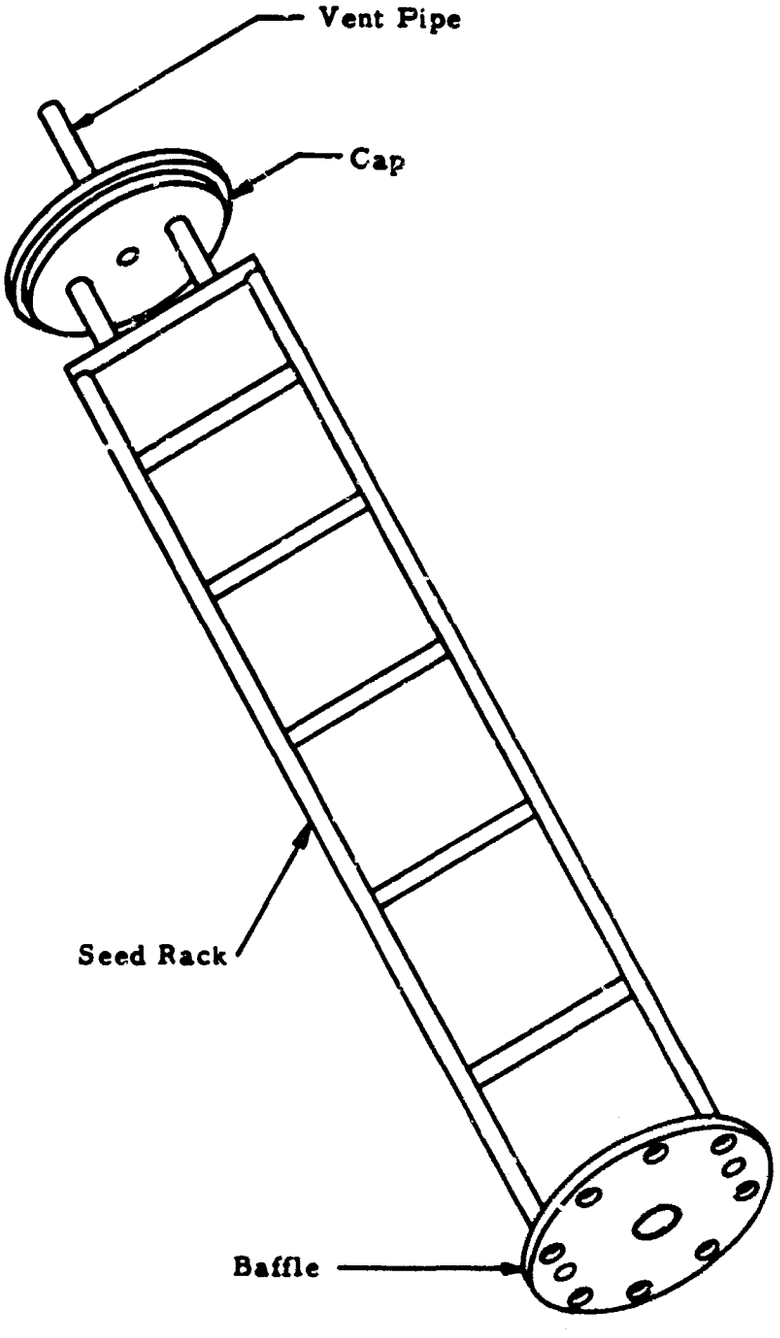

Figure 6. Seed Rack Design

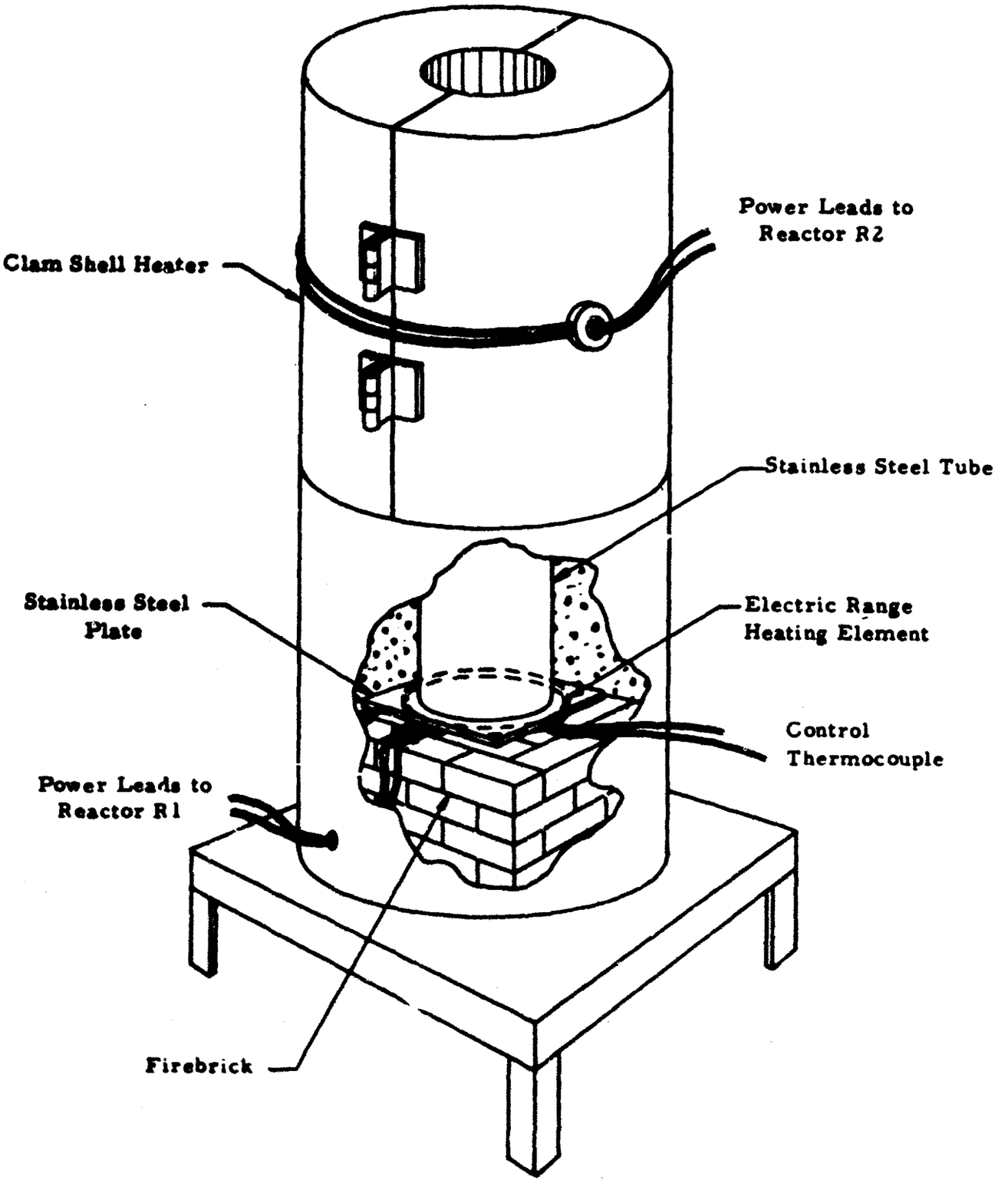

Figure 7. Furnaces Used to Heat Autoclaves

4.0 THE AUTOCLAVE

The autoclave represented a large portion of the investigation. Such things as design, fabrication, sealing technique, auxiliary apparatus and operational procedures were considered. These are discussed in the following sections. Table I contains the pertinent information about autoclaves used in this contract.

4.1 Design and Fabrication

Besides the short (1.5" I.D. x 15" I.L.) and intermediate (3" I.D. x 34" I.L.) vessels which were on hand, four other vessels were fabricated during the course of the contract. Two were purchased from Autoclave Engineers, Inc., and two were fabricated in accordance with Airtron designs.

The two vessels purchased from Autoclave Engineers (Figure 8) were pressure tested at both room and maximum rated temperatures. The vessels were hydrostatically tested to 48,000 psi at room temperature. This was the standard quality control test used by Autoclave Engineers at that time. In order to satisfy Airtron, Autoclave Engineers agreed to test the vessels at maximum rated temperature and pressure. Airtron insisted on this procedure because Autoclave Engineers' vessels had a previous history of holding pressure at temperatures less than approximately 400°C but developed leaks above that temperature range. Simultaneous testing of the high temperature and pressure was accomplished by overfilling the vessel with water and valving off the excess as the vessel was heated. Final conditions of 592°C and 30,000 psi were reached and maintained for one-half hour without loss of pressure. All sealing surfaces were then regenerated to Autoclave Engineers' specifications and shipped to Airtron.

It was our opinion that the half hour test was too short to show up a slow leak. Even an extremely small leak can cause failure of a crystal growth run since the duration can be two to three months. Also one-half hour was a rather short time to conclude that thermal equilibrium had been achieved in a vessel of this size.

Of the two vessels purchased from Autoclave Engineers one vessel operated satisfactorily with the seal in the "as received" condition from the factory. In the second vessel a crystal growth run was attempted (Run No. 132), but had to be shut down after two days because of a slow leak in the seal. However, another crystal growth run was made with no loss of pressure after the seal pieces were redressed in accordance with procedures developed by Airtron during Contract AF33(615)-2228. These are described in Section 4.2 on sealing the autoclave.

TABLE I

Autoclave Data

Autoclave Number	Length Inches	Inside Diameter Inches	Outside Diameter Inches	Fabricator
1	16	1	2.5	Airtron
1	52	3	6	Airtron
2A	21	1.5	6	Autoclave Engineers
2	52	3	6	Airtron
4	21	1	2.5	Airtron
5	42.75	3	6	Autoclave Engineers
6	42.75	3	6	Autoclave Engineers
7	48.75	3	6	Autoclave Engineers
9	26	1.5	3	Airtron

Note: All autoclaves fabricated from A-286 alloy.

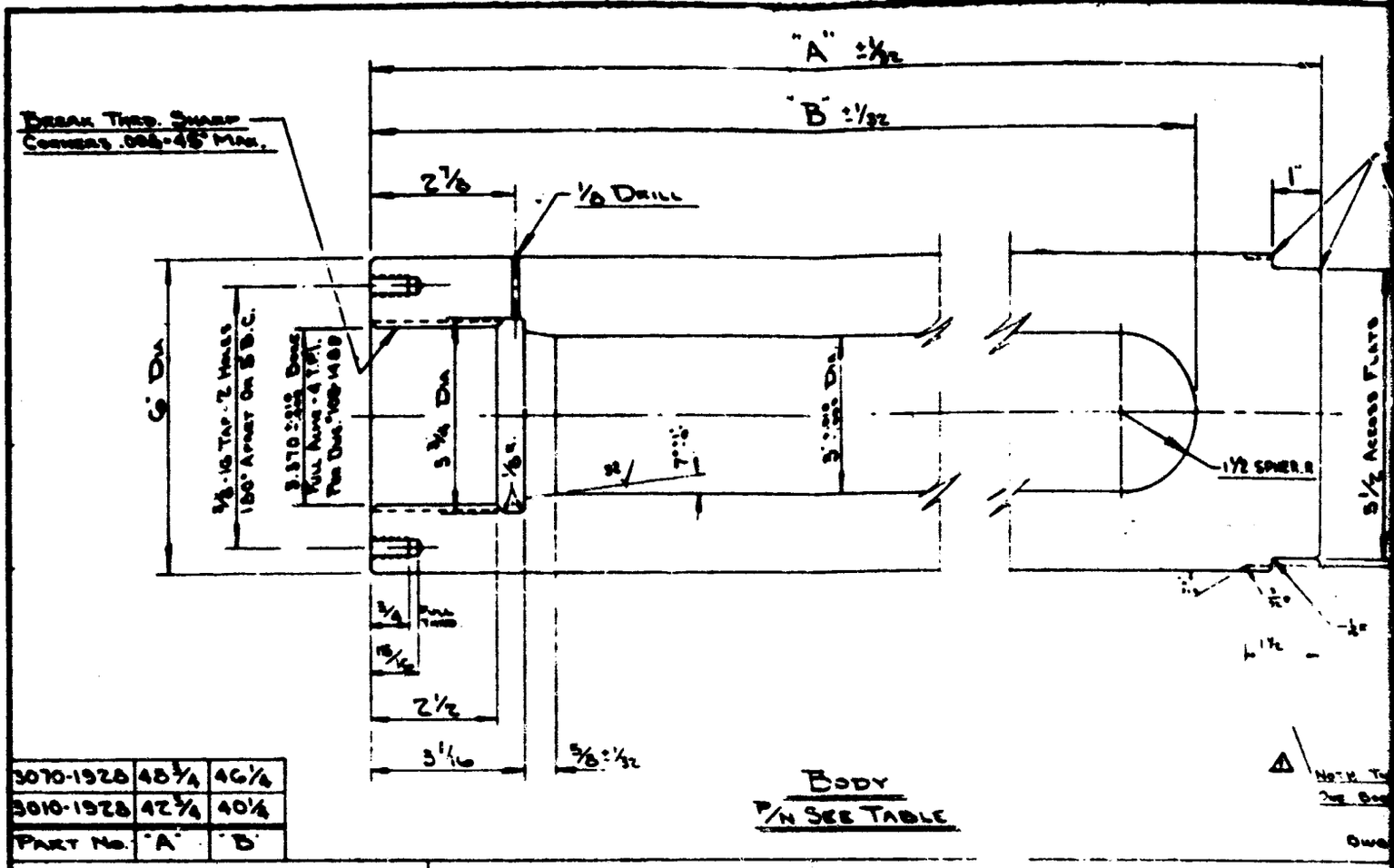

3070-1928	48 3/4	46 1/8
3010-1928	42 3/4	40 1/8
Part No.	"A"	"B"

Body
P/N See Table

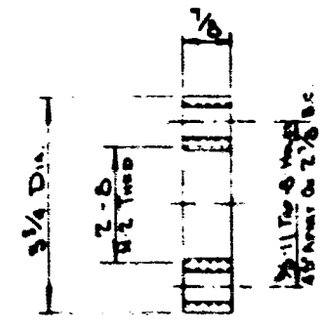

Lock Nut
P/N 3060-1928

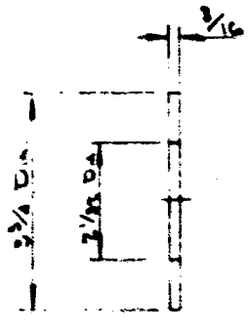

Thrust Washer
P/N 3050-1928

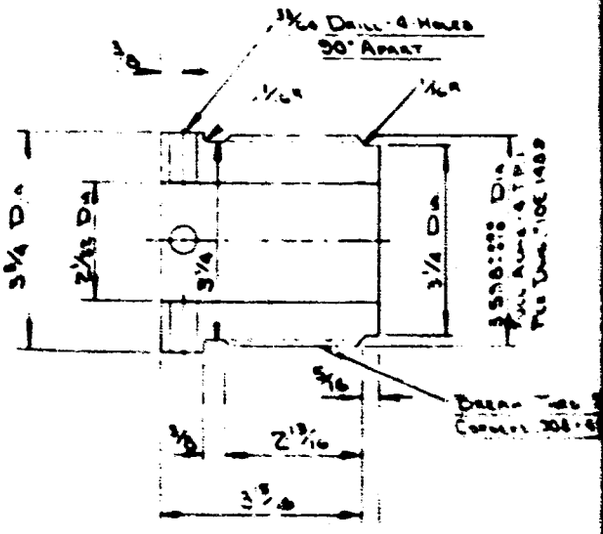

Main Nut
P/N 3040-1928

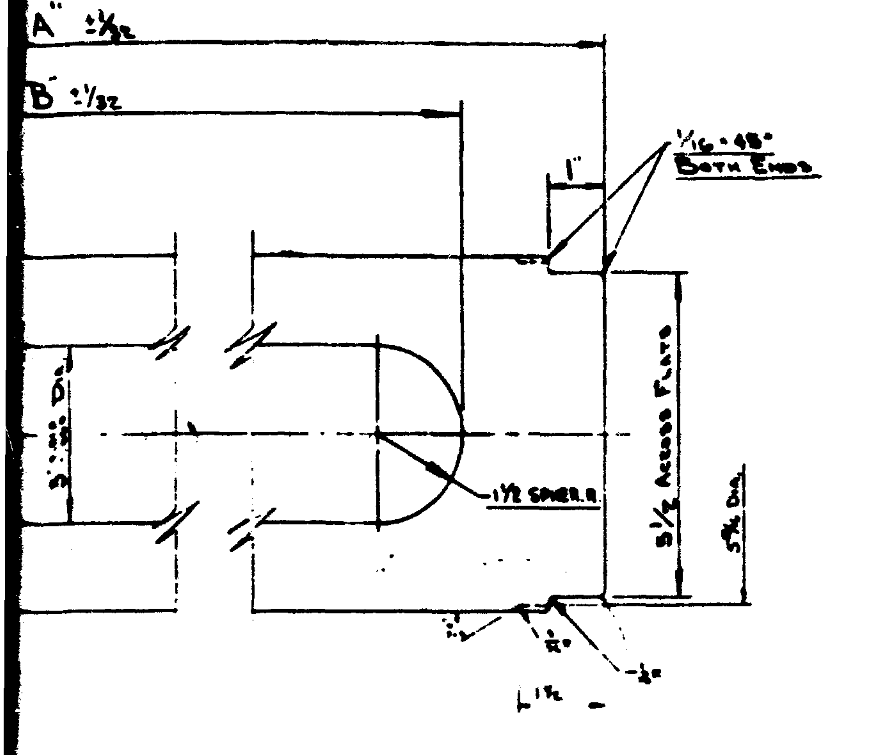

Body
See Table

Note – These Dim's Added To The Body

DWG # 30-1928

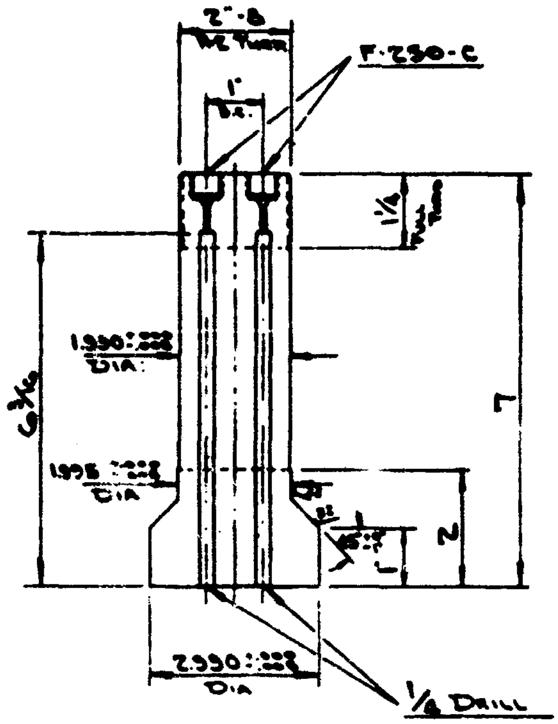

Cover
P/N 3020-1928

DWG # 30-1928

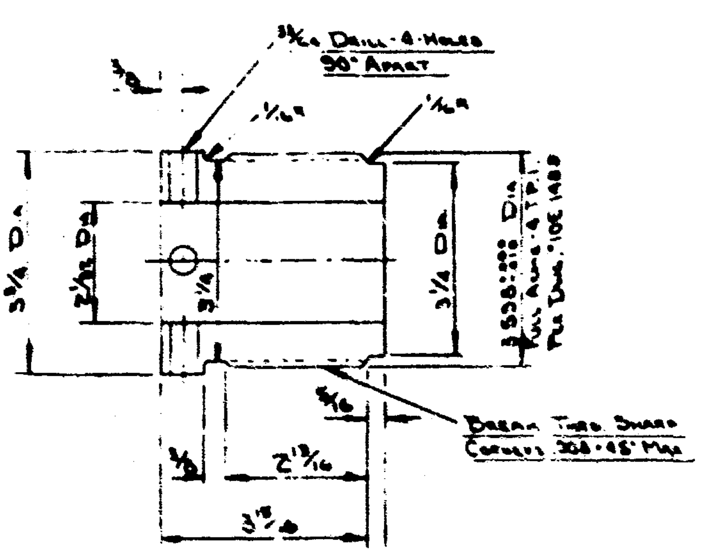

Main Nut
P/N 3040-1928

DWG # 30-1928

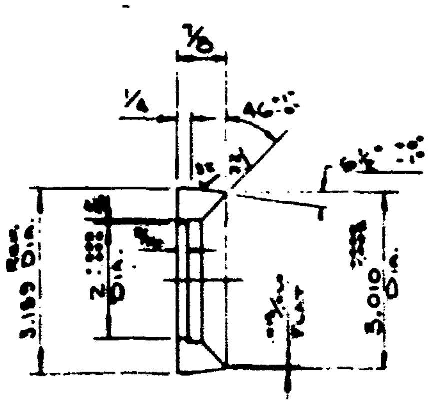

Seal Ring
P/N 3030-1928

REVISIONS	
1	[illegible]
2	[illegible]
3	[illegible]

AUTOCLAVE ENGINEERS, INC.
ERIE, PENNSYLVANIA

Reactor Details

ORDER	DR.	DRAWING
AL-5580	CH. / APP.	30-1928 B

The Autoclave (Continued)

The Airtron autoclave bodies were made from two forged ingots of A-286 alloy ultrasonically tested for flaws. The ingots were purchased from Universal Cyclops, Inc., Bridgeville, Pa. Sufficient A-286 material was purchased to make the closure parts and several spare sealing rings at the same time. The entire body was machined by Thul Machine Co., Plainfield, N. J., using conventional deep drilling techniques and machines. Female threads at the top of the autoclave body were fitted to a male member supplied by Airtron. All closure parts and seal rings were machined by Rame' Hart, Inc., Mt. Lakes, N. J. A drawing of the Airtron autoclave is shown in Figure 9. The two autoclaves were satisfactorily tested for 24 hours at 592°C and 30,000 psi prior to actual crystal growth runs.

The major difference between the autoclaves purchased under this contract and the ZnO Contract (AF33(615)-2228) was the thickness and shape of the vessel bottoms. The earlier vessels had a 1.5-inch thick bottom and a concave shape which was an area of high stress. The Phase II vessels had a hemispherical bottom which was 2.5 inches thick. The hemisphere should reduce the amount of stress created by internal pressure. Figure 9 shows this design.

It was thought that thickening and reshaping the vessel bottom would lengthen its life when caustic solutions were accidentally brought in contact with the autoclave interior due to seal leaking or faulty welding of the silver can. In actuality, after the sealing problems were resolved, stress corrosion failure was no longer a problem.

To solve the sealing problem, a modification was used to reduce the temperature of the seal parts during actual crystal growth conditions. In order to make the sealing area of the autoclave operate at a lower temperature, both Autoclave and Airtron's autoclave were designed longer. This did not significantly increase the autoclave cost but permitted cooler operation of the seal. The two autoclaves supplied by Autoclave Engineers were 48.75 inches long. The length of the two autoclaves fabricated by Airtron was increased from 42.5 inches to 52 inches. With the available furnaces, either 8 or 11 inches projected above the furnace top depending on which autoclave was used.

By using a standard length (33.30 inches) silver can, a void was generated above the can in the autoclave cavity. This void was filled with a stainless steel plug in order to reduce the external volume. Figure 10 shows the heater-autoclave configuration for a typical vessel, and the plug configuration. The intended effect was to keep T_{cryst} (crystallization temperature) and Δt the same within the growth cavity while the seal area was at much lower temperature.

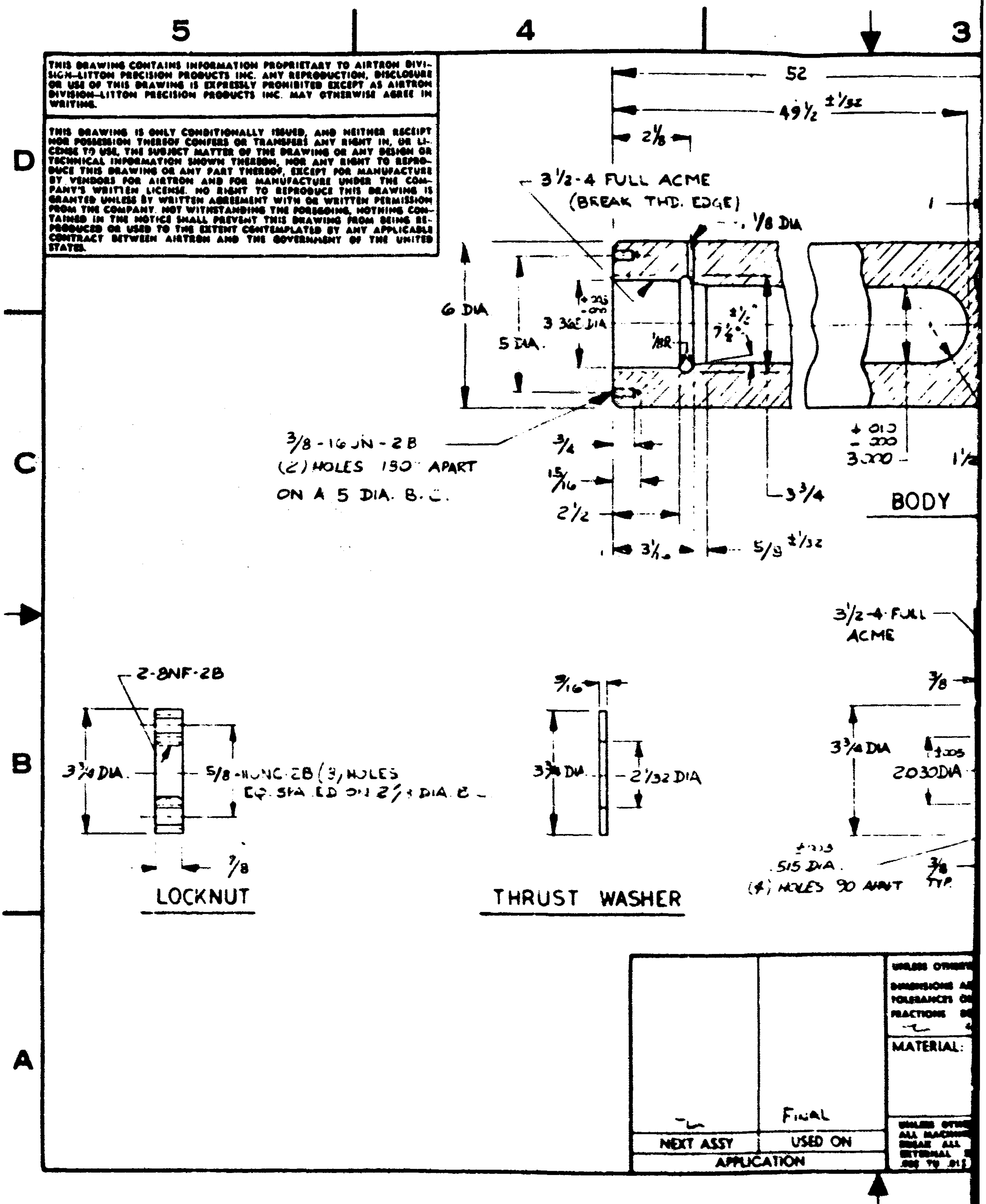

REVISIONS					
ZONE	LTR	CHANGE	DESCRIPTION	DATE	APPROVED
~	A	~		11-29-67	

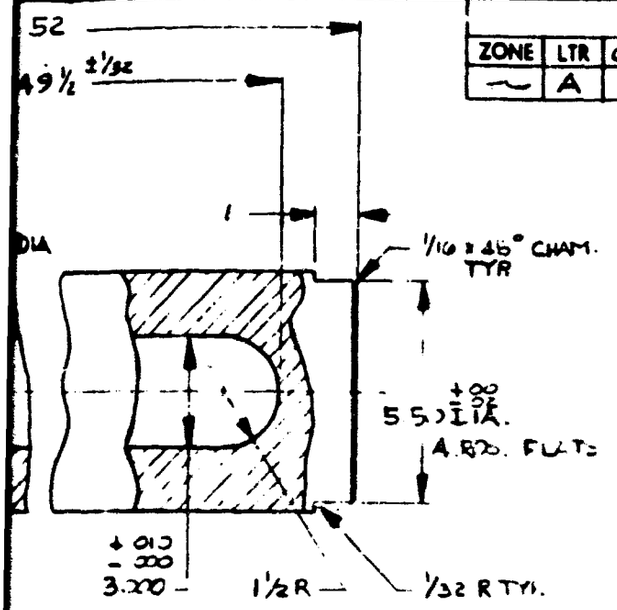

BODY

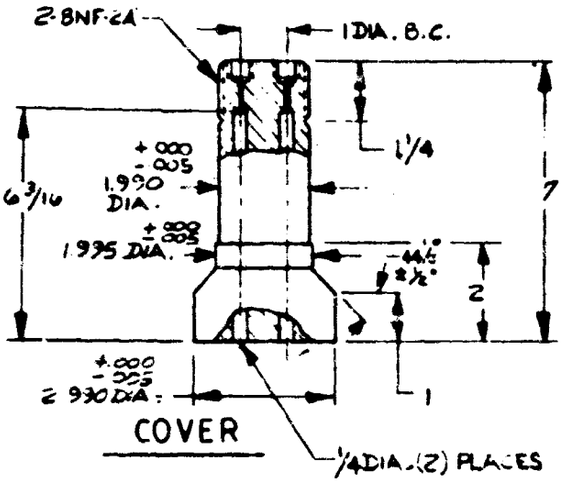

COVER

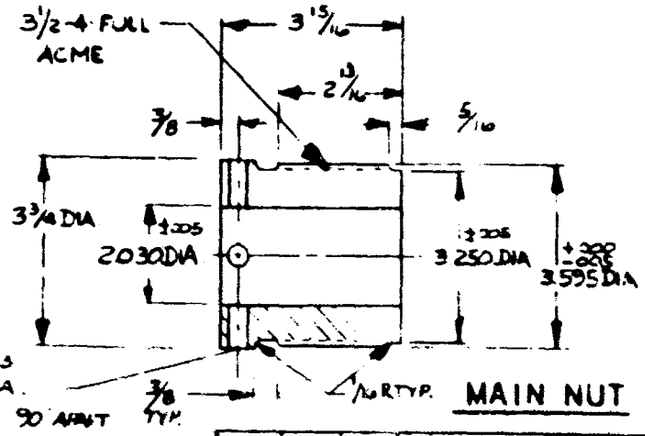

MAIN NUT

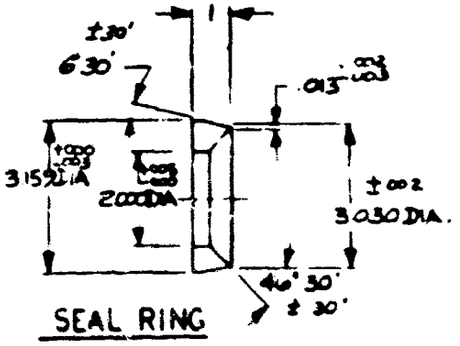

SEAL RING

ITEM NO.	QTY REQD	SYM	PART NO.	DESCRIPTION	MATERIAL	SPECIFICATION	CODE IDENT	UNIT WT

LIST OF MATERIALS

UNLESS OTHERWISE SPECIFIED
DIMENSIONS ARE IN INCHES
TOLERANCES ON
FRACTIONS DECIMALS ANGLES
~ ~ ~

MATERIAL:

FINAL
USED ON
ON

DRAWN BY H.W.
CHECKED
ENGR
MFG
DATE 11-29-67
APPROVED

CONTRACT NO.
CUSTOMER NO.
S.O. 880700Z
REV.

UNLESS OTHERWISE SPECIFIED ALL MACHINED SURFACES TO HAVE ALL INTERNAL AND EXTERNAL SHARP CORNERS [illegible] TO .015 RADIUS

APPROVED BY OTHER ACTIVITY

AIRTRON
DIVISION OF LITTON INDUSTRIES, INCORPORATED
MORRIS PLAINS LITTON INDUSTRIES NEW JERSEY

REACTOR DETAILS

SIZE	CODE IDENT NO.	DRAWING NO.	REV
B	80006	417235	A

SCALE ~ WT SHEET

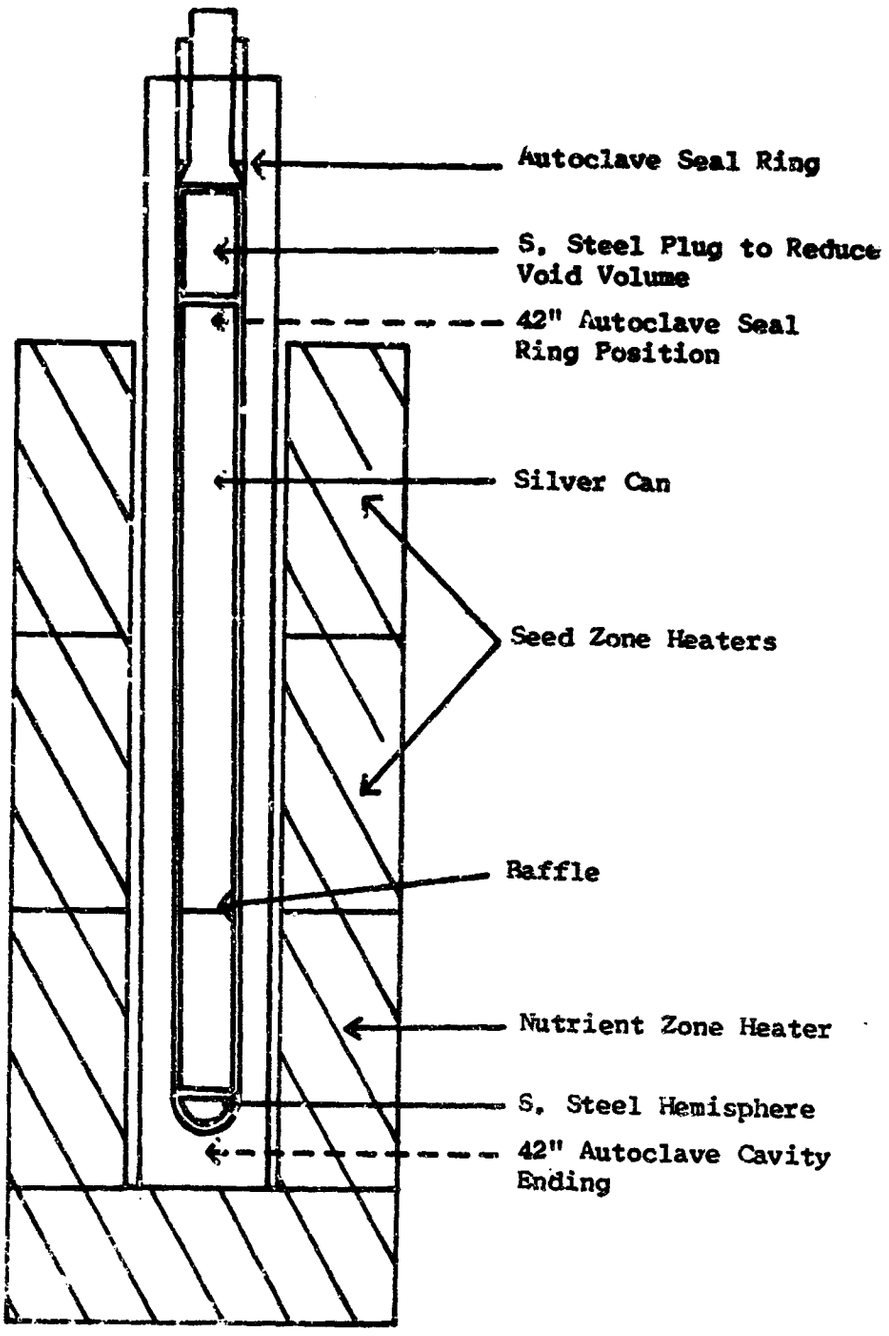

Figure 10. Heater Autoclave Configuration

The Autoclave (Continued)

Later in the program a sealing technique was developed which allowed both long and short autoclaves to operate without leaking. Unfortunately both Autoclave Engineers and Airtron vessels were in the final stages of fabrication before this was realized. This technology is described in detail in Section 4.2.

4.1.1 Gold Plated Autoclave

A one-inch internal diameter autoclave was electroplated with gold at Nu-Line Industries, Minneapolis, Minnesota, to test this coating under crystal growth conditions. A stainless steel tube was inserted into the autoclave for use as an anode. The bottom of the anode was constructed to prevent an electrical short with the autoclave. Gold solution was then gravity fed down through the center of the anode and siphoned out of the top of the autoclave. This technique provided the advantages of 1) internal agitation, 2) sufficient gold content within the plating chamber, 3) fresh solution to obtain the lowest porosity, 4) the highest plating efficiency, 5) adequate anode area to obtain the required finish. The amount of gold deposited on the inside surface of the autoclave was 0.25 mil thick. This was determined from a continued analysis of the gold solution and calculating the amount of gold removed. Knowing the surface area to be coated, the thickness of the deposit was easily obtained. A second continuous check was also made by using an amp-hour meter. The gold solution used was a proprietary composition supplied by Technic Company. It was a hard gold with cobalt as an inorganic brightener. The bath was a phosphate-type system.

Run No. 136 was made in this vessel. The conditions were a bottom temperature of 543°C, a top temperature of 506°C, and a pressure of 11,500 psi. The external fill was 12.2 ml of deionized water or 73.5%. The duration of the run was only four days because the low pressure suggested a possible leak.

Examination of the gold plating after the run was most interesting. The gold in the lower part of the vessel where the can had been located was completely gone. Above this region where the vessel was cooler there was still a trace of a gold coating but it was obvious that even in this region the gold had been attacked. The mechanism by which the gold was removed was not known. There was no evidence of transport and growth of gold needles such as has been observed in the case of silver corrosion[3]. In fact no trace of the removed gold could be detected in the liquid, in the vessel, or on the can. Possibly the gold diffused into the autoclave during the run. The use of this gold plating technique did not provide a corrosion resistant crystal growth vessel and thus was dropped.

The Autoclave (Continued)

4.2 Sealing Technology and Making the Seal

The inability of the autoclave closure to seal effectively at high temperatures had been the principal problem in the use of hydrothermal crystal growth equipment. This problem was most clearly demonstrated during the later stages of Phase I of this contract when the combination of more demanding pressures and temperatures resulted in unsatisfactory seal performance. Seals which were previously successful at low pressure and temperature conditions failed at the more severe conditions necessary for ruby crystal growth. Initially it was thought that cool seals would suffice so the autoclaves were made longer. While the vessels were being fabricated a sealing technique was developed which proved successful on both long and short vessels.

It has been our experience that there is no substitute for care, cleanliness, and attention to detail in producing highly reliable autoclave closures consistently. The machine shop should be instructed to wrap each seal ring and cover in paper after it is polished and inspected. This will prevent parts from hitting each other and possibly causing a disastrous nick or scratch. All parts should be scrupulously clean before assembly of the seal is attempted.

During each run the seal parts underwent plastic deformation which resulted in permanent dimensional changes in all three seal parts. The ring, cover, and autoclave seal areas had to be returned to their original dimensions and surface finish each time the autoclave was used. If this was not done the seal became unreliable. The preparation of each part is discussed in turn below.

In order to regenerate and polish the sealing surface of the autoclave properly, it was necessary to design and develop two tools, a lapping tool and a polishing tool. The final models of each are shown in Figures 11 and 12.

The lapping tool was made to generate a surface of the proper sealing angle (7°) whose bore was concentric with that of the threads. This particular alignment was found to be critical since the axis of the threads and that of the autoclave seal surface must be coincident. Deviations from this geometric configuration lead to seal leaks. The lapping section of the tool was made of cast iron; the surface of the lap was regenerated periodically by milling. The guide in the body of the tool was made of aluminum and was fitted specifically for one vessel. It was used only for that vessel thereafter.

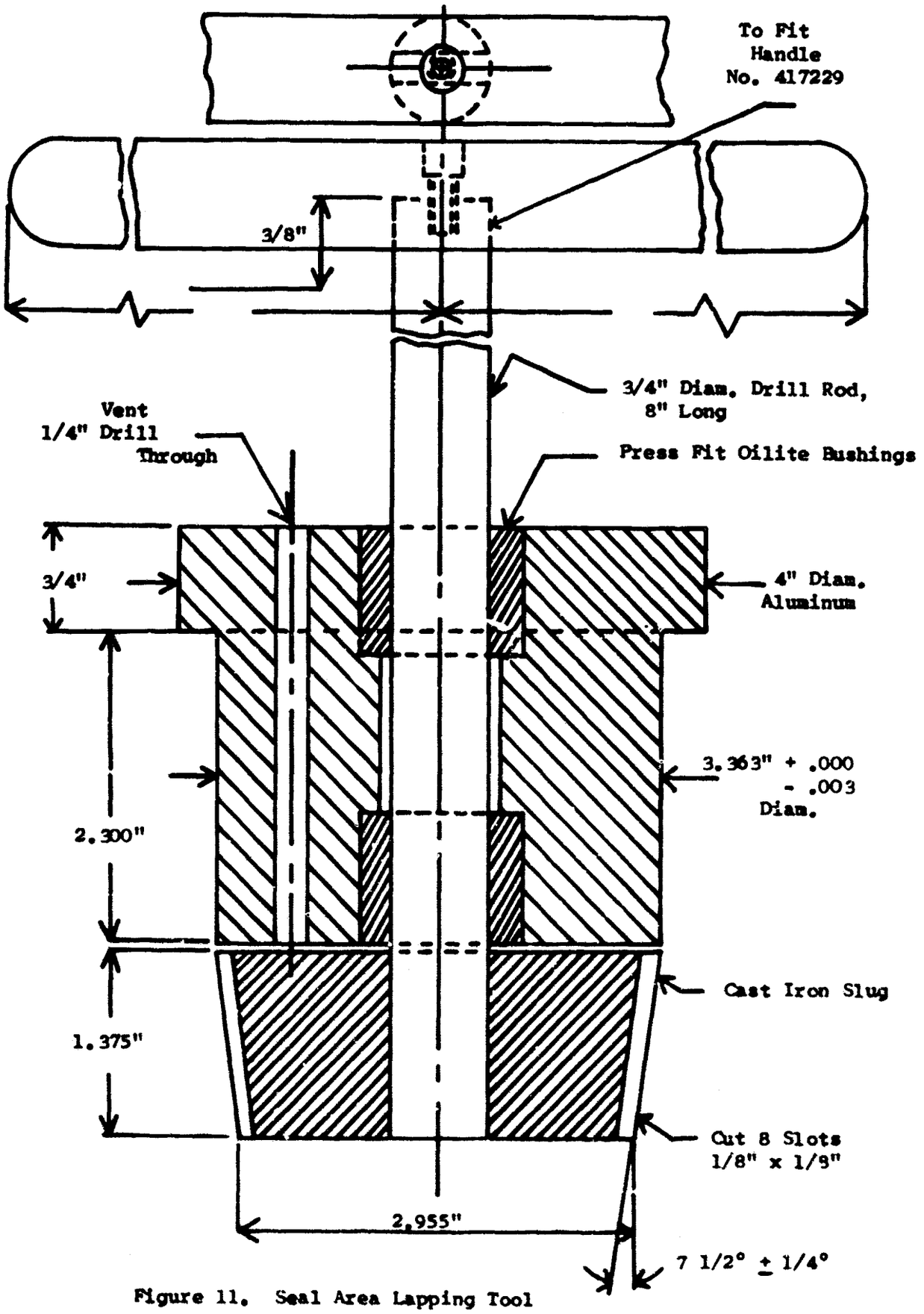

Figure 11. Seal Area Lapping Tool

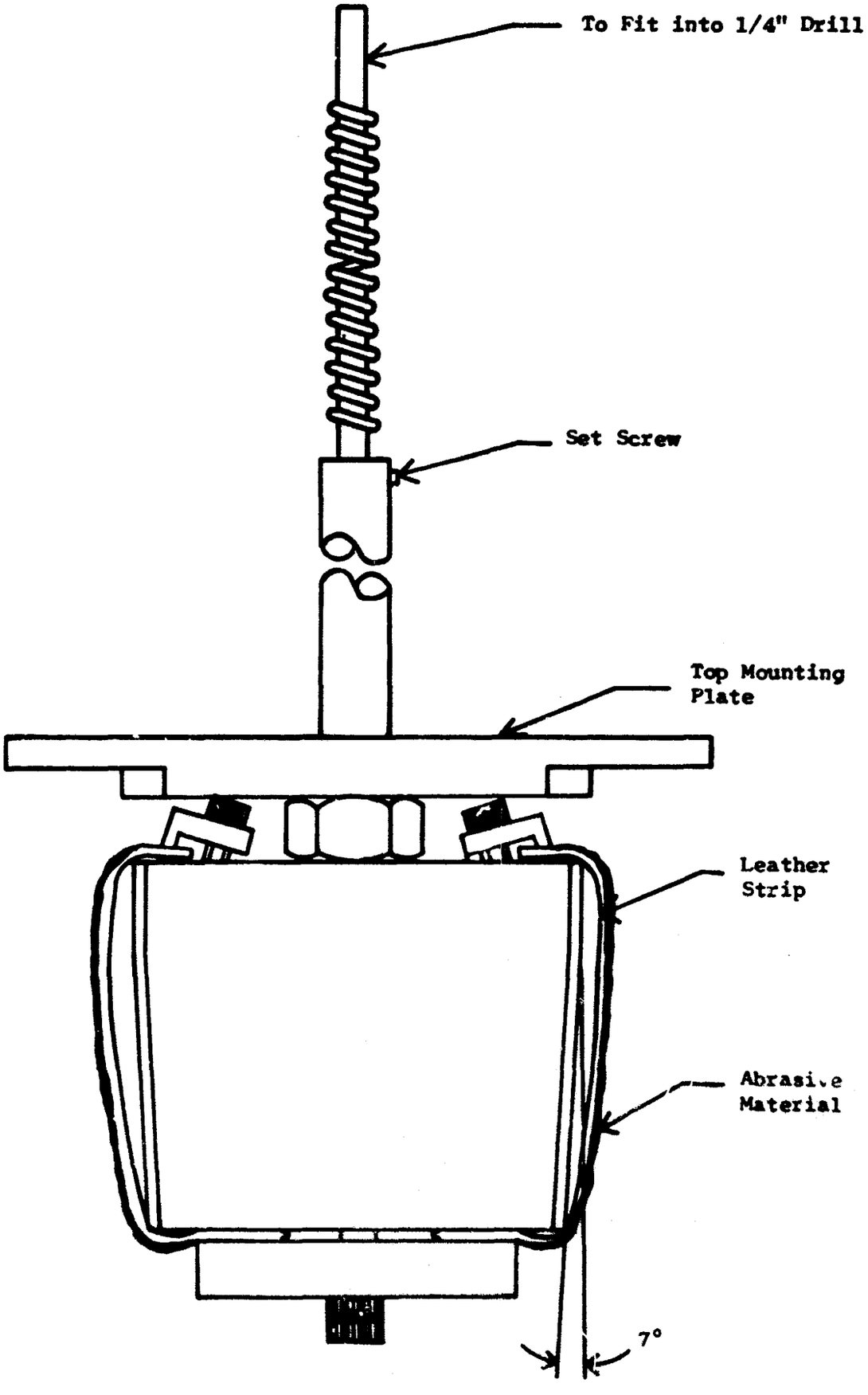

Figure 12. Polishing Tool

The Autoclave (Continued)

A polishing tool was also developed to be used after the seal surface had been ground with the lapping tool. The mirror polish produced by this tool was found to be essential in order to seal the autoclaves for use at combinations of high pressure-temperature conditions (>500°C and 20,000 psi).

The seal area of the autoclave was lapped with a mixture of 2 volumes of SAE 20 machine oil plus 1 volume of Norton No. 320 aluminum oxide abrasive using the lapping tool shown in Figure 11. Lapping was continued until all traces of former seal marks were removed. The autoclave was then washed with detergent and water to remove any residual grit. The seal area was polished with WETORDRY TRI-M-ITE PAPER No. 320 SILICON CARBIDE (3M Co., St. Paul, Minnesota) and SAE 20 machine oil. The paper was fixed to the polishing fixture (Figure 12) which was then rotated at 200 to 300 RPM. A good polish was required, i.e., no visible flaws were detected with the unaided eye.

An expanding mandrel shown in Figure 13 was used to hold the seal ring during the remachining of the sealing surfaces. A modified vernier caliper shown in Figure 14 was used to measure the critical dimension which was the minor outside diameter of the taper. The ring was machined to the angles and dimensions shown in Figure 15. The angles were slightly different from those prescribed by the manufacturer (Figure 8) but only with the specifications depicted in Figure 15 could reliable sealing be attained. Both inner and outer angular surfaces were then polished with No. 180 Al_2O_3 U BOND METAL CLOTH from Sandpaper, Inc., Rockland, Massachusetts.

The sealing surface of the cover was remachined to the angle shown in Figure 9. Polishing of the surface was done using the same No. 180 cloth as above.

All parts were scrubbed with detergent and hot water to remove any residual grit. Prior to assembly all surfaces were wiped with Kimberly-Clark type 900-S Kimwipes and acetone.

A final inspection of the seal ring and cover sealing surfaces was made before assembly. Particular attention was paid to the external surface of the seal ring. If a leak occurred it would probably be between the seal ring and the autoclave body. Leaks almost never occurred between the cover and inner ring surface. Bear in mind also that the initial seal was a line seal between the tip of the outside edge of the seal ring and the autoclave body. Therefore, even a slight nick barely visible to the unaided eye was intolerable if it occurred at the outside tip of the seal ring.

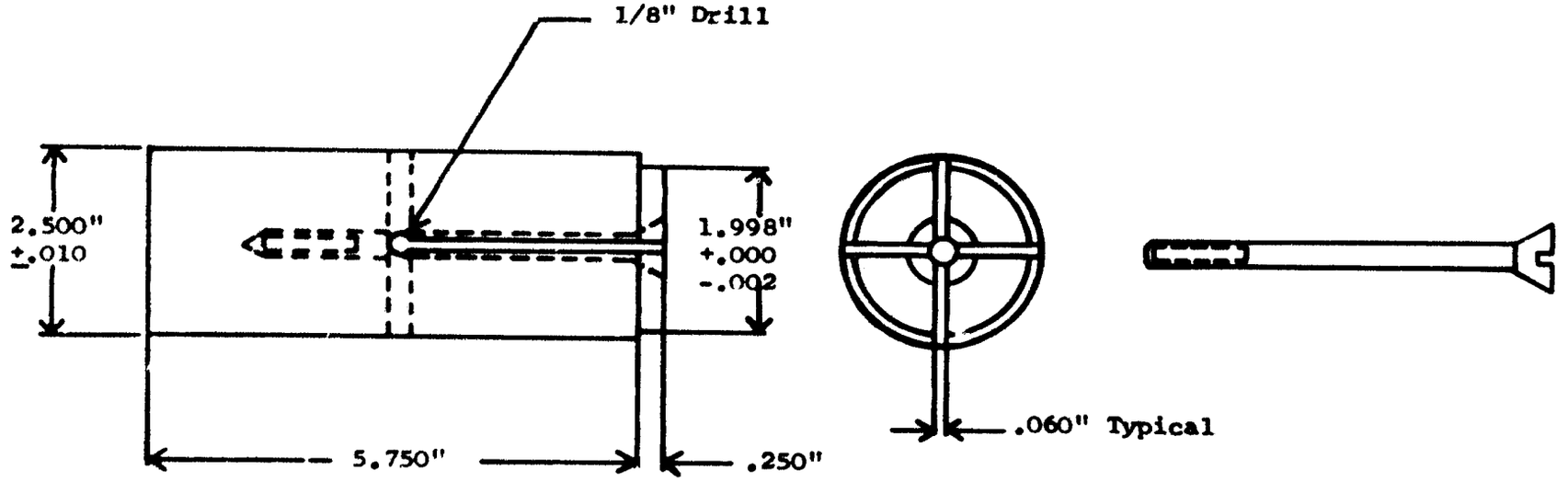

Figure 13. Expanding Mandrel for Remachining Seal Rings

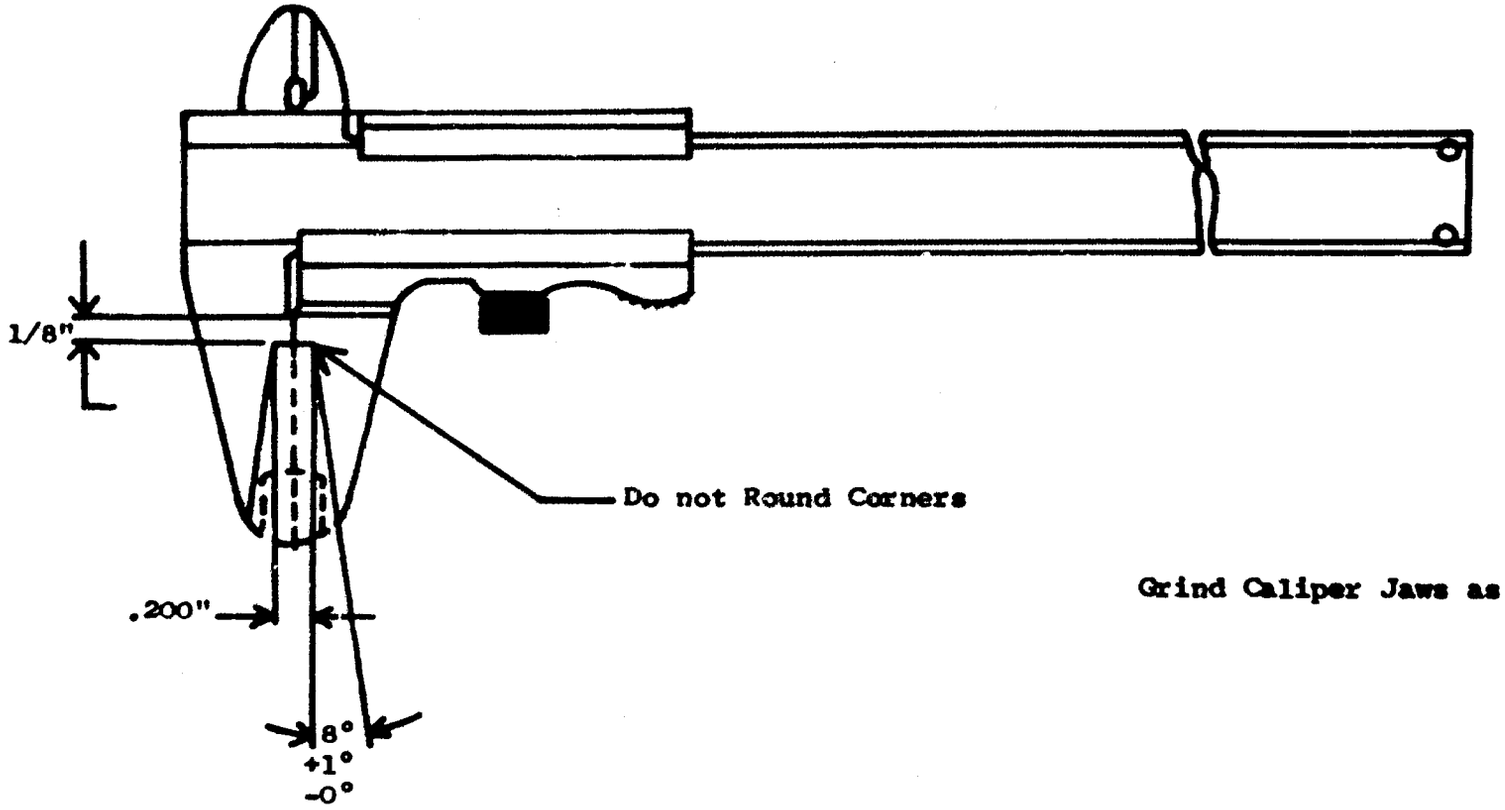

Grind Caliper Jaws as Shown.

Figure 14. Seal Ring Caliper

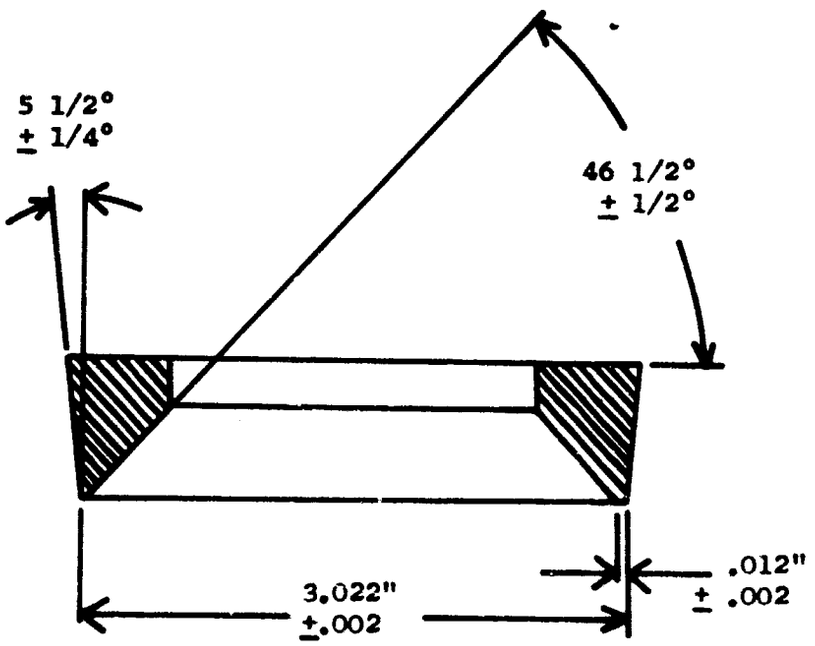

Figure 15. Seal Ring

The Autoclave (Continued)

The closure was assembled by placing the seal ring, main nut, thrust washer and lock nut onto the cover in that order. To insure proper seating of the seal ring into the autoclave the main nut was screwed into the autoclave with one hand while lifting up on the cover piece with the other. This maintained alignment of the seal ring until it touched the seat area in the autoclave. Two 1/2 inch diameter by 12 inches long steel rods were then inserted into opposite holes in the main nut. The main nut was tightened down firmly. If the main nut turned more than about 45° between hand tight and bar tight positions without bottoming, the seal would be taken apart and checked for interference. If interference was suspected the seal would be removed and disassembled. A test would then be performed using just two of the seal parts, the seal ring and main nut. The seal ring would be placed in the autoclave in its normal position. The main nut would be screwed down next, until hand tight. A dental mirror could then be inserted through the center of the main nut and the junction between the bottom of the nut and seal ring observed. The main nut should hit the seal ring without interference.

If there was no interference a torque wrench was used to tighten the eight screws in the locknut in the following manner. Opposite pairs of screws were tightened, successively proceeding to new pairs in a clockwise direction. Tightening was continued repeatedly until no screw moved under the applied torque of 10 foot pounds. This procedure was repeated for 15, 20, 25, and 30 foot pounds torque. The vessel was then sealed except for the pressure gauge connection.

4.3 Operating Procedures

4.3.1 Preparing the Silver Can and Loading the Autoclave

Before a can was loaded for a run, the silver pieces were cleaned of grease and oil with detergent (Figures 16 and 17), washed with concentrated HCl, thoroughly rinsed with deionized water, and then allowed to dry.

Most hydrothermal ruby crystal growth runs were of about one month duration. This provided ample time for even a very small leak in the silver can to cause serious damage to the autoclave. In fact, an autoclave could easily be rendered useless in a single run. Testing for leaks in the system before use was a prime requirement for successful operation of a crystal growth system.

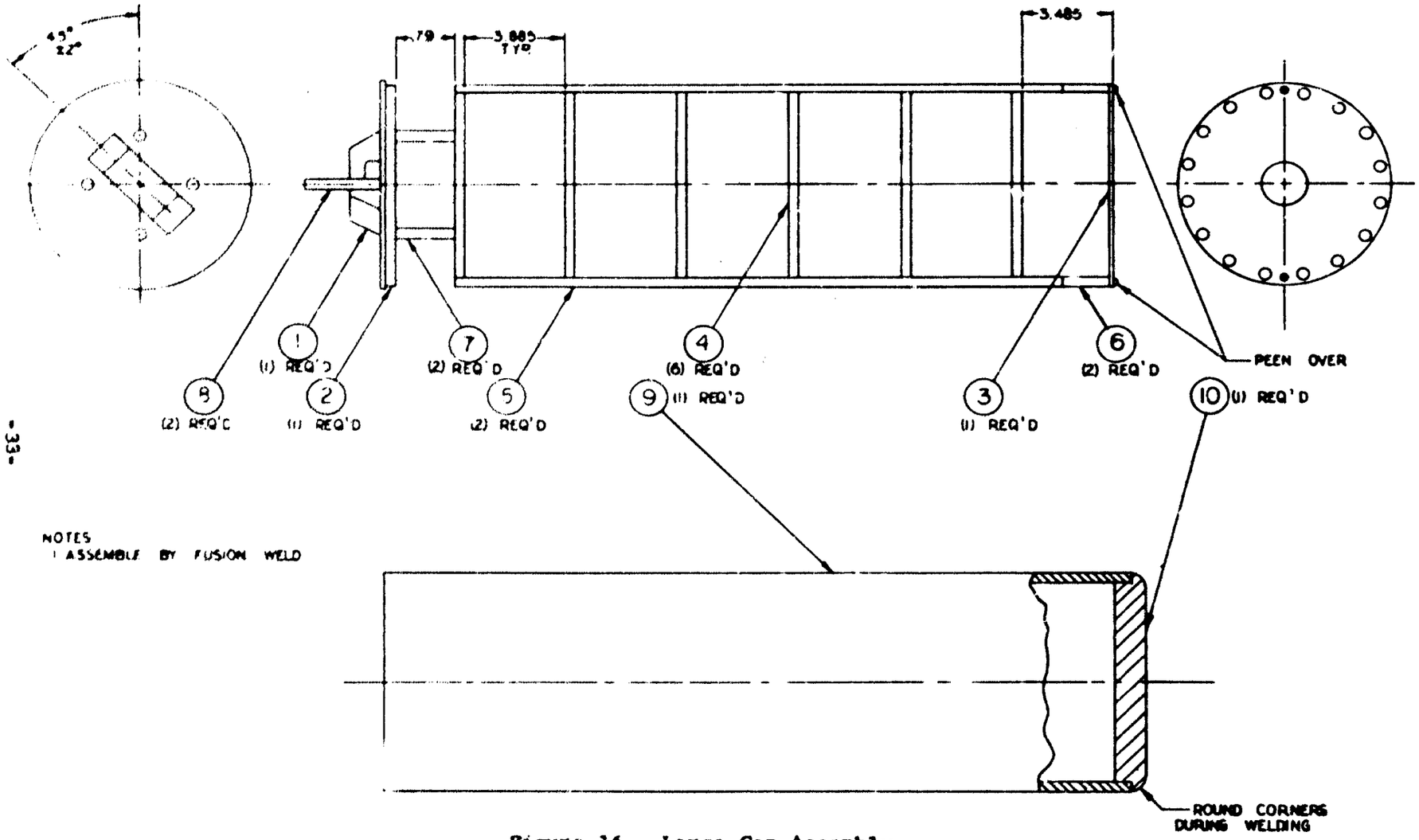

Figure 16. Large Can Assembly

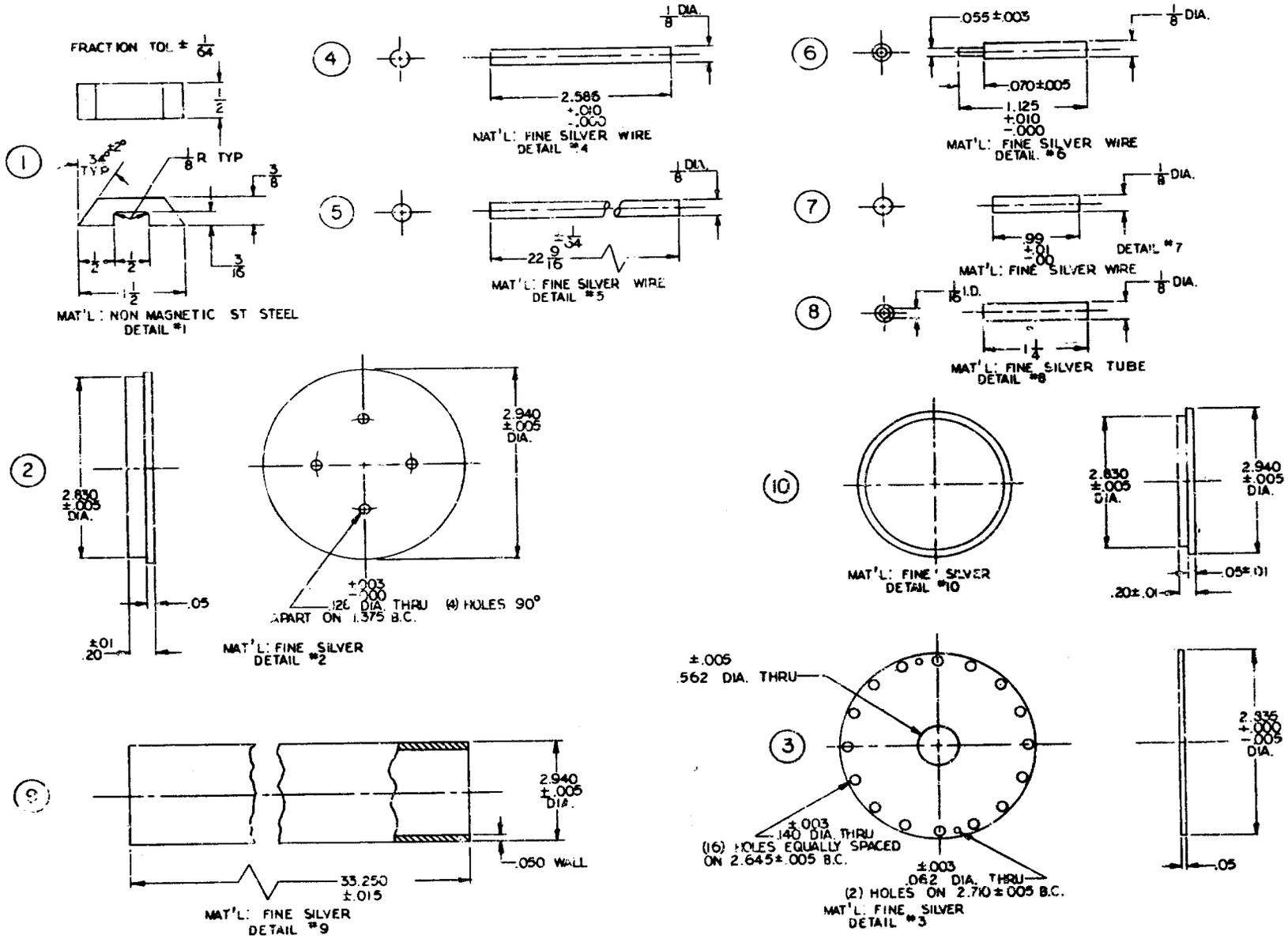

Figure 17. Engineering Drawing of Silver Can Parts

The Autoclave (Continued)

During construction of the cans all welds in subassemblies were subjected to a dye-penetrant test+ and any suspicious areas were welded and tested again. The seeds were attached to the seed rack with .020 inch diameter fine silver wire and the nutrient and zinc metal were placed in the bottom of the can. The seed rack and baffle subassembly were then welded to the can body. Any pressure within the can generated by the heat of welding was relieved through the twin vent tubes in the cover. The cover to body weld was then dye-checked and rewelded if necessary.

One hundred milliliters of deionized water were placed in the can through one of the vent tubes. The ends of both vent tubes were then flattened with heavy pliers and the tips were fused to seal the can. The can was then weighed to ± 1/2 gram. Final leak testing was done by heating the can to 110 to 120°C with a Briskeatt++ type D heating tape operated at 70 to 80 volts from a variable transformer. The can was kept hot for 15 to 16 hours and then weighed again. If there was no loss of weight the ends of the vent tubes were cut off and the test water boiled out. When all the water was removed, the KOH solvent was introduced through one of the tubes. The tubes were then flattened and resealed. Next, the can was placed in the autoclave, along with the appropriate external fill of deionized water. The vessel was closed, the pressure gauge was attached, and the vessel was placed in the furnace for operation. Autoclave sealing was described in detail in Section 4.2.

4.3.2 Warm-Up

Two different warm-up schemes were used in the course of this work: (a) programmed and (b) "as fast as possible". The programmed procedure was used only in the early part of this work when the operating pressure was low. In this case, the vessel was heated at a constant rate to operating conditions over 24, 48 or 96 hours by using the temperature programmer modification on the West Controller.

+ Spotcheck, Penetrant Type SKL-HF, Spotcheck Developer Type SKD-NF, Maganflux Corporation, Chicago, Illinois

++ Scientific Glass Co., Bloomfield, New Jersey

The Autoclave (Continued)

During the programmed warm-up a low gradient was maintained between the bottom and top sections of the autoclave. Since the seeds were so thin in the early part of the program, it was found a slow warm-up with a low temperature gradient would dissolve the seeds before growth conditions were established.

Drastic seed dissolution was prevented by heating the vessel to operating conditions "as fast as possible", with a high temperature gradient. This was accomplished by having the power inputs on the controller fixed at their ultimate position for operation and then switching on the controller.

Operating conditions were approached within 2-3 hours with an additional 3-4 hours required for the entire assembly of furnace, vessel, etc., to attain thermal steady state. This procedure prevented seed dissolution, and was used for the major part of the program.

4.3.3 Temperature Measurements

Temperatures were monitored with three chromel-alumel thermocouples attached to the autoclave exterior as depicted in Figure 18. The exact locations of the thermocouples are given in Table II. This was the usual procedure with the exception of a few experiments when internal measurements were made. These are described below.

The large growth rate differences of various runs made under similar measured conditions led to an investigation of the internal and external temperatures. The vessel used for this purpose was 1/2 the size of the large 52-inch long vessel. A stainless steel clad mineral insulated thermocouple was silver brazed into a standard 1/4-inch diameter pressure fitting of approximately 1/16-inch bore. A "dummy" silver can was made up with a hole in the top to permit introduction of the thermocouple inside of this can. An external thermocouple was attached on the surface of the vessel at the same vertical height. The autoclave was pressurized to 26,200 psi at an average temperature of approximately 485°C and allowed to equilibrate for 24 hours. At this time the inner and outer temperatures were measured and found to be approximately 30°C apart with the interior couple being the hotter. Twelve measurements were made of the temperature difference. The smallest difference recorded was 18°C and the highest was 34°C. The average value was 26.5°C.

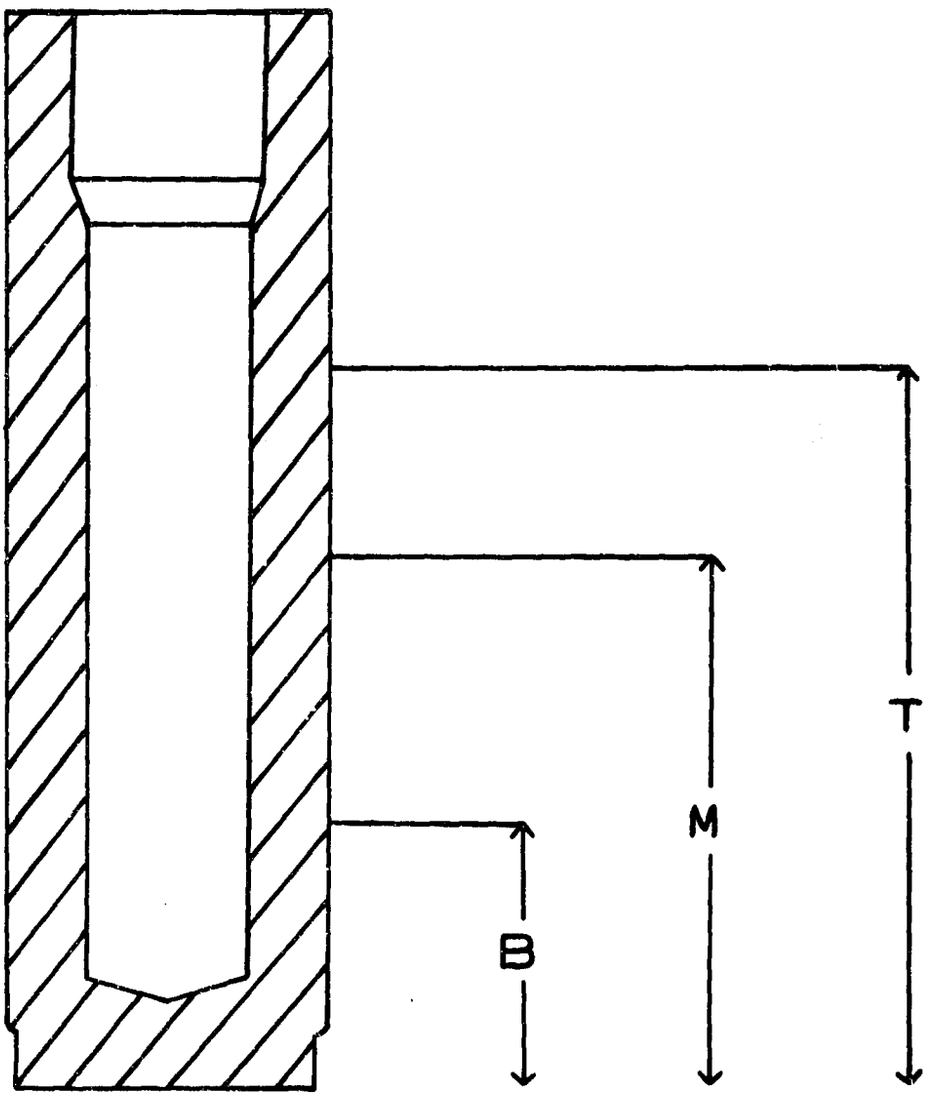

Figure 18. Thermocouple Location

TABLE II

Thermocouple Locations for Autoclaves

Autoclave Number	Diameter Inches	Bottom, B Inches	Middle, M Inches	Top, T Inches
1	1	3.75	8.50	11.25
1	3	8.75	20.75	34
2A	1.5	4.75	10.125	13.875
2	3	8.75	20.75	34
4	1	3.875	8.75	11.50
5	3	8.50	20.75	34.125
6	3	8.75	21	34.25
9	1.5	3.875	10	14
7	3	8.75	20.75	34.25

The Autoclave (Continued)

One unusual effect noted during the internal measurements was abrupt temperature cycles of liquid in the vessel. Temperature changes of 5 - 10°C in approximately 5 seconds were noted. This indicated that the liquid was in a violent convective state.

Two ruby runs in 1.5 inch cans were made while monitoring temperatures in two places just above the top of the can and outside the autoclave. In both cases the external temperature was about 30°C higher than the internal temperature. In one case the internal temperature was 462°C and in the other it was 473°C. The corresponding external temperatures were 493°C and 503°C. A higher external temperature was rather surprising since in the first experiments with a "dummy" can the opposite had been found, i.e., the interior was hotter. The internal temperature in this latter case had been measured inside of the can through a hole in the cover. It did not seem possible that there could be such a high gradient across the top of the silver lid since the thermal conductivity of silver is high.

4.3.4 Opening the Autoclave

At the end of the run, the power was switched off and the autoclave was air cooled; when zero gauge pressure was indicated, the cold water was then passed over the vessel until it reached room temperature.

Closure was achieved with manual force only, according to the technique described in Section 4.2. Opening of the autoclaves proved that the manufacturer's recommended technique and tools supplied for loosening the main nut after a run were far from adequate. In order to unscrew the main nut and to provide the only possible technique for removing it, a new anvil-type tool was developed (Figure 19). This tool was constructed so that it could easily be clamped onto the main nut by means of two bolts. When in place, two steel pins in the tool fitted into two opposing holes on the side of the main nut. The pins in these holes allowed for efficient transmission of the applied torque. For opening the autoclave, torque was provided by striking the arms of the anvil openers with ten-pound hammers. No pressure-temperature or leak condition produced sealing of the vessel which could not be opened by this tool. The opener was used in Step 5 described below.

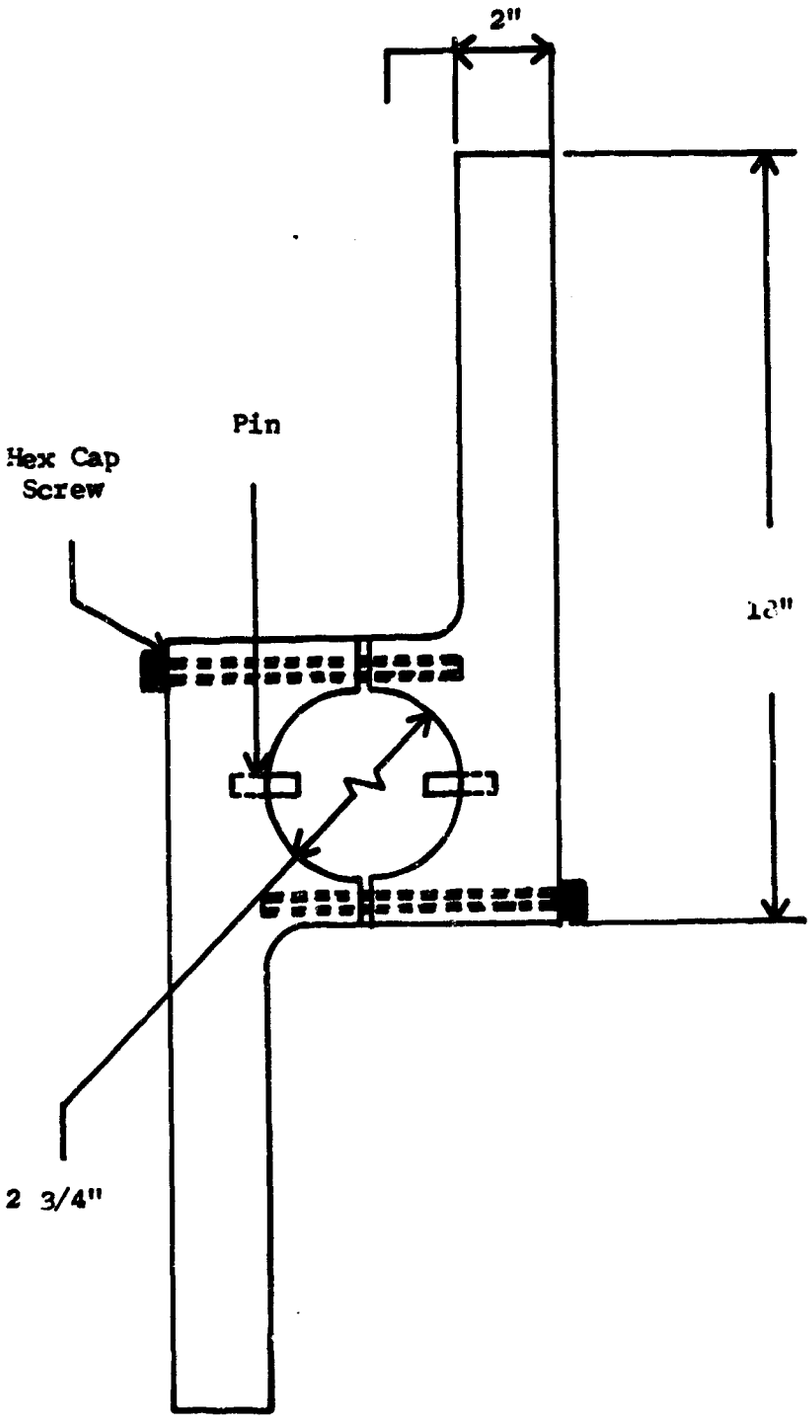

Figure 19. Main Nut Opener

The Autoclave (Continued)

After the run was completed and the vessel cooled to room temperature it was opened in the following way:

1. The pressure gauge was removed.
2. Eight screws in the locknut were loosened.
3. The locknut was backed off about 1/8 inch vertically.
4. The brass block was placed on top of the cover and struck with a hammer to break the cover loose from the seal ring.
5. The main nut opener (Figure 19) was bolted on and struck with a hammer to break loose the main nut.
6. The main nut was backed off approximately 1/4 inch vertically.
7. The locknut was screwed down hand tight.
8. Screws were tightened in the locknut until the seal ring was pulled free.
9. The main nut was unscrewed from the autoclave.

4.3.5 Extracting the Silver Can

Because of improper pressure balance or slow leaks in the entire system, there occurred in some cases a puffing up of the silver can. Due to the proximity of the autoclave walls, this expansion could not proceed too far. The movement of the can's wall was stopped by the autoclave walls. As a result of this large expansive force, the silver can walls were forced against the autoclave. Removal of the can was then extremely difficult.

While this expansion occurred in the small can and vessel, it was even a greater problem in larger cans (3 inch diameter). In order to remove the cans after a run, an extractor (Figure 20) was designed and constructed which could be used with vessels of both sizes. For the smaller can, a large screw was threaded into the top cap to provide a clasping handle. The cap of the larger can was provided with a clip. After engaging the handle in either case, the can was removed by driving the threaded rod with an electric drill. The extractor has removed cans which were impossible to remove manually.

4.4 Large Gradient Fill Determination

The longer vessels had an increased volume as a result of the increased length. In order to render this volume inactive, a steel plug designed to occupy as much volume as possible was placed on top of the silver can. Because of the length changes the temperature of the upper part of the vessel was much lower than the bottom.

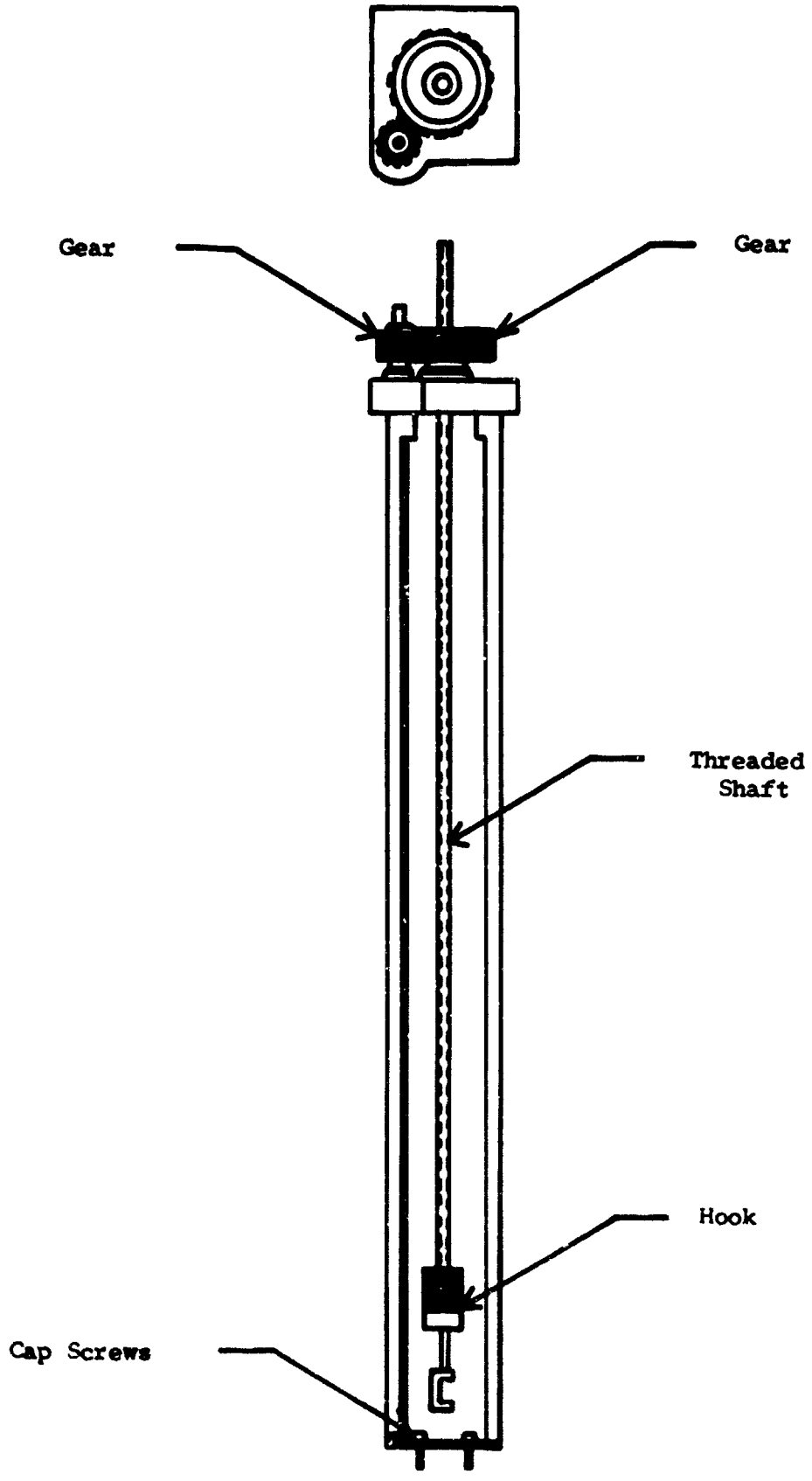

Figure 20. Can Extractor

The Autoclave (Continued)

Since the temperature distribution of the upper part of the vessel could not be known in advance, the proper amount of water to maintain pressure balance could not be determined either. The following scheme was used to determine the exact amount of water to use as external fill for a given pressure and temperature distribution.

A stainless steel solid "dummy" can was made. This was placed into the autoclave with a filler block and as much water as possible placed into the external space. The volume of the water in the external space was carefully measured. Then the vessel was heated to the desired thermal configuration, including the proper ΔT. Water in excess of that required to maintain the desired pressure was valved off and collected. Once equilibrium was attained the amount of water valved off was subtracted from the original amount of fill. The remainder was the fill required to produce the indicated pressure when the silver can was in its undistorted shape.

The data collected for this experiment are presented in Table III. The temperature reported in the table is an average temperature calculated from those measurements along the vessel corresponding to a crystal growth ΔT. The same data, pressure, temperature and fill are shown plotted in Figure 21. As indicated in the figure, seven points were observed to be equilibrium points; i.e., sufficient time had elapsed after a temperature or fill change was made so that the entire vessel could attain steady state conditions.

The P-T and fill conditions for these points are presented and a value for P/nT is calculated and presented in the last column of Table III. Considering the large thermal gradients along the autoclave, the very cool temperature at the seal and the high pressures involved, the constancy of this value is surprising.

The temperature at the seal was measured at the highest average temperature and found to be 337°C. The other temperatures were 550°C, 547°C, and 564°C for distances of 15 inches, 28 inches, and 40 inches from the seal. A crystal growth run using the fill data obtained in the test run was made. After opening the run almost no distortion of the silver can could be found. This indicated the accuracy of the method.

TABLE III

Pressure, Temperature, and Fill Data for Large Autoclaves

Day	Time	P(psi)	T(°C)	External Fill (ml)	P/nT(psi/°K)
1	1700	19,800	332	375	-
1	2145	21,700	-	375	-
2	0820	22,100	318	375	0.100
2	1100	18,900	319	366	-
2	1530	30,000	444	366	0.114
2	1530	25,000	444	353	-
2	1750	28,700	463	353	0.111
2	1750	23,700	463	337	-
3	0830	23,600	454	337	0.096
4	0830	25,800	487	337	-
5	0920	28,600	490	337	0.111
5	0920	25,000	490	327	-
5	1700	20,;00	532	325	0.111
5	1700	24,100	532	311	-
6	0815	25,500	534	311	-
7	0830	27,600	550	311	-
7	1430	28,400	554	311	0.110
7	1420	25,000	554	298	-

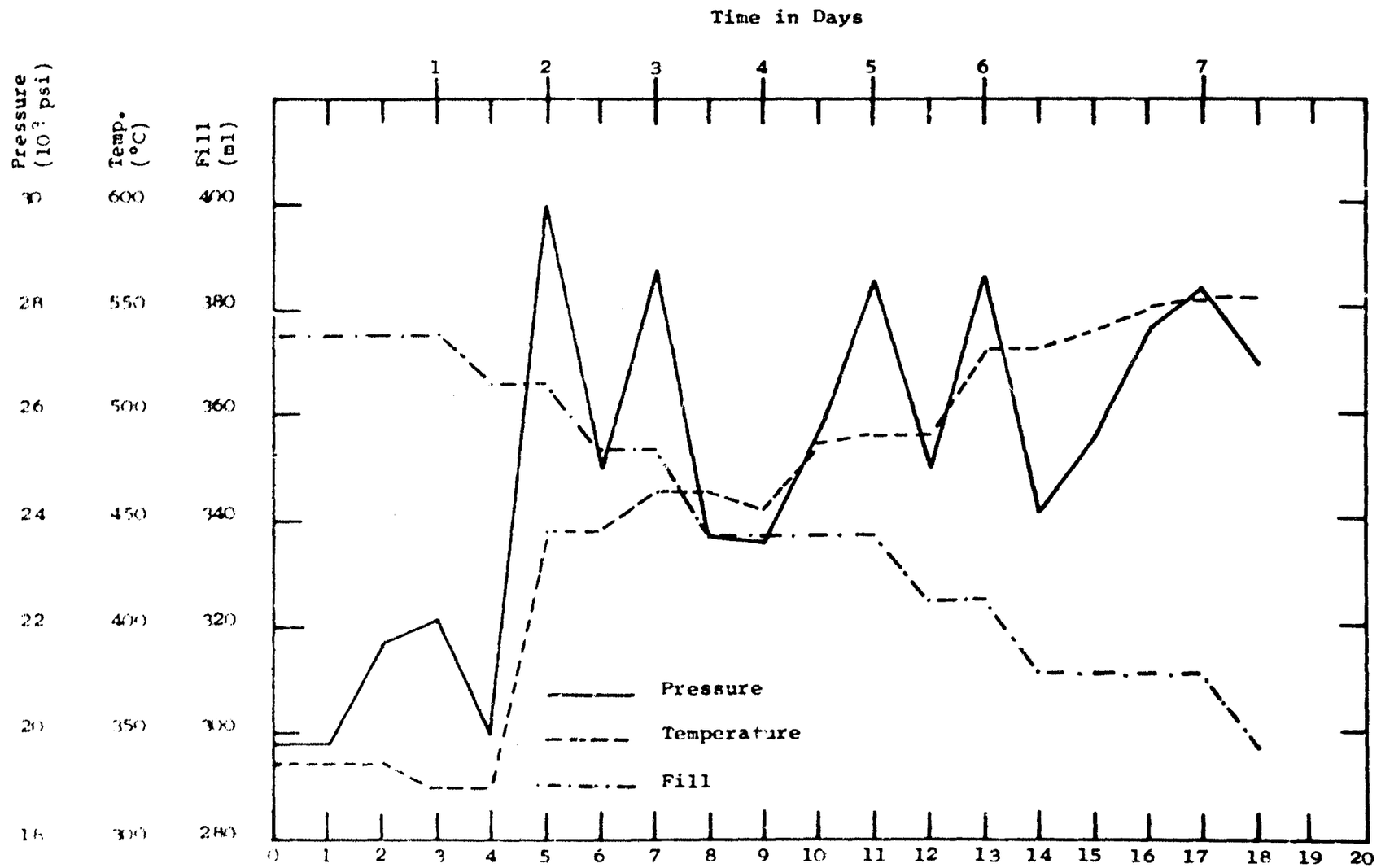

Figure 21. Pressure, Temperature, and Fill Data as a Function of Time

5.0 NUTRIENT PREPARATION

5.1 Introduction

The ruby nutrient must meet several requirements in order to be acceptable. First the nutrient cannot be composed of a powder. Powder settles to the bottom of the solution and prevents liquid circulation and heat transfer from the bottom of the crystal growth chamber. Also very small particles could be carried by the liquid into the growth chamber where they would function as seeds and begin to grow. If the size of the nutrient pieces are 10 to 20% of the diameter of the growth chamber adequate solution circulation should take place. When the nutrient is prepared by ceramic techniques it must be very dense so that the grains will not become separated and cause the pieces to revert to a wet powder.

Chromic oxide must be incorporated uniformly throughout the pieces of nutrient and not undergo preferential dissolution compared to the nutrient. In this way the amount of chromia taken up by growth on the seeds will be equal to the amount of nutrient that dissolves. If the solution solubility requirement for chromia is satisfied by a chromia addition, constant dopant concentration can be achieved: Purity consistent with the tolerable impurity levels in the grown crystals would have to be maintained. Since large scale hydrothermal ruby crystal growth is intended to be economically competitive with the Verneuil process, the latter method cannot be used for nutrient production.

In Phase I and II scrap flame fusion ruby was used as nutrient. The quantities of hydrothermal ruby proposed to be grown in Phase III will require large amounts of flame fusion scrap nutrient. A necessary objective of Phase II was to develop and alternate supply of nutrient. Three methods were investigated to try and produce a satisfactory substitute for the expensive flame fusion scrap. One method was a fused lump Al_2O_3 while the others employed a sintered powder.

5.1.1 Carbon Arc Fused Al_2O_3

In this method an a.c. arc is struck between carbon rods submerged in alumina powder. The powder located at a distance from the arc acts as an efficient heat insulator. Sufficient heat is produced in the arc to locally melt the alumina powder. When enough liquid has formed to bridge the carbon rods, the arc is extinguished by the conductive path through the molten alumina. Further heat is produced in the liquid by virtue of the I^2R loss between the carbon rods. The rods can be withdrawn slowly to produce a larger melt and powder can be fed continuously from the top. The process is used commercially and fused pieces of ruby have been made weighing several tons.

Nutrient Preparation (Continued)

The fused alumina was obtained from Simonds Abrasives Company, Philadelphia, Pennsylvania, and designated SF-1. Their starting material was a commercial grade alumina powder with a 99.9% purity. An amount of chromium oxide to produce 0.05 wt. % was added to the alumina and placed in a water-cooled iron crucible. The mixture was then fused by striking an arc between the high purity carbon electrodes near the bottom of the powders and withdrawing the electrodes from the melt as fusion occurred.

The color was a grey pink but closer inspection showed that the material was quite heterogeneous with various shades of pink and grey appearing in each piece. The appearance of this material was similar to a sponge with many holes formed by gas bubbles. This form gave the material a lower bulk density but provided a high surface area. This fused alumina sample was designated SF-1. A spectrographic analysis was made on SF-1 and the results are shown in Table IV. The fused alumina was quite impure with iron, magnesium and silicon appearing in objectionable quantities.

A second attempt at fusing alumina was made because the high density of the material and the inherent economy of the process were both desirable. A higher purity aluminum oxide (99.99+%) was purchased from United Mineral and Chemical Co. and mixed with 0.05 wt. % Cr_2O_3. The iron crucible was replaced with a thin walled alumina crucible which was water-cooled. Two difficulties were encountered which caused the second fusion attempt to fail. The crucibles cracked from thermal shock and allowed cooling water to enter the crucible. This effectively terminated the heating cycle. Secondly the 120 cycle power fluctuation of the arc caused a vigorous agitation of the air in the crucible. The alumina powder being fused was too fine and was blown out of the crucible before it was ever hot enough to fuse.

5.1.2 Sintered Al_2O_3

Dense sintered high alumina ceramics are routinely produced by industry. The technique in general is to ball mill a mixture of a decomposable aluminum compound such as aluminum nitrate or aluminum hydroxide with aluminum oxide. The ball milling reduces the particle size and increases the reactivity. After ball milling a mixture in the form of a slurry, the liquid portion is removed by filtering and slow evaporation leaving a "cake". The cake is then fired at a high temperature for a long enough time to allow the material to approach theoretical density. The nitrates or hydroxides decompose during the firing, react with oxygen to form Al_2O_3, and "cement" the particles together. Pieces of the large sintered mass can then be used directly for the nutrient.

TABLE IV

Spectrographic Analysis of Nutrients from Various Sources*

Element	Flame Susion FF-1	Associated Ceramics Sintered SNB-4	Simonds Sintered SS-1	Simonds Fused SF-1	National Beryllia NBL-1	Airtron A-1	Airtron A-2
Aluminum	High	High	High	High	High	High	High
Chromium	0.05	0.04	0.56	0.10	0 .08	0.07	0.07
Calcium	X	X	X	X	0.04	X	X
Copper	X	0.002	X	X	X	X	X
Iron	X	0.04	0.03	0.09	0.05	0.04	0.001
Gallium	X	0.001	X	X	0.03	X	0.001
Lead	X	X	X	X	X	X	X
Magnesium	0.001	0.12	X	0.02	0.007	X	0.005
Manganese	X	0.001	X	0.001	X	X	X
Columbium	X	0.15	X	X	X	X	X
Silicon	0.01	0.78	0.04	0.03	X	0.04	X
Sodium	X	X	X	X	X	X	0.03
Titanium	0.002	0.001	X	0.002	0.005	X	X
Vanadium	X	X	X	X	0.005	X	X
Zirconium	X	0.002	X	X	0.005	X	X

* All results are reported in weight percent.
X Not detected.

Nutrient Preparation (Continued)

An alternate possibility for a nutrient source is that of a pelletized sintered alumina to which the proper quantity of chromia had been added. After mixing the starting materials, standard pelletizing technique and carbide die materials can be used to prepare the pellets. Sintering may be achieved by firing the pellets in a travelling-bed, gas-fired furnace. One of the main points of concern was whether or not, as a result of subjection to the hydrothermal conditions, the pellets would disintegrate into a sludge which would settle to the bottom of the tube and be unsatisfactory as a nutrient form. This had occurred with $LaAlO_3$ pellets prepared in a similar manner. It was found that no sludge would form from the Al_2O_3 if a good sintered bond was prepared by reaction above 1700°C.

Several forms of pellets were prepared from powdered alumina and chromia. The first type was manufactured by National Beryllia Co., Haskell, N. J., (Sample NBL-1) and consisted of pressed pills. The starting material was a high purity Al_2O_3 to which the Cr_2O_3 was added in the 0.05 wt. % range. The size of the pellets was 3/8 inch diameter and 3/16 inches thick. The pellets were fired at 1700°C after pressing to give a hard, durable, and compact nutrient.

An alternate supplier was contacted who effectively used the same approach. In this case the company was Associated Ceramics of Butler, Pennsylvania. One preparation was made by them, (Sample SNB-4). Pellets were again prepared from pressed powders of Al_2O_3 and Cr_2O_3. The size of the pellets in this case was 1/2 inch diameter x 3/4 inches long. The pellets were fired at an unknown high temperature to give a dense sintered mass of pink ruby.

The two above forms of sintered pellets, possessed a high impurity content which was introduced principally through the preliminary processing. One further attempt was made to prepare a higher purity sintered nutrient. A ten-pound lot of 99.99+% Al_2O_3 was purchased from United Mineral Co. and Cr_2O_3 was added at Airtron in the form of powder. This mixture was sent to Simonds Abrasives Co., Philadelphia, Pa.

The powder was milled using a rubber lined ball mill. Balls for the mill were fused ruby lumps produced by Simonds. After milling, the batch was filtered to remove the water then air dried to form a "cake". The "cake" was fired at a temperature in excess of 1700°C for four nours. The result was a dark pink material of very high strength and density. This sample was designated SS-1. The analysis of SS-1 in Table IV shows iron and silicon as the only detected impurities other than chromium. (This was due to the large weight loss of the impure high chromium content ruby used as balls.)

Nutrient Preparation (Continued)

Another experiment was planned in which flame fusion boules would be used for balls in the ball mill. Once a sufficiently large batch of sintered material was made a portion of it could be broken up and returned to mill the next batch. This experiment was not completed by the end of the contract.

5.1.3 Airtron Preparation

The preparation of high purity Al_2O_3 and Cr_2O_3 suitable for further sintering can be accomplished by thermal degradation of aluminum or chromium salts. One of the most frequently used salts is an alum of the type $K\,Al(SO_4)_2 \cdot 12H_2O$ but other compounds are also amenable. Preliminary experiments were designed to obtain a uniform mixture of Al_2O_3 and Cr_2O_3 where the Cr_2O_3 concentration was close to 0.05 wt. %.

An initial batch of material was prepared at Airtron by coprecipitating aluminum and chromium hydroxides by addition of ammonium hydroxide to a solution of the proper ratio of aluminum alum ($Al_2(SO_4)_3 \cdot (NH_4)_2SO_4 \cdot 24H_2O$), and chromium alum ($CrK(SO_4)_2 \cdot 12H_2O$). Alum is inexpensive and in bulk costs less than one dollar per pound. The precipitation of aluminum and chromium hydroxides produces a homogeneous mixture and provides a purification step. This moisture of hydrated oxides was then washed, dried and fired at 1000°C in a platinum beaker thus converting it to the α-Al_2O_3 phase. The spectrographic analysis for this material (A-1) is presented in Table IV. As can be seen, a relatively high purity mixture was obtained. The chromium content obviously needed adjustment which was relatively simple and the only other elements to show in the analysis were iron and silicon. A second batch (A-2) was prepared using the same technique but with recrystallized alum in order to reduce the iron content. Ammonium carbonate rather than the hydroxide was used in order to reduce the silicon content. This material, when fired in a high temperature furnace similar to that used in preparing other sintered samples, was expected to provide an inexpensive, high purity, satisfactory form of nutrient material. Even though the product was definitely high purity, the laboratory process was not economical. Commercial large scale production facilities would have to be used in order to lower the price. This area of investigation was totally outside the scope of the contract. It may be added that no hydrothermal runs were made from A-1 or A-2 material because of the supply situation. Technically there was no reason to believe the materials were not satisfactory.

5.1.4 Analysis of Materials

All nutrients used in the hydrothermal growth of ruby were analyzed by optical spectrographic methods. Early in the program flame fusion grown ruby was found to be entirely satisfactory as a nutrient. Throughout Phase II this material has remained a standard high purity nutrient. Table IV contains the results of analyses performed on alternate nutrient sources. Comparison should be made with

Nutrient Preparation (Continued)

column 2 which gives the principal impurities in a flame fusion sample (FF-1). The total impurity content for the latter is not more than 100 ppm. It should be stressed that this purity is directly related to the powder source since the flame fusion method does not purify per se. A typical powder preparation for flame fusion is derived from thermal decomposition of the alums.

The nutrients listed in columns 3-6 were all derived from commercially available alumina powders of different purities. The highest purity of Al_2O_3 was 99.99%. The starting purity is generally maintained throughout either a sinter or a mass fusion. The most abundant impurity is iron although other elements are present at 10-1000 ppm. The presence of iron in the nutrient occurs at a level almost equal to that of the Cr^{+++} necessary for pink ruby and laser action. Iron would lead to poor quality crystals particularly because of possible segregation and chemical effects with the solvent. A green-yellow coloration is also imparted to the crystal from Fe^{+++}. The resulting optical absorption is detrimental to laser action.

The Airtron materials (A-1 and A-2) prepared in laboratory amounts illustrate the purity attainable with recrystallized hydroxides or alums. Notice that the A-2 sample is almost as pure as the flame fusion ruby. The small amount of Pb is not thought to be a consistent impurity. It probably occurred from the large amounts of PbO and PbF_2 used as fluxes in nearby furnaces. Certainly the thermal decomposition of alum is to be recommended as the best source of Al_2O_3 from a purity viewpoint.

5.1.5 Nutrient Material Tests

Not all the runs made under Phase II of this program were specifically designed for nutrient tests. Originally only flame fusion ruby was the nutrient but as other sources became available they were immediatly tested. Table V is a summary of all runs performed during the program. The information on Table V is concerned only with the nutrients and does not add other specific reasons for initiating the run. Runs 121, 124, and 125 were the first ones to incorporate an alternate nutrient. Seed and crystal data are given in Tables IX, XII, and XIII. In these cases sintered pellets were tried. The materials were obtained from National Beryllia Co. (NBL-1) and their preparation was described in Section 5.1.2. The performance of the pellets was satisfactory but the high impurity content was detrimental. Run 127 was the first attempt at growing from an arc fused nutrient as described in Section 5.1.1. Here again the physical state was perhaps optimized but large gradients of Cr^{+++} existed in the pieces. Also the impurities were much too high for good ruby growth.

TABLE V

Nutrients Used for Hydrothermal Growth of Ruby

Run Number	Nutrient Used	Source of Nutrient	Amount (grams)	Physical State or Size
120	flame fusion scrap pink ruby	Adolph Meller Co.	180	crushed boules, 0.2 cm^3
121	sintered pellets of Al_2O_3 + Cr_2O_3	National Beryllia Co.	180	3/16" thick x 3/8" dia.
122	flame fusion ruby	Adolph Meller Co.	180	crushed boules
123	flame fusion ruby	Adolph Meller Co.	180	crushed boules
124	sintered pellets of Al_2O_3 + Cr_2O_3	National Beryllia Co.	150	3/16" thick x 3/8" dia.
125	sintered pellets of Al_2O_3 + Cr_2O_3	National Beryllia Co.	150	3/16" thick x 3/8" dia.
126	flame fusion ruby	Adolph Meller Co.	150	crushed boules
127	arc fused Al_2O_3 + Cr_2O_3	Simonds Abrasives Co.	100	1/4" to 1/2" pieces
128	flame fusion ruby	Adolph Meller Co.	50	crushed boules
129	flame fusion ruby	Adolph Meller Co.	1000	crushed boules
130	flame fusion ruby + 0.12 g Cr_2O_3	Adolph Meller Co.	1000	boule pieces and powder
131	flame fusion ruby	Adolph Meller Co.	1000	boule pieces
132	flame fusion ruby + 0.12 g Cr_2O_3	Adolph Meller Co.	1000	boule pieces and powder

TABLE V (Continued)

Nutrients Used for Hydrothermal Growth of Ruby

Run Number	Nutrient Used	Source of Nutrient	Amount (grams)	Physical State or Size
133	flame fusion ruby + 0.13 g Cr_2O_3	Adolph Meller Co.	1000	boule pieces and powder
134	flame fusion ruby + 0.13 g Cr_2O_3 + 2.2 g Al	Adolph Meller Co.	1300	boule pieces and powder
135	flame fusion ruby + 0.13 g Cr_2O_3 + 0.1 g Al	Adolph Meller Co.	1300	boule pieces and powder
136	flame fusion ruby	Adolph Meller Co.	50	small pieces
137	flame fusion ruby + 0.13 g Cr_2O_3 + 0.1 g Al + 18.4 g KNO_2 + 8.0 g Li_2CO_3	Adolph Meller Co.	1300	small pieces and powder
138	flame fusion ruby + 0.13 g Cr_2O_3 + 0.1 g Al	Adolph Meller Co.	1300	small pieces and powder
139	sintered pellets of Al_2O_3 + Cr_2O_3	Associated Ceramics	44	1/2" dia. x 3/4" long
140	flame fusion ruby + 0.13 g Cr_2O_3 + 0.1 g Al + 8.054 g Li_2CO_3	Adolph Meller Co.	1300	small pieces and powder
141	sintered pellets of Al_2O_3 + Cr_2O_3	National Beryllia Co.	45	3/16" thick x 3/8" dia.
142	arc-fused Al_2O_3 + Cr_2O_3	Simonds Abrasives Co.	45	1/4" - 1/2" lumps
143	flame fusion ruby + 0.13 g Cr_2O_3 + 0.1 g Al	Adolph Meller Co.	1300	crushed boules

TABLE V (Continued)

Nutrients Used for Hydrothermal Growth of Ruby

Run Number	Nutrient Used	Source of Nutrient	Amount (grams)	Physical State or Size
144	flame fusion scrap	Adolph Meller Co.	45	crushed boules
145	flame fusion ruby + 0.13 g Cr_2O_3 + 0.1 g Al + 8.0175 g Li_2CO_3	Adolph Meller Co.	1300	crushed boules and powder
146	arc-fused Al_2O_3 + Cr_2O_3	Simonds Abrasives Co.	45	small lumps
147	flame fusion ruby + 0.13 g Cr_2O_3	Adolph Meller Co.	1300	crushed boules and powder powder
148	flame fusion ruby + 0.13 g Cr_2O_3	Adolph Meller Co.	1300	crushed boules and powder
149	flame fusion sapphire	Adolph Meller Co.	150	crushed boules
150	flame fusion ruby + 0.14 g Cr_2O_3	Adolph Meller Co.	1300	crushed boules and powder
151	flame fusion ruby + 0.14 g Cr_2O_3	Adolph Meller Co.	1300	crushed boules and powder
152	flame fusion ruby + 0.12 g Al	Adolph Meller Co.	150	crushed boules and powder
153	flame fusion ruby + 0.12 g Al	Adolph Meller Co.	150	crushed boules and powder

Nutrient Preparation (Continued)

Four crystal growth runs (Nos. 139, 141, 142, and 144) were made in one-inch vessels to test the nutrient materials available in large amounts. Simonds arc fused (SF-1), National Beryllia pellets (NBL-1), Associated Ceramics pellets (SNB-4), and a flame fusion (FF-1) were chosen for comparison. The growth conditions for these runs are summarized in Table VII. It can be seen from these data that the conditions for each run were not duplicated. However, all runs were in regions where substantial growth occurred in the operating time. The crystal and seed data for the runs are given in Tables XXVII, XXIX, XXX, and XXXII, for Associated Ceramics (SNB-4), National Beryllia (NBL-1), Simonds fused (SF-1) and flame fusion (FF-1) nutrients, respectively. In the cases of the Associated Ceramics (SNB-4) and National Beryllia (NBL-1) materials, very little <0001> growth occurred and only slight growth occurred with Simonds fused (SF-1) material. The crystals from the runs with National Beryllia (NBL-1) and Associated Ceramics (SNB-4) also had some lateral growth. This growth was pale yellow in color and was probably caused by the high iron content of the nutrient. Similarly the crystals from the Simonds fused (SF-1) material were also discolored. The lack of growth with the National Beryllia (NBL-1) and Associated Ceramics (SNB-4) nutrient can probably be attributed to poisoning caused by one or more of the various impurities. The growth in the run in which scrap flame fusion nutrient was used was similar to that obtained in the larger vessels.

It was found that both the fused lumps and sintered pellets were satisfactory physical states for the nutrient. Neither would carry powdered particles to the growing crystal where additional nucleation sites may develop. The amount of sludge formation from non-uniform dissolution of the nutrient was also negligible provided the material was coherent. The fused ruby gave no trouble. The sintered samples had to be fired at 1700°C for best results.

5.1.6 Final Nutrient Preparation

Two approaches were found to be most attractive for large amounts of nutrient required in the hydrothermal growth of ruby. First the coprecipitation of the aluminum and chromium hydroxides from a solution of the alums is recommended. This method leads to a very high purity powder with the Al and Cr in the proper ratio for growing pink ruby. The resulting mixture of hydroxides can be either dried and then fired or else hydrostatically pressed in pellet form and then sintered. The net result is an ideal nutrient which is compact, does not form sludge, and slowly dissolves.

The alums necessary for starting materials can be purchased from reliable chemical supply houses. Some of these are Fisher Scientific, Pittsburgh, Pa., E. H. Sargent and Co., Springfield, N. , who may provide quantities in 100-pound lots. For requirements stil-

Nutrient Preparation (Continued)

are rated in tons it may be necessary to begin your own pilot plant or work with a small company who is willing to prepare the desired quantity.

The other remaining method for large scale nutrient preparation involves the direct purchase of a high purity Al_2O_3 from commercial suppliers. The Cr_2O_3 may be added in the form of powder and the resulting mixture can be subsequently ball milled to disperse the Cr_2O_3 evenly. After an efficient mixing, the material can be processed again by two different procedures to bring about a coherent mass. Thus the caked mixture can be sintered in large lumps or pressed into a convenient sized pellet and sintered.

High purity powdered Al_2O_3 can be purchased from an increasing number of companies at this time. Among these are Johnson Mathey, Ltd., London, England, Alcoa, Pittsburgh, Pa., Linde Division, Union Carbide Co., New York, N. Y., Consolidated Aluminum Corp., Switzerland. The Al_2O_3 in high purity is basically prepared in much the same manner. The preferential method is a thermal decomposition of an alum. The resulting purity is 99.99% and better. However, new and easier methods may also lead to Al_2O_3. The impetus for further development is dependent on the proposed market. Since the amount used only for ruby laser crystals is rather limited, few companies have invested time and money in purification schemes.

6.0 SEED CRYSTAL PREPARATION

As a part of the Phase I work, it was found that the quality of the hydrothermally grown crystal was extremely dependent upon the quality of the seed crystal. Furthermore, only seed crystals grown by molten salt technique were found to be usable for the growth of high quality crystals. Fortunately, the Solid State Laboratory had both the necessary laboratory furnaces and experience in the growth of ruby crystals by the molten salt technique so that the crystals for seed material were available for Phase I of the hydrothermal ruby growth program.

In order to replenish the seed supply for the preliminary investigation of Phase II, twelve runs, shown in Table VI, were made during the program. The crystals were grown in 8 inches x 8 inches platinum crucibles holding 54 pounds of melt. Seven pounds of alumina, 47 pounds of lead fluoride and 1.6 grams of Cr_2O_3 constituted a charge. The alumina and lead fluoride were premixed in a clean 5-gallon plastic garbage can with an aluminum scoop. The platinum crucible was charged to 3/4 full with powder and placed in the heated furnace for about one hour. Considerable consolidation and shrinkage of the powder took place. More powder was then added to take up the remaining space. Two premelts were sufficient to get all the powder in the can. The Cr_2O_3 was added with the last of the powder.

The crucible was "soaked" (held at constant temperature) at 1250°C for 24 hours to assure complete liquification of the components. After soaking, the crucible was cooled at a linear rate to approximately 950 to 1000°C over a period of 4 to 10 days. All molten material was poured out of the crucible at 950°C and the crystals were left behind. Typical yields of 50% or 3-1/2 pounds of ruby crystals were obtained per run. The largest plates obtained were approximately 2 x 3 inches across the (0001) faces.

Three slight departures from the normal growth procedures were attempted. In runs No. 12 and No. 13, after the soak period was maintained at nearly isothermal conditions in the center of the furnace, the crucible was lowered four and six inches respectively in order to impose a vertical gradient on the melt. At this position in the furnace the bottom of the crucible is in the cooler section. It was hoped that crystallization of the plates would occur at the bottom of the crucible and continue upward as the cooling progressed. No significant changes were noted. The crystals continued to grow at the surface of the melt.

The second and third deviations from the growth of ruby were performed by adding a trace of La_2O_3 in Run No. 14 and a large quantity of Cr_2O_3 in Run 10 to the melt. It had been reported that such additions were effective in changing the habit to the rhombohedral form.[4] The possession of such crystals would allow study of the quality and growth rates in crystallographic directions other than the <0001>. No significant changes in habit were noted. Runs 14 and 15 completed the series made for obtaining seed crystals. The procedures and compositions were identical to those described previously.

TABLE VI

Molten Salt Crystal Growth of Ruby Seeds

Run No.	Al_2O_3 (kg)	PbF_2 (kg)	Cr_2O_3 (gm)	Soak Temp. (°C)	Soak Time (hours)	Cool Rate (°C/hr)	Pour Temp. (°C)	Comment
BR-4	3.2	21.4	1.59	1300	12	5.0	1000	Melt capped over by undissolved Al_2O_3. Many small plates underneath cap.
BR-5	3.2	21.4	1.59	1300	24	6.5	1100	Small plates.
BR-6	3.2	21.4	1.59	1300	24	7.6	1000	Small yield - crystals at top of crucible.
BR-7	3.2	21.4	1.59	1300	24	6.5	1000	Layers of crystal plates.
BR-8	3.2	21.4	1.59	1270	24	10.0	840	Many large crystals.
BR-9	3.6	22.3	1.82	1292	24	4.3	820	Many large crystal plates.
BR-10	3.6	22.3	18.2	1265	24	4.7	801	Many large dark plates.
BR-11	3.6	22.3	1.82	1262	24	4.7	807	Many large dark plates.
BR-12	3.6	22.3	1.82	1271	24	4.1	810	Large crystal plates.
BR-13	3.6	22.3	1.82	1290	24	3.8	842	Large crystal plates.
BR-14	3.6	22.3	1.82	1278	24	4.5	838	58.4 gm La_2O_3 added to melt. No morphology change.
BR-15	3.6	22.3	1.82	1367	16	-	-	Furnace shut down after 16 hrs. because of mechanical failure.

7.0 HYDROTHERMAL CRYSTAL GROWTH

7.1 Introduction

During the course of the contract 34 crystal hydrothermal growth runs were made. Crystal growth was carried out in equipment of various sizes. Systems from 1/4 inch diameter x 4 inches long to 3 inch diameter x 34 inches long were used. The main purpose of all the crystal growth runs was to grow high quality ruby crystals large enough to yield laser rods 1/4 inch diameter by 3 inches long. The data obtained are shown in Table VII. A detailed description of each run is presented below.

7.2 Experiments

Both Waspalloy vessels used during Phase I had failed by the start of this contract because of corrosion caused by the leakage of growth solutions. A vessel numbered A-1 was available with the same size as those used in Phase I but it was fabricated from A-286. In order to perform some experiments the A-286 vessel was used. The pressure temperature rating of the Waspalloy vessels was 40,000 psi at 700°C. On the other hand the A-286 vessel of the same size was rated at 30,000 psi at 590°C.

To produce the proper temperature distribution it was necessary to operate the Waspalloy vessel with the bottom at approximately 650°C. Since this was well above the rating for A-286 the bottom temperature had to be reduced. This was accomplished by adding an additional heater for the lower third of the vessel. This greatly increased the area for heat input to the vessel and decreased the maximum bottom temperature. Runs 120 through 127 used this heater configuration.

Run 120, Vessel 2A-1.5

Toward the end of Phase I the major crystal growth problem appeared to be too high a growth rate. In order to better control the growth rate a low gradient run was tried first in the newly available A-286 vessel. A temperature difference of only 3°C was used. Everything appeared normal throughout the run. The hot plate was set at 1/2 the power of the side heater.

When the silver can was opened it was found that the seeds had actually lost weight instead of gaining. See Table VIII. However, the seed crystals had well developed faces. This indicated that they dissolved to some extent, were in equilibrium temporarily with the solution, or perhaps had grown very slowly.

Since the heater configuration was changed it appeared that the internal temperature difference did not have the same relationship to the external temperature difference that was experienced with the Waspalloy vessel.

TABLE VII

Crystal Growth Operational Data

Run No.	Internal Fill (%)	Bottom Temp. (°C)	Average Top Temp. (°C)	ΔT (°C)	Average Temp. (°C)	Average Pressure (psi x 10^3)	K_2CO_3 Concentration (molal)	Growth Period (days)	Average Growth Rate (mils/day)	Autoclave Number and Diam. (inches)
120	84	523	520	3	521	22.3	6.0	10	-	2A-1.5
121	84	545	520	25	530	24.5	6.7	7	-	2A-1.5
122	82	540	502	38	515	18.2	6.0	7	5.4	2A-1.5
123	73	526	495	31	505	20.0	1.5	4	8.4	2A-1.5
124	86	521	488	33	499	25.8	6.0	7	.32	2A-1.5
125	73	525	492	32	593	19.7	1.5	6	1.9	2A-1.5
126	76	522	492	30	590	22.2	1.5	7	3.7	2A-1.5
127	76	490	443	47	459	16.0	1.5	2-3	-	2A-1.5
128	76	521	487	34	498	22.9	1.5	7	22.6	1-1
129	76	507	483	23	491	25.9	1.5	10	3.2	6-3
130	78	505	478	27	490	27.0	1.75	24	9.4	1-3
131	76	502	476	26	486	25.0	1.50	31	0.90	5-3
132	78	519	480	39	495	26.2	1.75	33	10.0	7-3
133	77	509	489	20	492	26.5	1.75	30	8.86	1-3
134	78	494	454	40	468	26.0	1.75	3	-	7-3
135	78	524	487	37	498	28.4	1.75	20	18.6	7-3

TABLE VII (Continued)

Crystal Growth Operational Data

Run No.	Internal Fill (%)	Bottom Temp. (°C)	Average Top Temp. (°C)	ΔT (°C)	Average Temp. (°C)	Average Pressure (psi x 10^3)	K_2CO_3 Concentration (molal)	Growth Period (days)	Average Growth Rate (mils/day)	Autoclave Number and Diam. (inches)
136	78	543	506	37	519	11.6	1.75	4	-	4-1
137	77	509	479	30	488	26.0	1.75	17	12.8	1-3
138	78	495	487	8	489	27.4	1.75	35	-	7-3
139	85	535	505	30	516	27.2	1.75	6	6	3-1
140	77	509	484	25	491	27.2	1.75	22	12.9	1-3
141	85	482	444	38	457	28.5	1.75	8	-	4-1
142	85	477	435	42	449	28.1	1.75	7	6.10	3-1
143	78	[illegible]	490	17	495	27.0	1.75	30	8.02	7-3
144	80	[illegible]	464	43	478	23.6	1.75	7	12.8	3-1
145	[illegible]	511	495	16	500	26.4	1.75	33	10.8	1-3
147	78	515	491	24	499	25.8	1.75	20	18.8	7-3
148	77	500	480	20	486	26.8	1.75	19	23.7	1-3
149	77	510	473	37	486	27.7	1.75	12	17.8	9-1.5
150	75	548	540	8	545	23.4	2.0	34	2.9	1-3
151	76	548	540	8	542	25.8	4.0	19	0.83	2-3
152	65	546	520	26	529	17.0	6.0	5	-	9-1.5
153	68	551	512	39	525	23.9	2.0	4	-	9-1.5

TABLE VIII

Seed and Crystal Data, Run 120

Crystal Number	Weight (grams) Before	After	Seed Type-Orientation *
120-1	5.4	3.9	MS-c
120-2	8.7	6.0	MS-c
120-3	10.2	6.2	MS-c
120-4	3.6	1.5	MS-c
120-5	0.9	-	MS-c

* MS - Molten salt
c - Major crystal face; Dana, ref. 6

Hydrothermal Crystal Growth (Continued)

Run 121, Vessel 2A-1.5

Run 121 was a nutrient test and is discussed in Section 5. Table IX gives the pertinent seed and crystal growth data.

Run 122, Vessel 2A-1.5

A temperature difference of 38°C was used in this run to cause growth to occur. A relationship betwen the measured temperature and the growth rate rate was required. The power setting was changed to equal power for hot plate and side heater. This raised the average temperature of the lower section of the vessel and increased the heat input to the hydrothermal system.

Growth did occur as concluded from the data in Table X. The highest rate was 13.4 mils/day in the "C" direction of the second seed from the top. All seeds were flux grown ruby plates from 1/6 to 3/16 inches thick. The growth was of poor quality generally and consisted of many cracks and veils.

The two bottom seed crystals did not grow at all. Probably the extra heat input to the bottom area of the autoclave flowed up the relatively thick walls of the vessel. Heat could have been conducted around the baffle keeping the lower seeds too warm.

The conditions measured for Run 122 were quite similar to those measured near the conclusion of Phase I. However, crystal quality was much lower. Since the heater configuration had to be changed to protect the A-286 autoclave from over-heating, the exact conditions used at the end of Phase I could not be reproduced.

Several runs were made during Phase I at low base concentrations in a range of 0.5 to 2 molal K_2CO_3. During this period only poor quality flame fusion seeds were available. Growth was obtained at rapid rates. The crystals were of fair quality on poor flame fusion seeds. It was felt that a combination of the low molality conditions, and the use of high quality flux grown seeds might produce the desired increase of quality.

Run 123, Vessel 2A-1.5

Run 123 was made with 1.5 molal K_2CO_3 and had a temperature difference of 31°C. All seeds were flux grown plates. The run suffered an accidental shut-down and continued only 4 days. See Table VII. The heater connections were interchanged so that the variable autotransformer now was connected to the side heater instead of the hot plate heater as before. The side heater was set at 30% of the hot plate power to

TABLE IX

Seed and Crystal Data, Run 121

Crystal Number	Weight (grams) Before	Weight (grams) After	Seed Type-Orientation *
121-1	4.8	3.8	MS-c
121-2	5.1	4.3	MS-c
121-3	2.7	1.8	MS-c
121-4	4.5	3.5	MS-c
121-5	2.1	1.5	MS-c

* MS - Molten salt
c - Major crystal face; Dana, ref. 5

TABLE X

Seed and Crystal Data, Run 122

Crystal Number	Weight (grams) Before	Weight (grams) After	Thickness (mils) Before	Thickness (mils) After	Growth Rate (mils/day)	Seed Type-Orientation *
122-1	7.1	15.4	152	215	9.0	MS-c
122-2	9.7	17.1	181	275	13.4	MS-c
122-3	4.3	9.0	105	136	4.4	MS-c
122-4	2.7	3.5	72	74	0.29	MS-c
122-5	2.8	3.6	72	73	0.14	MS-c

* MS - Molten salt
c - Major crystal face; Dana, ref. 6

counteract the low growth rate on the bottom seeds. The data are given in Table XI. Growth rates were from 7 to 10 mils per day in the "C" direction. Only the bottom seed showed no sign of growth. The quality was good and the hydrothermally grown portion of the crystal was very clear with a minimum of cracks and flaws.

Run 124, Vessel 2A-1,5

Run 124 was a nutrient test run and is discussed in Section 5. Seed and crystal growth data are given in Table XII.

Run 125, Vessel 2A-1,5

Run 125 was a nutrient test run and is discussed in Section 5. Seed and crystal growth data are given in Table XIII.

Run 126, Vessel 2A-1,5

Conditions for Run 126 were essentially the same as for Run 123 except all the power was delivered to the hot plate heater and none to the side heater. The measured growth rates were more uniform. See Table XIV. Rates of 3.6 mils per day on the bottom seed and 3.4 mils per day on the top seed were measured. Nutrient was scrap flame fusion ruby. All growth was of high quality. The can leaked slightly due to a leaky autoclave seal. Vessel 2A-1,5 subsequently failed while in use on another project ending this series of runs.

Run 128, Vessel 1-1

The dimensions of vessel 1-1 were 1 inch I.D. x 2-1/2 inch O.D. It was fabricated from A-286 alloy. A ruby run was made using approximately the same conditions as Runs 123 and 126 to see if the vessel size and shape seriously changes the growth conditions while keeping measured temperatures the same. A temperature difference of 34° was used.

Growth rates as high as 25 mils per day occurred. A minimum rate was found at approximately 22 mils per day on the bottom seed. See Table XV. There was a large amount of spontaneous nucleation in the upper part of the silver can. All the nutrient was consumed. Quality was poor but consistent with very high growth rates. The bottom seed actually started to dissolve. Everything about the run indicated that it had operated with a gradient that was much too large. Yet the measured external conditions were very similar to Runs 123 and 126. These data strongly suggested that thermal conditions which produce good growth in a small system will not necessarily produce good growth in a much larger system.

TABLE XI

Seed and Crystal Data, Run 123

Crystal Number	Weight (grams) Before	Weight (grams) After	Thickness (mils) Before	Thickness (mils) After	Growth Rate (mils/day)	Seed Type - Orientation *
123-1	3.6	9.1	74	116	10.50	MS-c
123-2	2.6	5.1	75	104	7.30	MS-c
123-3	4.5	-	103	-	-	MS-c
123-4	4.7	3.1	80	110	7.5	MS-c
123-5	2.5	4.1	79	56	-	MS-c

* MS - Molten salt
c - Major crystal face; Dana, ref. 6

TABLE XII

Seed and Crystal Data, Run 124

Crystal Number	Weight (grams) Before	Weight (grams) After	Thickness (mils) Before	Thickness (mils) After	Growth Rate (mils/day)	Seed Type-Orientation *
124-1	7.7	10.5	118	121	0.43	MS-c
124-2	3.8	4.9	73	74	0.14	MS-c
124-3	6.0	8.3	113	117	0.57	MS-c
124-4	3.0	3.7	84	85	0.14	MS-c
124-5	4.8	6.6	140	140	-	MS-c

* MS - Molten salt
c - Major crystal face; Dana, ref. 6

TABLE XIII

Seed and Crystal Data, Run 125

Crystal Number	Weight (grams) Before	After	Thickness (mils) Before	After	Growth Rate (mils/day)	Seed Type-Orientation *
125-1	5.0	-	110	111	0.17	MS-c
125-2	3.7	-	69	104	4.2	MS-c
125-3	4.7	-	75	77	.33	MS-c
125-4	3.2	-	92	92	-	MS-c
125-5	5.5	-	97	95	-	MS-c

* MS - Molten salt
c - Major crystal face; Dana, ref. 6

TABLE XIV

Seed and Crystal Data, Run 126

Crystal Number	Weight (grams) Before	Weight (grams) After	Thickness (mils) Before	Thickness (mils) After	Growth Rate (mils/day)	Seed Type-Orientation *
126-1	4.0	10.3	108	132	3.4	MS-c
126-2	3.6	13.9	98	402	43.4	H-r
126-3	6.6	10.6	117	124	1.0	MS-c
126-4	6.0	11.6	124	170	6.6	MS-c
126-5	9.5	13.7	130	155	3.6	MS-c

* MS - Molten salt
H - Hydrothermal
r,c - Major crystal face; Dana, ref. 6

TABLE XV

Seed and Crystal Data, Run 128

Crystal Number	Weight (grams) Before	Weight (grams) After	Thickness (mils) Before	Thickness (mils) After	Growth Rate (mils/day)	Seed Type-Orientation *
128-1	1.6	10.6	56	214	22.6	MS-c
128-2	2.4	11.9	64	208	20.6	MS-c
128-3	2.2	14.5	58	235	25.3	MS-c
128-4	1.3	7.9	46	199	21.9	MS-c

* MS - Molten salt
c - Major crystal face; Dana, ref. 6

Hydrothermal Crystal Growth (Continued)

Run 129, Vessel 6-3

Vessel 6 was 3" I.D. x 6" O.D. x 42.75" long. This vessel was procured under another contract. Conditions were similar to Runs 123 and 126 except the temperature difference was 23°C instead of 30°C. A wide variety of seeds was used. These ranged from good molten salt seed plates to poor quality flame fusion material. Table XVI gives the pertinent information about the seeds. A fast warm-up to operating conditions was used. Duration of the run was 10 days.

The growth on all of the molten salt seed plates was of high quality. Figure 22 shows four of the crystals. Little or no veiling occurred and the crystals were quite clear. The growth rate on the flux plates varied from 0.8 mils per day on the bottom seed to 6.7 mils per day on the top seed. Growth rates of the flame fusion seeds with other orientations were generally somewhat higher than the flux seed rate, but of much lower quality. A notable exception to this were the "d" oriented seeds. There were two "d" seeds No. 129-2C on the second rung and No. 129-6B on the bottom rung of the seed rack. The upper one grew at 27.2 mils per day and the lower one at 19.9 mils per day. The quality of the "d" grown ruby was approximately the same as that grown on the other flame fusion seeds. If a high quality seed of "d" orientation were available this would be a good growth direction to investigate further. It would be most desirable to use an orientation capable of yielding high quality growth at rates greater than that obtainable in the "c" direction. Examination under crossed polaroids of the high quality crystals grown on flux seeds showed very little strain present.

When growth begins on the seed, sapphire is laid down first to a thickness of approximately 50 mils. After this colorless band the crystal turns a definite pink and increases in color toward the surface of the crystal. It is believed this is caused by differences in amounts of Al_2O_3 and Cr_2O_3 required to saturate the growth solution. The relative amount of Cr_2O_3 in solution must be greater than the relative amount of Cr_2O_3 in the ruby nutrient. This causes the solution to become saturated with Al_2O_3 before it becomes saturated with Cr_2O_3. As more ruby nutrient dissolves, the solution retains the Cr_2O_3 but deposits Al_2O_3 causing the sapphire band. When the solution becomes saturated with respect to Cr_2O_3 the growth becomes pink.

If Cr_2O_3 is added to the system in the proper amount the solution will become saturated with Al_2O_3 and Cr_2O_3 at the same time eliminating the sapphire band. Crystal 129-3B was cross-sectioned and the sapphire band was measured. It was found to be 104 mils on one side and 56 mils on the other as shown in Figure 23. There was no ruby growth. All the growth was sapphire indicating that the solution was not yet saturated with Cr_2O_3. The amount of Cr_2O_3 in solution at the termination of Run 129 had to be supplied by the nutrient. Weighing the

TABLE XVI

Seed and Crystal Data, Run 129

Crystal Number	Weight (grams) Before	Weight (grams) After	Thickness (mils) Before	Thickness (mils) After	Growth Rate (mils/day)	Seed Type-Orientation *
129-1A	16.6	30.6	106	173	6.7	MS-c
129-1B	11.2	14.0	125	130	0.5	FF-u
129-2A	2.0	3.1	86	121	3.5	FF-n
129-2B	16.8	22.1	167	194	2.7	MS-c
129-2C	9.4	23.4	159	431	27.2	FF-d
129-3A	2.5	2.8	-	-	-	FF-r
129-3B	20.7	33.2	99	144	4.5	MS-c
129-3C	4.5	6.7	-	-	-	FF-r
129-4A	8.7	19.2	118	211	9.3	FF-u
129-4B	4.8	6.6	113	128	1.5	MS-c
129-4C	4.5	7.6	92	168	7.6	FF-r
129-5A	7.6	10.9	95	120	2.5	MS-c
129-5B	12.1	19.9	97	136	3.9	MS-c
129-5C	7.1	10.7	160	-	-	FF-u
129-6A	4.5	6.5	65	73	0.8	MS-c
129-6B	11.0	23.4	165	364	19.9	FF-d

* MS - Molten salt
FF - Flame fusion
n, d, r, c, - Major crystal face; Dana, ref. 6
u - Orientation unknown

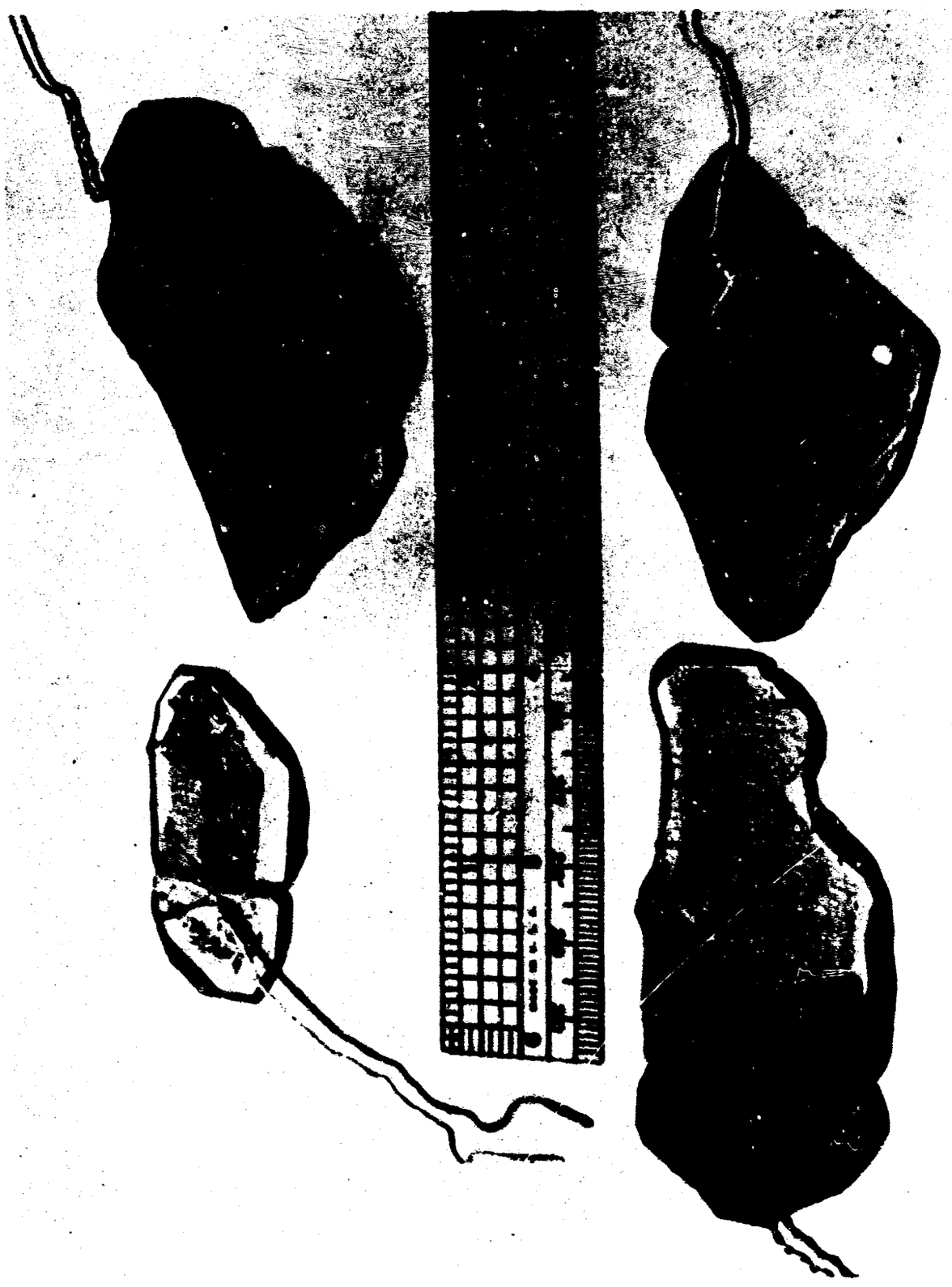

Figure 22. High Quality Crystal Growth on Molten Salt Seed Plates

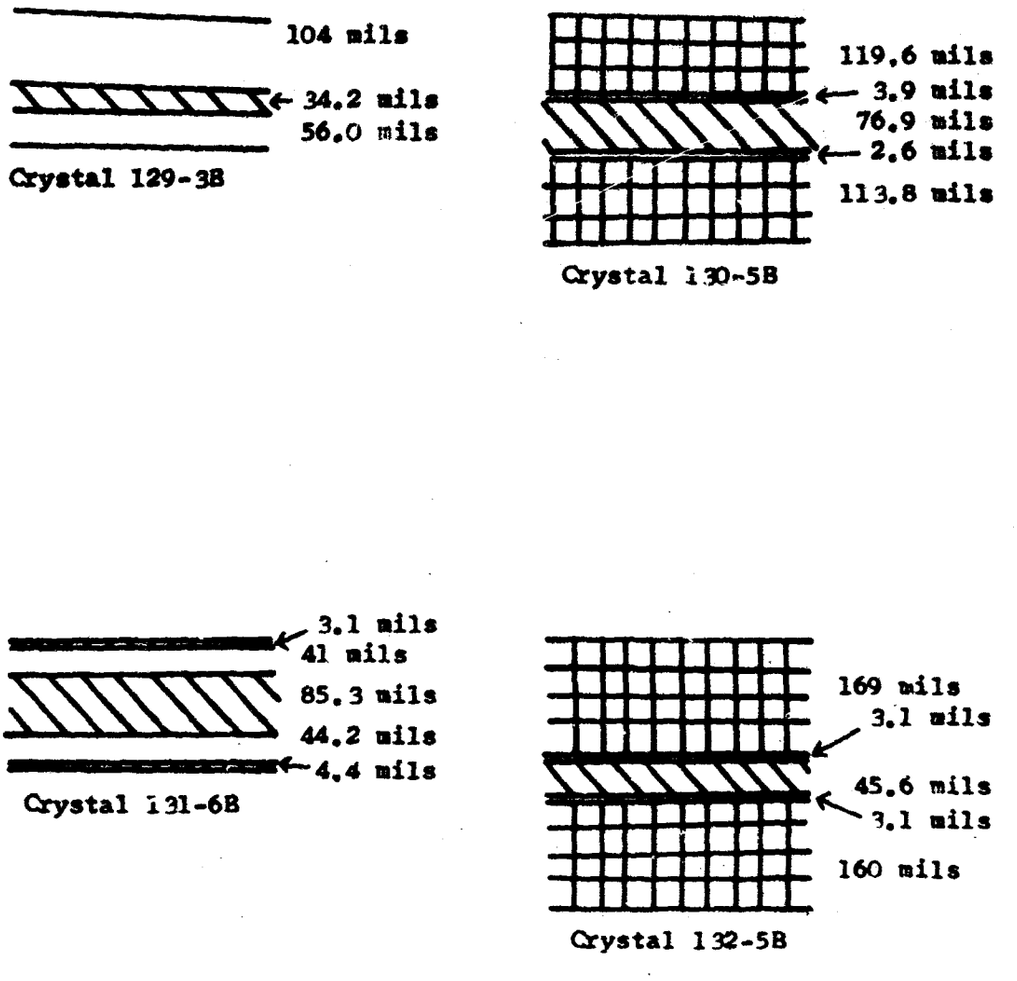

Figure 23. Drawing of Cross Sections of Ruby Crystals Nos. 129-3B, 130-5B, 131-6B and 132-5B

residual nutrient determined how much ruby had dissolved. The amount of Cr_2O_3 in solution must closely approximate the amount of Cr_2O_3 contained in ruby nutrient which had dissolved. Two hundred and forty-one grams of nutrient had dissolved. At approximately 0.05 weight percent Cr_2O_3 the 241 grams of ruby nutrient contained 0.1205 grams of Cr_2O_3. Since ruby had not yet started to grow in Run 129 the 0.1205 g could not be too large an addition. This amount was used in the next Run 130.

Run 130, Vessel 1-3

The two main reasons for Run 130 were to test the Cr_2O_3 addition discussed above and to use a 52 inch long vessel made by Airtron. The molality was also increased to provide more solubility. Otherwise the run was arranged to operate at the same conditions as Run 129.

Results of the run can be seen in Table XVII. The average growth rate was 9.4 mils/day compared to 3.2 mils per day in Run 129. The general quality of the crystals was good. However, there were cracks and veils in some areas of each crystal. The cracking was most severe on the largest and thickest crystals.

Run 131, Vessel 5-3

Run 131 was designed to duplicate the conditions of Run 129. The growth period was 33 days. Run 131 used the same type of vessel as Run 129. The actual conditions of growth can be seen in Table VII. These conditions were very similar as judged by the measurements. A slightly larger temperature difference was maintained to increase the growth rate a small amount.

In Table XVIII the results of Run 131 are shown. The growth rate was even lower than that of Run 129. Run 131 averaged 0.90 mils per day compared to 3.2 mils per day for Run 129. The quality was very high but the total amount grown was approximately the same as Run 129. No apparent reason for the difference could be found in the data.

It was felt that the very high quality ruby resulting from low growth rates would permit later growth at higher rates. Therefore Run 132 was designed to grow slowly at the beginning to promote healing and high quality. The temperature difference would then be increased to effect a higher growth rate.

Run 132, Vessel 7-3

Chromium oxide was added to this run to decrease the width of the sapphire band next to the seed. A slow programmed warm-up was used to control the rate of heating. The bottom temperature heating rate

TABLE XVII

Seed and Crystal Data, Run 130

Crystal Number	Weight (grams) Before	Weight (grams) After	Thickness (mils) Before	Thickness (mils) After	Growth Rate (mils/day)	Seed Type-Orientation *
130-1A	11.3	73.7	65	309	10.2	MS-c
130-1B	13.9	53.2	127	378	10.5	MS-c
130-2	33.2	99.5	155	389	9.7	H-c
130-3A	8.4	40.1	55	249	8.1	MS-c
130-3B	30.8	84.8	168	400	9.7	H-c
130-4	11.8	83.7	57	310	10.5	MS-c
130-5A	10.8	35.4	118	306	7.8	MS-c
130-5B	14.0	57.8	85	317	9.7	MS-c
130-6A	11.2	45.1	169	948	32.4	FF-d
130-6B	8.1	38.7	68	270	8.4	MS-c

* MS - Molten salt
FF - Flame fusion
H - Hydrothermal growth on MS see
d, c, - Major crystal face; Dana, ref. 6

TABLE XVIII

Seed and Crystal Data, Run 131

Crystal Number	Weight (grams) Before	Weight (grams) After	Thickness (mils) Before	Thickness (mils) After	Growth Rate (mils/day)	Seed Type-Orientation *
131-1	11.1	43.5	69	135	2.12	MS-c
131-2A	12.5	21.6	114	124	0.32	MS-c
131-2B	8.0	19.8	53	94	1.32	H-c
131-3A	19.8	28.8	129	159	0.97	MS-c
131-3B	7.7	13.3	81	100	0.61	MS-c
131-4	54.4	72.4	209	228	0.61	MS-c
131-5A	6.8	14.9	74	100	0.84	MS-c
131-5B	13.4	24.1	76	104	0.90	MS-c
131-6A	8.4	11.9	84	98	0.45	MS-c
131-6B	15.0	23.6	150	178	0.90	MS-c

* MS - Molten salt
H - Hydrothermal growth on MS seed
c - Major crystal face; Dana, ref. 6

Hydrothermal Crystal Growth (Continued)

was controlled by a cam to approximately 200°C per day. Temperature was raised manually to about 300°C and then programmed to 500°C. On the second day a loss of pressure was noted and the run was shut down. The autoclave was made by Autoclave Engineers, Inc., Erie, Pa. It was used in the condition as received. After opening the autoclave, it was found that leakage had occurred across the seal area. All seal parts were remachined to Airtron Specifications. The can had not leaked although it had expanded. This was verified by the fact that the sealed can still weighed the same as before the run. Since the can had not leaked, the run was restarted after the seal parts were machined.

Due to time schedules the run was warmed-up fast on the rerun. The growth period was 33 days. No pressure loss was detected in this interval. The temperature difference was 39°C. Very fast growth was obtained as recorded in Table XIX. A growth rate of 11.8 mils per day was measured on the top seed. All nutrient was transported and most of it grew on the seeds. Some spontaneously nucleated crystals formed a ring and cap on the upper 2.5 inches of the can. It was assumed that the puffed can actually contacted the autoclave walls and presented much better thermal conductivity. Subsequently a cold spot was formed which caused a much higher internal temperature difference than the external measurements would indicate. As the autoclave cooled it contracted around the spontaneously nucleated crystals. This made removal of the can extremely difficult. The crystals from Run 132 were heavily veiled and cracked.

Discussion of Runs 129 - 132

A 50 mil thick cross section was cut from one crystal selected from Run Nos. 129, 130, 131, and 132 in order to measure the width of the sapphire and ruby bands. After cutting and preparing the samples for microscopic examination, they were viewed under low power (8-30x). The seed width and band widths of ruby and sapphire were measured using a calibrated reticule in the eyepiece. The results of these measurements are shown in Figure 23. There were two note-worthy conclusions. The widths of the sapphire band in contact with the seed were greatly reduced by the addition of chromic oxide to the solvent. Crystal 129-3B was included in the examination for complete coverage of all large runs completed up to this point. For this crystal, it appeared that sapphire alone had been deposited with a thin band of ruby just at the crystal surface. When viewed through a microscope it was difficult to distinguish between a true thin ruby band at the crystal surface and any pink reflection from the seed. For crystal No. 131-6B, a 3-4 mil thick band of ruby at the crystal surface was observed. In both crystals, 129-3B and 131-6B, the sapphire band between the seed and surface was 41-104 mils thick.

Crystals 130-5B and 132-5B demonstrated the efficacy of the chromic oxide addition. Only a 3-4 mil band of sapphire grew on the

TABLE XIX

Seed and Crystal Data, Run 132

Crystal Number	Weight (grams) Before	Weight (grams) After	Thickness (mils) Before	Thickness (mils) After	Growth Rate (mils/day)	Seed Type-Orientation *
132-1A	13.6	104.0	105	477	11.3	MS-c
132-1B	8.9	66.2	87	476	11.8	MS-c
132-2A	8.2	95.8	58	420	11.0	MS-c
132-2B	4.3	48.9	51	402	10.6	MS-c
132-3A	8.0	51.2	102	450	10.6	MS-c
132-3B	22.4	108.2	120	449	10.0	MS-c
132-4A	4.7	46.7	60	395	10.2	MS-c
132-5A	17.6	83.3	114	409	8.9	MS-c
132-5B	4.3	39.9	60	381	9.7	MS-c
132-6A	5.7	33.7	38	292	7.7	MS-c
132-6B	4.3	20.5	77	356	8.5	MS-c

* MS - Molten salt
c - Major crystal face; Dana, ref. 6

Hydrothermal Crystal Growth (Continued)

seed. This sapphire band was then followed by a homogeneously doped ruby band growing out to the crystal surface.

Differences in the crystal thickness may be found. They can result from measurements made on different portions of the crystal or by different techniques. Seed thickness differences are due to the initial dissolution which occurs as the vessel is brought to operating temperatures. It is questionable how narrow this sapphire band can be made by the addition of Cr_2O_3 before the reverse condition would arise in which a ruby band of high chromium content would be deposited on a seed.

The two runs No. 130 and No. 132 in which the sapphire bands were narrowed were also runs in which the growth rate was high. It is not believed that the high rate should cause the sapphire banding which is a result of non-saturation of the fluid with chromium. Furthermore, if a slow rate was the contributing factor to the sapphire band, one would have expected to see a sapphire band at the surface of crystal No. 132-5B. In this case nutrient had been depleted and the rate must have slowed down.

The differences in growth rates for the four runs (Table XX) cannot be explained simply on the basis of the data for the conditions presented in the table. The reason for the different rates may be the combination of the autoclave length, filler plug, and can configuration. In the long vessel the filler plug rests on the top of the silver can and extends 6-9 inches above the top of the can into the top of the autoclave. The top of the autoclave also extends out of the furnace heaters about 10 linear inches. The plug appears to provide a heat sink for the can and the exposed autoclave surfaces serve to dissipate this heat.

In the short vessel there is no plug to act as a heat sink and only the external fill fluid may act as the heat absorber. In addition the autoclave barely extends out of the furnace and top insulation. A sketch showing the positions of three different autoclaves is presented in Figure 24. Because of the plug-can-autoclave configuration in the long autoclave, the comparable internal temperatures are lower than those of the short vessel. As a result, even though the external temperatures on long and short vessels are the same, there is a greater internal ΔT in the long vessel. This larger internal ΔT would then be responsible for the faster growth rate in the longer vessel.

Support for this proposition is given in data of Table XX. These data clearly show that higher growth rates were obtained only when the longer 48-inch and 52-inch vessels were used. It was concluded that the internal ΔT in these vessels was much larger than that of the short vessels even though the externally measured ΔT's were nearly the same.

TABLE XX

Autoclave Length, Steel Plug and Crystal Growth Rate for Runs Nos. 129, 130, 131, and 132

Run No.	Average "C" Direction Growth Rate (mils/day)	Autoclave Length (inches)	Steel Plug Length (inches)
129	3.2	42	-
130	9.4	52	9
131	0.9	42	-
132	10.0	48	6

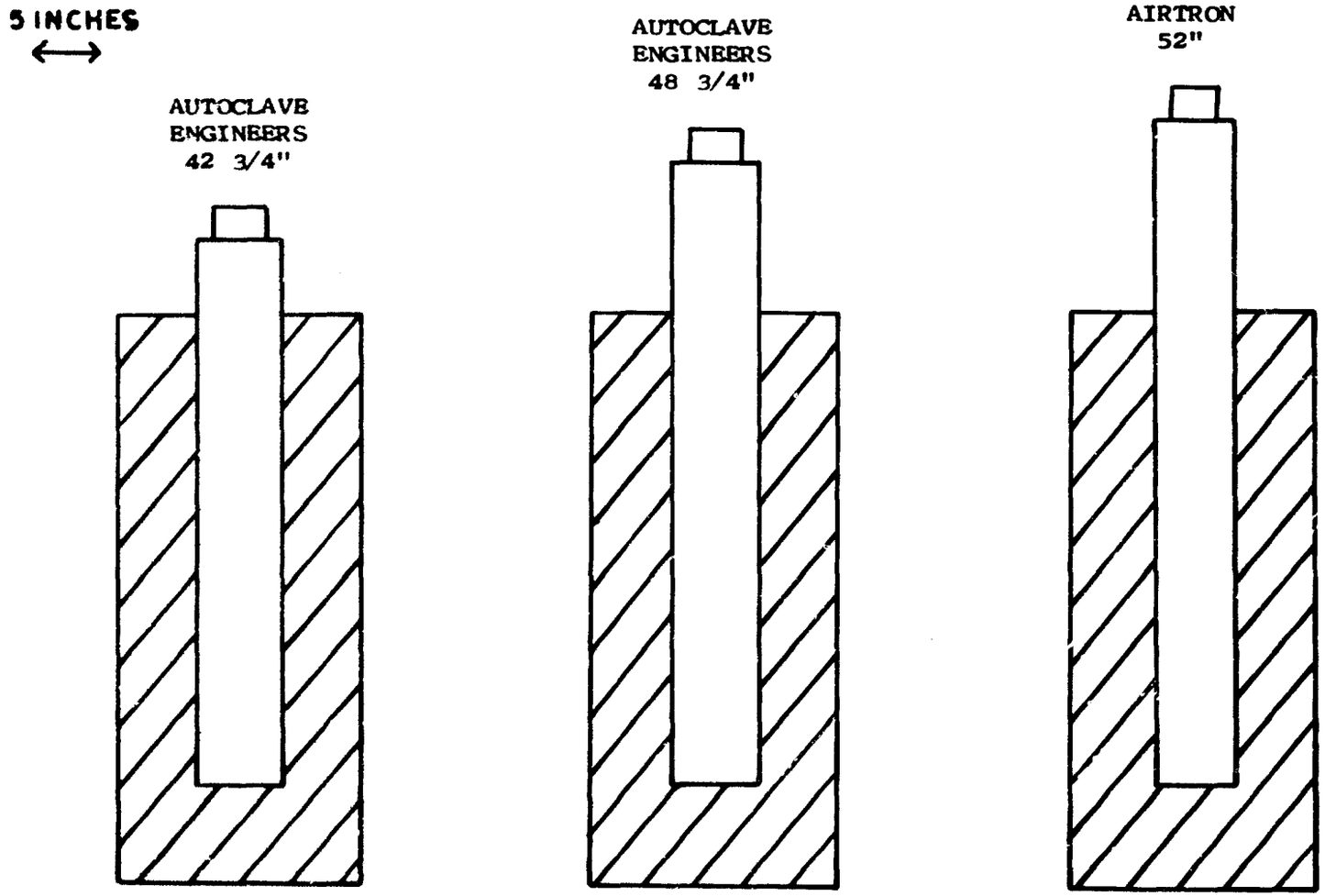

Figure 24. Positions of Autoclaves in Furnace

Hydrothermal Crystal Growth (Continued)

Further discussion of internal-external autoclave measurements using a special thermocouple probe was presented at the end of Section 4.0 of this report.

Run 133, Vessel 1-3

Three of the seeds in Run 133 were annealed at 1200°C for 12 hours to determine if crystal quality would be improved. Two molten salt seeds and one hydrothermal seed were annealed. Conditions similar to the last four runs were selected. Run duration was thirty days. All the nutrient was transported. Very heavy spontaneous nucleation was present. The liquid portion of the run was colored dirty yellow. Some silver attack was also seen. The top crystal was quite large and weighed approximately 90 grams. The silver attack had weakened the supporting wire for the top seed and it had fallen to the bottom sometime near the end of the run. This seed had dissolved back considerably. Growth on all the seeds was generally quite good except for the presence of cracking and other numerous defects. The growth rates reported in Table XXI should be considered minimum values since all the nutrient had dissolved. No difference in the quality of ruby was detected on the annealed seeds.

Run 134, Vessel 7-3

Run 134 had a programmed warm-up. The seed data are presented in Table XXII. On the third day of operation the bottom cylindrical heater of the furnace failed. As a result of this failure a negative temperature difference of more than 100°C occurred. The top section was more than 100°C higher in temperature than the bottom. The run was shutdown immediately. The growth data showed a surprising result. Even though a large inverted temperature difference existed the seeds were still intact. An addition of 0.13 g of Cr_2O_3 was made to the nutrient. Also 2.2 g of aluminum metal was added to inhibit the silver attack[3] experienced in several previous runs. When the can was opened a considerable amount of hydrogen escaped. No silver attack was noted after the run.

Run 135, Vessel 7-3

Run 135 was made to repeat Run 134. The only change made was to reduce the amount of aluminum metal from 2.2 g to 0.1 g since so much hydrogen had escaped from Run 134. Operating conditions were maintained for 20 days. Data are recorded in Table XXIII. When the can was opened a slight amount of gas escaped. No traces of silver attack were found. Almost no liquid was left in the can. The can was full of a white, creamy substance with a greenish tint. Massive spontaneous nucleation occurred in the top section of the can. Growth on the seed crystals was of very poor quality. Most of the regrown ruby was milky in appearance. The nutrient was almost depleted and the upper seeds had dissolved to "feed" the spontaneously nucleated crystals in the top of the can.

TABLE XXI

Seed and Crystal Data, Run 133

Crystal Number	Weight (grams) Before	Weight (grams) After	Thickness (mils) Before	Thickness (mils) After	Growth Rate (mils/day)	Seed Type-Orientation *
133-1	25.1	88.7	80	260	6.0	H-c
133-2A	20.5	93.6	149	555	13.5	H-c
133-2B	22.1	107.6	160	614	15.1	H-c
133-3A	24.3	104.4	104	407	10.1	H-c
133-3B	11.1	80.0	68	392	10.8	MS-c
133-4	35.5	131.5	144	444	10.0	H-c
133-5A	13.5	34.5	100	266	5.5	H-c
133-5B	14.0	44.7	145	356	7.1	MS-u
133-6A	21.7	25.2	116	240	4.1	H-c
133-6B	15.1	39.7	102	294	6.4	H-c

* MS - Molten salt
H - Hydrothermal
c - Major crystal face; Dana, ref. 6
u - Orientation unknown

TABLE XXII

Seed and Crystal Data, Run 134

Crystal Number	Weight (grams) Before	Weight (grams) After	Thickness (mils) Before	Thickness (mils) After	Growth Rate (mils/day)	Seed Type-Orientation *
134-1	32.7	29.1	136	128	-	H-c
134-2	38.3	35.9	146	129	-	H-c
134-3	23.7	23.9	129	113	-	H-c
134-4	40.4	38.4	182	168	-	H-c
134-5	27.1	27.3	97	87	-	H-c
134-6	36.0	34.7	174	156	-	H-c

* H - Hydrothermal
c - Major crystal face; Dana, ref. 6

TABLE XXIII

Seed and Crystal Data, Run 135

Crystal Number	Weight (grams) Before	Weight (grams) After	Thickness (mils) Before	Thickness (mils) After	Growth Rate (mils/day)	Seed Type-Orientation
135-1	29.1	181.6	128	582	22.8	H-c
135-2	35.9	183.7	129	584	22.9	H-c
135-3	23.9	123.9	113	505	19.6	H-c
135-4	38.4	148.7	168	533	18.2	H-c
135-5	27.3	125.2	87	370	14.1	H-c
135-6	34.7	110.0	156	441	14.2	H-c

* H - Hydrothermal
c - Major crystal face; Dana, ref. 6

Hydrothermal Crystal Growth (Continued)

Run 136, Vessel 4-1

This run proceeded only four days due to a suspected leak. Low pressure forced termination of the run. The major objective was to test the effectiveness of a protective plating of gold. Gold plating of the vessel was ineffective. A detailed description of this run appears in Section 4.1.1 of this report. The seed and crystal data are listed in Table XXIV.

Run 137, Vessel 1-3

It has been shown[5] that an addition of lithium nitrite ($LiNO_2$) to the growth solution will significantly reduce the hydroxyl ion and water content of hydrothermally grown quartz. Infrared absorption measurements on hydrothermally grown ruby presented in Section 8.3.5 have revealed the presence of either hydroxyl ion or other hydrated species. Run 137 was made to test an addition of $LiNO_2$ to the ruby growth liquid to see if the hydroxyl ion or water content could be reduced. Eight grams of Li_2O_3 and 18.4 grams of KNO_2 were added to the K_2CO_3 solution. Operating conditions were maintained for 17 days. The seed data are presented in Table XXV.

Upon opening the can a considerable amount of gas was expelled. The liquid was a lemon-lime color and about one liter in volume. There was silver attack on the autoclave can liner. The lid of the silver can was coated with small silver crystals. The uppermost ruby crystal had small crystalline flecks of silver incorporated into it. The nutrient was not depleted. There was a complete lack of spontaneously nucleated ruby crystals in the system. The white coating normally present on the crystals was easily removed. Growth on the seeds looked quite good considering the high growth rate of 15 mils/day. Cracks were the main defects and were large in size and number. The chromium concentration appeared to be rather low. The crystals were veiled to about the same extent as found in other runs. However the ruby in between the veils was exceptionally clear compared to crystals from other runs. The most probable reason for the oxidizing conditions in the system was because of the nitrite ion which can act as either an oxidizing or reducing agent. In this case the nitrite ion acted as an oxidizing agent.[5]

Run 138, Vessel 7-3

The objective for Run 138 was a low temperature difference to produce a growth rate consistent with high quality. At the same time the amount of spontaneously nucleated ruby crystals may be reduced. A temperature difference of 8°C was used. Additions to the system were 0.13 g Cr_2O_3 and 0.1 g of aluminum metal. Operating conditions were maintained for 35 days. The seed data are given in Table XXVI. When the

TABLE XXIV

Seed and Crystal Data, Run 136

Crystal Number	Weight (grams) Before	After	Thickness (mils) Before	After	Growth Rate (mils/day)	Seed Type-Orientation *
136-1	2.8	3.0	193	200	-	H-c
136-2	4.3	3.8	116	115	-	H-c
136-3	1.3	1.0	32	31	-	MS-c
136-4	1.6	1.3	67	70	-	FF-n

* MS - Molten salt
FF - Flame fusion
H - Hydrothermal
n, c - Major crystal face; Dana, ref. 6

TABLE XXV

Seed and Crystal Data, Run 137

Crystal Number	Weight (grams) Before	Weight (grams) After	Thickness (mils) Before	Thickness (mils) After	Growth Rate (mils/day)	Seed Type-Orientation *
137-1	89.0	175.1	260	522	15.4	H-c
137-2	43.6	134.5	125	380	15.0	H-c
137-3	52.3	125.1	192	427	13.8	H-c
137-4	19.8	55.5	90	263	10.2	H-c
137-5	64.0	127.3	215	399	10.8	H-c
137-6	45.2	86.0	180	331	8.9	H-c

* H - Hydrothermal
c - Major crystal face; Dana, ref. 6

TABLE XXVI

Seed and Crystal Data, Run 138

Crystal Number	Weight (grams) Before	Weight (grams) After	Thickness (mils) Before	Thickness (mils) After	Growth Rate (mils/day)	Seed Type-Orientation *
138-1	82.7	75.9	265	262	-	MS-c
138-2	44.6	42.2	180	170	-	H-c
138-3	80.4	72.5	249	249	-	MS-c
138-4	28.9	26.5	156	149	-	H-c
138-5	39.9	37.5	293	287	-	H-c
138-6	47.5	42.1	231	229	-	MS-c

* MS - Molten salt
H - Hydrothermal
c - Major crystal face; Dana, ref. 6

system was opened it appeared to have been isothermal during the entire run. No significant growth was obtained. Only an equilibrium type growth occurred such as corner and chip filling in.

Run 139, Vessel 3-1

The objective of Run 139 were to repeat the conditions of Run 136 (gold-plated autoclave) and to determine the reason for the low pressure condition. The autoclave was plagued by seal leaks but the can did not leak. When the autoclave finally was able to hold pressure, the amount was still too low for the fill used when compared to the 3-inch diameter runs. The seed data are listed in Table XXVII. A small net growth occurred in the short operating time.

Run 140, Vessel 1-3

Run 140 was designed to measure the effects of the warm-up procedure on crystal quality. It may postulated that during a rapid warm-up, high temperature differences may be produced as a result of the rate of heating. As the system approaches the actual growth conditions it does so with a large temperature difference. This may cause a rapid and highly flawed growth even on a high quality seed. In an effort to eliminate this possible problem the system was heated to operating conditions with a controlled temperature difference of 20°C. Growth conditions were maintained for 22 days. The seed data are listed in Table XXVIII.

In order to control the ΔT an additional pair of chromel-alumel thermocouples were installed on the vessel at positions B and T (Fig. 18). These were connected in opposition to one another and the difference was fed to the input section of a Leeds & Northrup Speedomax H temperature controller. The controller output in turn was connected to the saturable reactor which fed power to the top two circular heater sections of the furnace. Since the top had to be colder than the bottom and the L&N controlled power only to the top section, the system was thermally unstable. When this condition was noted the L&N was switched to the bottom unit and the West Controller (which had been controlling the bottom) was switched to the top section. This seemed to remedy the situation. However, the next day an insensitivity developed in the L&N which could not be removed. This led to rather severe cycling. At this point No. 6 West Controller (temporarily unused) was substituted for the L&N. But the West sensitivity was too low for a differential thermocouple configuration so the bottom temperature was controlled directly. Somehow the program or cam drive switch was turned on and the temperature of the bottom rose to 556°C. This resulted in a maximum 68°C ΔT. The cam was reversed and the temperature was programmed back down to 509°C.

When the run was opened a fairly heavy deposit of spontaneously nucleated ruby crystals was found in the top of the can. However in con-

TABLE XXVII

Seed and Crystal Data, Run 139

Crystal Number	Weight (grams) Before	Weight (grams) After	Thickness (mils) Before	Thickness (mils) After	Growth Rate (mils/day)	Seed Type-Orientation *
139-1	3.0	3.0	200	199	-	H-c
139-2	3.8	4.0	114	114	-	H-c
139-3	2.3	2.4	200	199	-	H-c
139-4	2.2	2.4	93	95	-	H-c

* H - Hydrothermal
c - Major crystal face; Dana, ref. 6

TABLE XXVIII

Seed and Crystal Data, Run 140

Crystal Number	Weight (grams) Before	Weight (grams) After	Thickness (mils) Before	Thickness (mils) After	Growth Rate (mils/day)	Seed Type-Orientation *
140-1	57.8	208.5	164	509	15.7	H-c
140-2	55.8	148.1	261	566	13.9	H-c
140-3	46.3	157.6	137	441	13.8	H-c
140-4	21.8	77.9	124	391	11.3	H-c
140-5	37.6	124.5	124	373	11.[illegible]	H-c
140-6	40.2	89.2	244	470	10.6	H-c

* H - Hydrothermal
c - Major crystal face; Dana, ref. 6

Hydrothermal Crystal Growth (Continued)

sideration of the large temperature difference of 68°C, this deposit did not seem excessive. The liquid was clear and about one liter was collected. Spontaneously nucleated crystals appeared to "rain" down onto the baffle plate, and completely covered it except for the central hole. Small grains about one mm across were found. They were very loosely joined and formed a conical pile on the baffle plate. Overgrowth on the seed crystals was very poor and much flawing was present.

Run 141, Vessel 4-1

The main objective of Run 141 was a nutrient test which was discussed in the nutrient preparation, Section 5.1.5. A pressure of 28,500 psi was produced with an average temperature of only 457°C. This high pressure indicated that the previous one-inch diameter runs had leaked slightly even though no evidence could be found. Seed data are presented in Table XXIX.

Run 142, Vessel 3-1

Run 142 was likewise a nutrient test run. A pressure of 28,100 psi was produced at an average temperature of 449°C. This would seem to be consistent with Run 141 and further substantiate some sort of difficulty with previous one-inch diameter runs. A discussion of this run appears in the nutrient tests, Section 5.1.5. A net growth rate was measured and is given in Table XXX.

Run 143, Vessel 7-3

The objective of Run 143 was to repeat Run 138 with a larger temperature difference. A 17°C difference was chosen for Run 143 while Run 138 had a 12°C difference. Additions were 0.13 g Cr_2O_3 and 0.1 g of aluminum metal. Operating conditions were maintained for 30 days. The seed data are presented in Table XXXI. The growth was very poor with many cracks and veils. It was definitely the worst to this point considering the low average growth rate of about 8 mils per day. There was no noticeable loss of gas on opening the can. A small amount of Cr_2O_3 could be seen in the bottom of the vessel.

Run 144, Vessel 3-1

The main objective of Run 144 was to test nutrient. This run was discussed in the nutrient tests, Section 5.1.5. A high growth rate was measured (Table XXXII) but the quality was poor.

Run 145, Vessel 1-3

The objectives of Run 145 were to test the effect of Li_2CO_3 on crystal quality and to attempt a programmed warm-up. The warm-up

TABLE XXIX

Seed and Crystal Data, Run 141

Crystal Number	Weight (grams) Before	Weight (grams) After	Thickness (mils) Before	Thickness (mils) After	Growth Rate (mils/day)	Seed Type-Orientation *
141-1	1.7	2.2	125	145	-	MS-c
141-2	1.4	1.7	56	55	-	MS-c
141-3	1.5	1.7	73	72	-	MS-c
141-4	1.9	2.2	68	68	-	MS-c

*MS - Molten salt
c - Major crystal face; Dana, ref. 6

TABLE XXX

Seed and Crystal Data, Run 142

Crystal Number	Weight (grams) Before	Weight (grams) After	Thickness (mils) Before	Thickness (mils) After	Growth Rate (mils/day)	Seed Type-Orientation *
142-1	1.3	3.2	60	123	9.0	MS-c
142-2	1.8	3.7	66	117	7.3	MS-c
142-3	1.8	3.3	125	125	-	MS-c
142-4	1.6	2.4	123	136	1.9	MS-c

* MS - Molten salt
c - Major crystal face; Dana, ref. 6

TABLE XXXI

Seed and Crystal Data, Run 143

Crystal Number	Weight (grams) Before	Weight (grams) After	Thickness (mils) Before	Thickness (mils) After	Growth Rate (mils/day)	Seed Type-Orientation *
143-1	57.0	178.7	157	456	10.0	H-c
143-2A	12.1	42.2	122	411	9.6	H-c
143-2B	12.1	48.1	98	367	9.0	H-c
143-3	3.2	15.7	118 133	246 321	4.3 6.3	FF-u
143-4	51.4	133.9	154	380	7.5	H-c
143-5	29.5	77.6	191	381	6.3	MS-c
143-6	54.4	116.7	156	326	5.7	H-c

* MS - Molten
FF - Flame fusion
H - Hydrothermal
c - Major crystal face; Dana, ref. 6
u - Orientation unknown

TABLE XXXII

Seed and Crystal Data, Run 144

Crystal Number	Weight (grams) Before	Weight (grams) After	Thickness (mils) Before	Thickness (mils) After	Growth Rate (mils/day)	Seed Type-Orientation *
144-1	1.3	5.4	58	189	18.7	MS-c
144-2	1.5	5.7	71	186	16.4	MS-c
144-3	1.9	5.5	75	180	15.0	MS-c
144-4	1.1	1.1	71	80	1.3	MS-c

* MS - Molten salt
c - Major crystal face; Dana, ref. 6

was designed to make the transition from room temperature to operating conditions as beneficial as possible. The vessel was heated as quickly as possible to 425°C with a temperature difference of only 10°C. The vessel was then held at these conditions for 24 hours. It was felt that the warm-up with only 10°C ΔT would dissolve some of the seed surface which could then "heal" during the 24-hour period. After the hold period elapsed, the warm-up was continued by heating the growth section slowly to 485°C over a 24-hour period. The 10°C ΔT was maintained during the warm-up. Finally the ΔT was increased to 20°C by cooling the growth section at 1°C per hour. The growth obtained was very poor. The Li_2CO_3 certainly made a negative contribution. A good growth rate was maintained (Table XXXIII) which was uniform for all seeds. From this standpoint the programmed warm-up was partially successful.

Run 147, Vessel 7-3

The objectives of Run 147 were to improve crystal quality by a programmed warm-up which did not use any metallic aluminum addition. Furthermore the L&N temperature controller used with Run 140 was arranged to control the ΔT at 24°C throughout the warm-up and operating times. Chromium oxide in the amount of 0.13 g was added.

The insensitivity present during Run 140 was actually caused by 60 cycle a.c. on the autoclave body. This 60 cycle "noise" was damped out by the galvanometer movement in the West Controllers but the L&N is an electronic device which cannot function properly in the presence of a large a.c. signal. The trouble was corrected by properly grounding the autoclave and shorting out the a.c. signal.

The growth rate was quite high and averaged 18.8 mils per day (Table XXXIV). All the nutrient was transported so the growth rates must be considered a minimum. The bottom crystals had dissolved to "free" the top ones. No gas evolution was noted when the can was opened. The quality of the crystals was good considering the high growth rate. There was severe spontaneous nucleation on the underside of the lid and on the upper 2 to 3 inches on the can wall. A small amount of silver attack was evident.

Run 148, Vessel 1-3

The objective of Run 148 was to reproduce Run 147 using a lower temperature difference. A temperature difference of 20°C was used. The growth period was 19 days. The nutrient was almost depleted and just 43 grams remained. The calculated average growth rate was 23.7 mils per day, (Table XXXV). The actual growth rate was probably somewhat higher since the surface area of the nutrient was small enough to limit the growth rate. The growth rate of Run 147 could well have been near 30 mils per day. It was not know when the nutrient was depleted sufficiently to affect the growth rate. Run 148 had significantly less spontaneously nucleated ruby crystals than did Run 147. This indicated that the actual temperature difference was actually lower for Run 148. The quality was good except for numerous veils.

TABLE XXXIII

Seed and Crystal Data, Run 145

Crystal Number	Weight (grams) Before	Weight (grams) After	Thickness (mils) Before	Thickness (mils) After	Growth Rate (mils/day)	Seed Type-Orientation *
145-1	41.5	146.0	167	521	10.7	H-c
145-2	30.2	133.6	112	494	11.7	H-c
145-3	47.7	167.9	221	603	11.6	MS-c
145-4	53.7	173.5	158	510	10.7	H-c
145-5	54.2	171.4	159	491	10.1	H-c
145-6	42.0	126.1	188	511	9.8	H-c

* H - Hydrothermal
MS - Molten salt
c - Major crystal face; Dana, ref. 6

TABLE XXXIV

Seed and Crystal Data, Run 147

Crystal Number	Weight (grams) Before	Weight (grams) After	Thickness (mils) Before	Thickness (mils) After	Growth Rate (mils/day)	Seed Type-Orientation *
147-1	117.0	316.5	325	735	20.5	H-c
147-2	26.8	113.4	149	527	18.9	H-c
147-3A	4.7	47.2	72	480	20.4	MS-c
147-3B	6.6	45.2	115	514	20.0	H-c
147-4	72.7	262.1	251	624	18.7	H-c
147-5	14.6	110.5	60	390	16.5	MS-c
147-6A	4.0	31.1	65	398	17.0	MS-c
147-6B	10.4	37.4	132	497	18.3	H-c

* H - Hydrothermal
MS - Molten salt
c - Major crystal face; Dana, ref. 6

TABLE XXXV

Seed and Crystal Data, Run 148

Crystal Number	Weight (grams) Before	Weight (grams) After	Thickness (mils) Before	Thickness (mils) After	Growth Rate (mils/day)	Seed Type-Orientation *
148-1	42.4	213.5	170	678	26.8	H-c
148-2A	8.9	86.9	88	556	24.6	MS-c
148-2B	1.1	12.5	50	-	-	CR-u
148-2C	6.1	92.4	54	545	25.8	MS-c
148-3A	6.4	56.1	73	467	20.7	H-c
148-3B	7.4	90.8	84	567	25.4	MS-c
148-4A	16.7	169.5	71	563	25.0	MS-c
148-4B	0.8	5.9	49	-	-	CR-u
148-5	13.2	148.6	93	542	23.6	MS-c
148-6A	7.5	70.3	67	474	21.4	MS-c
148-6B	9.3	40.0	128	490	19.1	H-c

* H - Hydrothermal
MS - Molten salt
CR - Czochralski Ruby Seed
c - Major crystal face; Dana, ref. 6
u - Orientation unknown

Hydrothermal Crystal Growth (Continued)

Run 149, Vessel 9-1,5

The objective of Run 149 was to test the relationship between the veiling problem and the Cr_2O_3 in the system. Molten salt sapphire seed plates were used as seeds and scrap flame fusion sapphire was used for the nutrient. The conditions were similar to those used for the recent 3-inch diameter Runs 145, 147, and 148. The growth time was 12 days. Seed data are given in Table XXXVI.

Spontaneous nucleation was present on the upper ladder and can wall but very little occurred on the under side of the cover. Moderate silver attack was noted. The growth rate averaged about 18 mils per day. The quality of the growth was good but veils were still present. The absence of chromium in the system did not seem to have any effect on veiling.

Run 150, Vessel 1-3

The objective for Run 150 was a lower gradient than that utilized in Run 148. The measured gradient was approximately 10°C. A programmed warm-up with a 5°C ΔT was used. An addition of 0.14 g Cr_2O_3 was made. The molality was increased from 1.75 in the previous runs to 2 molal for Run 150.

The internal fill was also decreased so that a higher temperature could be used. It was felt that a higher growth temperature would yield a larger absolute solubility and enhance crystal growth. The growth period extended 34 days. No aluminum metal was added.

The can was severely crushed during the run. A crack could be seen in the bottom weld of the can. The external fill was found to be basic and thus some leakage had occurred from the can. The external fill of 190 c.c. was definitely too large for the temperature imposed during operation.

Silver attack was absent. Very heavy spontaneous nucleation was found in the top of the can. A deposit approximately one-inch thick was attached to the underside of the cover. The quality of the growth was extremely poor considering the average growth rate was only 2.9 mils per day (Table XXXVII). Few conclusions were drawn from this run since the leak could very well have "breathed" and pulled impurities into the can from the autoclave.

Run 151, Vessel 2-3

The purpose of Run 151 was to investigate the use of more concentrated K_2CO_3 solutions. The solvent concentration was increased from 1.75 m to 4 m. Growth temperature was 540°C. The seed and crystal data are given in Table XXXVIII.

TABLE XXXVI

Seed and Crystal Data, Run 149

Crystal Number	Weight (grams) Before	Weight (grams) After	Thickness (mils) Before	Thickness (mils) After	Growth Rate (mils/day)	Seed Type-Orientation *
149-1	2.9	27.0	46	305	21.5	MS-c
149-2	7.1	34.1	98	327	19.0	MS-c
149-3	2.9	16.4	46	224	14.8	MS-c
149-4	2.2	14.4	48	271	18.6	MS-c
149-5	2.4	15.1	42	221	14.9	MS-c

* MS - Molten salt
c - Major crystal face; Dana, ref. 6

TABLE XXXVII

Seed and Crystal Data, Run 150

Crystal Number	Weight (grams) Before	Weight (grams) After	Thickness (mils) Before	Thickness (mils) After	Growth Rate (mils/day)	Seed Type-Orientation *
150-1	39.5	226.3	168	538	-	FF-a
150-2	4.6	35.2	34	188	4.5	MS-c
150-3	18.1	50.0	127	260	3.9	H-c
150-4	30.6	55.1	155	224	2.0	H-c
150-5A	11.9	20.3	136	201	1.9	H-c
150-5B	10.1	16.2	143	172	0.8	H-c
150-6A	11.9	21.7	153	183	0.9	H-c
150-6B	6.2	38.8	119	617	-	H-d

* FF - Flame fusion
MS - Molten salt
H - Hydrothermal
a, c, d - Major crystal face; Dana, ref. 6

TABLE XXXVIII

Seed and Crystal Data, Run 151

Crystal Number	Weight (grams) Before	Weight (grams) After	Thickness (mils) Before	Thickness (mils) After	Growth Rate (mils/day)	Seed Type-Orientation *
151-1	65.9	77.0	204	295	-	FF-a
151-2A	27.1	14.7	229	234	0.26	MS-c
151-2B	5.5	3.8	65	63	-	MS-c
151-3	16.1	11.4	115	94	-	H-c
151-4	26.0	11.4	124	56	-	H-c
151-5A	5.8	5.7	106	131	1.32	MS-c
151-5B	3.9	3.3	90	107	0.90	MS-c
151-6A	5.6	2.1	120	56	-	H-c
151-6B	5.4	-	126	-	-	H-d

* FF - Flame fusion
MS - Molten salt
H - Hydrothermal
a, c, d - Major crystal face; Dana, ref. 6

Hydrothermal Crystal Growth (Continued)

Very little growth occurred. The average growth rate was 0.83 mils per day. Only the top seed had any significant growth. The bottom seed had dissolved completely and the remaining seeds all lost weight. Slight silver attack was noted and also the extent of the spontaneously nucleated ruby crystals was slight. Only 180 g of nutrient had dissolved out of 1300 g initially charged.

Run 152, Vessel 9-1,5

Run 152 was made using KOH as the solvent. Six molal KOH was used at an internal fill of 65%. An addition of 0.12 g of aluminum metal was added to the nutrient. The run progressed for 5 days. No growth was obtained. The seed data are given in Table XXXIX.

Run 153, Vessel 9-1,5

Two molal KOH was used as the solvent in Run 153. Operating conditions were maintained for 4 days. The internal fill was raised to 68%. An average temperature of 525°C and a pressure of 23,900 psi were recorded. Again no growth occurred. The seed data are given in Table XL.

7.3 Platinum Capsule Investigation

The major quality problem connected with the hydrothermal growth of ruby crystals was that of veiling and cracking. An investigation was made using an HR-1B hydrothermal unit (Fig. 3) manufactured by Tem-Pres Research, Inc., State College, Pa. The unit accepts capsules up to about one-quarter inch in dameter. The capsule is fabricated from seamless platinum tubing with a 0.005" wall thickness. A seed is suspended in the solution by a platinum wire which is fused into the top weld. This technique was described in detail in the final report[1] of Phase I. All runs were made at temperatures of 550°C, 600°C or 700°C. One run was made at 17,000 psi while the rest were at 25,000 psi or 30,000 psi. Temperature gradients were not measured. However, previous work has shown them to be around 50°C.

Table XLI contains the data pertinent to the capsule runs. Two problems related to the solvent were investigated, 1) effects of oxidizing or reducing conditions, and 2) the possibility of using a solvent other than K_2CO_3.

In several 3" diameter runs aluminum metal had been added to the contents to eliminate transport of the silver can. Generally the crystals grown were of poor quality when aluminum metal was added to the system. There may have been a correlation between the oxidizing or reducing conditions and crystal quality. Three runs were made with aluminum metal additions. Run 169 used one gram of crushed flame fusion ruby as nutrient. Aluminum wire in the amount of 0.25 mg was added to

TABLE XXXIX

Seed and Crystal Data, Run 152

Crystal Number	Weight (grams) Before	Weight (grams) After	Thickness (mils) Before	Thickness (mils) After	Growth Rate (mils/day)	Seed Type-Orientation *
152-1	3.3	-	107	-	-	H-c
152-2	2.2	-	40	-	-	MS-c
152-3	5.7	-	131	-	-	H-c
152-4	1.9	-	35	-	-	MS-c
152-5	1.6	-	40	-	-	MS-c

* H - Hydrothermal
MS - Molten salt
c - Major crystal face; Dana, ref. 6

TABLE XL

Seed and Crystal Data, Run 153

Crystal Number	Weight (grams) Before	Weight (grams) After	Thickness (mils) Before	Thickness (mils) After	Growth Rate (mils/day)	Seed Type-Orientation *
153-1	8.0	7.5	181	177	-	H-c
153-2	5.8	5.4	93	91	-	H-c
153-3	8.8	8.2	178	172	-	H-c
153-4	5.4	5.1	94	94	-	H-c
153-5	8.1	7.0	122	111	-	H-u

* H - Hydrothermal
c - Major crystal face; Dana, ref. 6
u - Orientation unknown

TABLE XLI

Data for Platinum Capsule Runs

Run No.	Pressure 1000 psi	Bottom Temp. (°C)	Run Duration (days)	Concentration and Solvent	Additive	Seed Weight (grams) Before	Seed Weight (grams) After
166	25	600	5	2.5 m K_2CO_3	H_2O_2	.376	1.004
169	25	600	4	2.5 m K_2CO_3	Al	.404	1.109
173	25	600	3	2.0 m K_2CO_3	Li_2CO_3	.376	1.021
174	25	600	3	2.0 m K_2CO_3	Al	.401	1.033
176	30	600	2	0.5 NaCl	-	.129	.129
182	30	600	3	2.0 m K_2CO_3	Al	.128	.531
186	25	600	3	1N H_2SO_4	-	.099	.099
194	25	600	3	5 m $CaCl_2$	-	.189	.196
197	25	600	2	0.2 wt.% H_3BO_3	-	.124	.124

TABLE XLI (Cont'd.)

Data for Platinum Capsule Runs

Run No.	Pressure 1000 psi	Bottom Temp. (°C)	Run Duration (days)	Concentration and Solvent	Additive	Seed Weight (grams) Before	Seed Weight (grams) After
198	25	600	2	H_2CO_3	-	.167	.167
201	25	600	2	0.25 wt.% AlF_3	-	.108	.100
204	17	550	2	6 m KOH	-	.155	.128
205	25	550	2	50% 6 m KOH	50% 6 m K_2CO_3	.143	.149
206	25	550	7	90% 6 m K_2CO_3	10% 6 m KOH	.106	.103
207	25	550	7	10 m H_2SO_4	-	.117	-
208	25	550	7	10 m H_2SO_4	-	.140	.105
209	25	550	7	10 m H_3PO_4	-	.125	.128
211	25	550	4	95% 6 m K_2CO_3	5% 6 m KOH	.133	.390

Hydrothermal Crystal Growth (Continued)

the capsule. The capsule was run for four days. All the nutrient was transported. Heavy growth was found on the seed and it was of good quality. However some veils could be seen. Run 174 contained 0.5 mg of aluminum wire. Growth was fair to good with large crack type flaws. Run 182 contained 1.0 mg of aluminum wire. Growth was again fair to good but many large crack type flaws were present. In addition a violet layer could be seen next to the seed where growth started. There was a trend toward more flaws as more aluminum metal was added.

Since the use of a reducing agent produced poor growth it was postulated that the use of oxidizing conditions may contribute to better growth. Run 166 used an H_2O_2 addition. It was found difficult to seal tubes containing H_2O_2 and only one successful run was made. The H_2O_2 generated pressure in the capsule preventing a tight weld in the closure. Run 166 had a large amount of growth of good quality. The crystal had flaws but they were relatively few and small. This result was sufficiently encouraging to warrant further investigation in the use of oxidizing agents.

The second area of investigation concerned the use of solvents other than K_2CO_3. Eight different solvents were tried. Run 176 used sodium chloride, Runs 186, 207, and 208 used sulphuric acid, Run 194 used calcium chloride, Run 197 used boric acid, Run 198 used carbonic acid, Run 201 used aluminum fluoride, Run 204 used potassium hydroxide, Run 209 used phosphoric acid. None of the above solvents showed very promising results.

Mixtures of K_2CO_3 and KOH were also tried. Run 205 was made with 50% 6 m KOH and 50% 6 m K_2CO_3. Run 206 was made with 90% 6 m K_2CO_3 and 10% 6 m KOH. Neither run showed any evidence of growth. Run 211 was 95% 6 m K_2CO_3 and 5% 6 m KOH. In this run the seed just about tripled in weight. The growth was of very good quality. There were still veils present. As an additive in small amounts KOH showed some promise.

8.0 CRYSTAL QUALITY

8.1 Introduction

8.1.1 Ruby Crystals

Although the growth of large single crystals of ruby is highly desirable, many factors other than size have gained in relative importance. Among these are optical clarity, homogenous doping at specified levels, absence of large angle grain boundaries and strain. Most of these factors have been the subject of individual studies relating to the performance of the crystals as a laser.[7,8] Unfortunately, the existing state of crystal growth has limited the source of the crystals to those grown only by the flame fusion method. As a result of the nature of the growth process, it has been well verified that flame fusion ruby crystals are poor in crystallographic quality.[9]

8.1.2 Growth Methods

It is interesting that ruby is one of the few crystals that has been grown by alternate techniques. Thus far the Verneuil, flux,[10] Czochralski,[11] and hydrothermal[12] methods have all been reported to give single crystals of sufficient size for many applications. Some preliminary work in a few laboratories has indicated that the crystal quality can be very high.[13] Programs have been initiated to obtain large, high quality, uniformly doped crystals by flame fusion, Czochralski, and hydrothermal methods in order to (1) study and compare crystals grown by the various methods, and (2) examine in more detail flux and hydrothermal rubies for defects incurred during growth. From the data obtained one may then understand the seed-crystal boundary requirements and thus be able to modify the crystal growth parameter to optimize the boundary condition and propagate high quality growth.

8.1.3 Crystal Seed Source

The growth of hydrothermal ruby is experimentally dependent on the availability of seed material. At the present stage of development, flux grown ruby has been the major source of seeds. Until larger and more perfect hydrothermal crystals are consistently obtained, the flux ruby will continue to serve as a high quality seed. This has been very fortunate because it is now known that flux ruby has very few dislocations, grain boundaries, and low strain. All of this information has been confirmed by means of Lang x-ray topographic studies on flux ruby.

8.1.4 X-Ray Examination

It is well known that in hydrothermal growth or in any epitaxially grown material, the inherent defects of the substrate can be propagated to the overgrowth. In order to assess the quality of

Crystal Quality (Continued)

hydrothermal ruby, it is quite essential to separate if possible defects caused by the seed and those caused strictly by the hydrothermal growth variables. Therefore, the x-ray studies have been directed along the following plan. First, the flux ruby has been studied to provide a comprehensive survey of its prominent defects. Second, flux grown sapphire is examined to attempt to separate defects caused solely by the presence of Cr^{+3}. A further purpose behind the sapphire work is the fact that in hydrothermal growth of ruby, the initial growth is frequently depleted of any Cr^{+3}. The large gradient of Cr^{+3} may sometimes be sufficient to initiate strains and cracking. Third, the program involves a more thorough review of the hydrothermal crystals themselves. Part of this has been performed and part reserved for the future when larger crystals are available. The latter are necessary in order to provide samples of up to 1-cm length in any direction. A good three-dimensional study of defects will then be possible.

8.1.5 Line Widths

In addition to x-ray topographic methods for determining crystal perfection, x-ray line widths obtained from a double crystal spectrometer are a powerful and reliable procedure. The two techniques are complementary because Lang topography reveals internal imperfections not readily apparent from a line width measurement. Likewise, some crystals with imperfections could conceivably give a uniform intensity in transmission and only a line width study could assess the true perfection. The fact that ruby can be grown by several methods has prompted some recent studies on x-ray line widths. One result[14] for Czochralski ruby was mentioned in early 1965. Birks, Hurley, and Sweeney[15] published a more detailed paper on Vernueil, flux, and Czochralski ruby. During Phase II some rather large single crystals of ruby have been grown by the hydrothermal method in Airtron's laboratories. X-ray topographic studies have shown that such crystals are somewhat strained but no effort was made to determine the overall perfection. In order to evaluate properly hydrothermal ruby, double crystal x-ray measurements were made on some of our best samples. At the same time, flux grown ruby and sapphire were examined because it was believed that their perfection was higher than indicated in Birks report.[15] The growth of hydrothermal ruby has also utilized flux ruby as seed material. Therefore, the relative perfection is of interest to (1) verify whether defects have propagated from the seed and (2) to determine how certain growth variables may change perfection. To the present time no other reports on hydrothermal ruby have appeared in the literature.

8.2 Experimental

8.2.1 Crystal Sampling and X-ray Technique

The single crystal flux grown rubies for this program

Crystal Quality (Continued)

were obtained from melts composed of PbF_2. The thin crystals were examined with their natural faces intact. These large area faces were of the {0001} type. Flux grown rubies up to a size of 3 x 2 x 1 cm were also obtained. These crystals were sectioned with a diamond wheel and polished with successively finer diamond grits. The final mechanical polish was performed with a 1 μ or 1/4 μ diamond abrasive. Hydrothermally grown ruby crystals were obtained from growth on flux ruby seeds. These crystals were also cut and polished with diamond tools and abrasives. The source of the Czochralski ruby was the Linde Company. It was obtained as a 90° rod. All crystals were oriented by optical and x-ray back reflection methods. The surface condition of the cut and polished crystals was quite sensitive to technique. All polishing scratches had to be removed by fine diamond pastes prior to chemical polishing. Final chemical polishing was performed with a PbF_2-PbO eutectic mixture at 550-650°C to give a defect-free surface.

All crystals were examined with a Rigaku-Denki Lang camera using MoK_α radiation. A Dunlee commercial x-ray tube served as the source. The focal spot was viewed "end on". The source to crystal distance was increased to 50-60 cm by means of a brass tube. The horizontal divergence was fixed at 90 seconds and the vertical at 1° by means of fine slits. The resulting horizontal and vertical resolutions were 1 μ and 8 μ respectively. Preliminary exposures were made on Kodak No Screen X-ray Film. All the final topographs in this work were recorded on Kodak Type M X-ray Films. Total exposure times ranged from 2 to 10 hours depending on scan length, thickness, and orientation.

The double crystal spectrometer utilized in the program was assembled by combining a standard Picker x-ray diffractometer with a Rigaku Denki Lang Camera. The first crystal was a nearly perfect silicon crystal provided by the Dow Chemical Company. The dislocation density by etch pit count was no more than a few hundred per cm^2. The crystal was cut and polished and finally at least 0.1 mm of the surface was removed by chemical means. The major face was (111). The second crystal was always the sample crystal and was mounted on a goniometer head contained on the Lang camera. The latter instrument was capable of measuring directly to 1 second of arc. The spectrometer was always operated in the parallel arrangement[16] and utilized the (333) reflection from silicon and the (00·12) reflection from ruby and sapphire. The latter was chosen because the growth morphology provided a large area (00·1) face on both flux and hydrothermal crystals. This natural face was highly flat and free from any surface damage. The crystals were not polished or etched because surface damage is rather difficult to remove.

The radiation used was CuK_α. Soller slits and plain slits were incorporated to limit the horizontal and vertical divergence to 1° and 2° respectively. The axes of rotation of both crystals were vertical. Two slits were used in front of the second crystal at differ-

Crystal Quality (Continued)

ent times. In one case a 1 mm x 1 mm aperture was employed and in the other a 1 mm x 0.2 mm slit. The distance between crystals was approximately 40 cm. Radiation was detected with a scintillation counter incorporating a pulse height analyzer. The rocking curve was obtained by rotating crystal 2 through the Bragg angle. The intensity was recorded at each two seconds of arc after manually turning the crystal. The resulting data were plotted for each crystal and the width at half maximum intensity determined. These widths were readily reproducible to a few tenths of a second.

8.3 Results and Discussion

8.3.1 Flux Grown Ruby Topography

Some confusion has existed between the designation of planes in the morphological and true structural unit cell of α-Al_2O_3. Kronberg[17] has presented a valuable description of the proper relationships. In our investigations we have adhered to the use of the hexagonal x-ray structural unit cell. The d spacings and indices have been fully tabulated for this unit cell.[18]

Enough evidence has been published on flame fusion rubies to show that typical dislocation densities are nearly always in the range of 10^5-$10^6/cm^2$. Grain boundaries of 1-2° are present and the crystals are often severely strained. The fruitful application of the Lang method[19] requires a crystal of much lower dislocation density in order to prevent severe overlap of defects. Small rubies of high quality can be prepared by means of the flux growth method. Etching studies have verified that ruby crystals with dislocation densities as low as $10^2/cm^2$ could be prepared.[20] For this reason and because flux grown rubies are used as seeds for hydrothermal growth, preliminary topographic work was restricted to flux grown plates.

The first crystal examined was a flux grown ruby plate with (0001) faces. The area of the face was about 1.0 x 1.5 cm and the thickness was 0.22 mm. Preliminary microscopic examination showed very few defects on the surface. One tiny particle of ruby adhered to the surface of one face. This was probably caused by sudden nucleation and growth during the cooling cycle. No sign of PbF_2 inclusions was visible. This was confirmed by a later x-ray spectographic analysis which showed less than 0.25% Pb in the entire plate. The use of crossed polarizers in a view parallel to the optic axis showed no evidence of strain or grain misorientation. The crystal was thoroughly cleaned in HNO_3 before all tests and x-ray topographs were taken with the (0001) natural faces intact. Figure 25 is a photograph of the crystal and shows the orientation of the a axis. The c axis or [0001] is perpendicular to the plane of the figure. The bounding faces are planes of the type $(01\bar{1}2)$, $(11\bar{2}0)$ and $(10\bar{1}4)$. Figure 26 is the x-ray topograph of the crystal taken from the $(11\bar{2}0)$ planes which were vertical during the exposure. Some of the

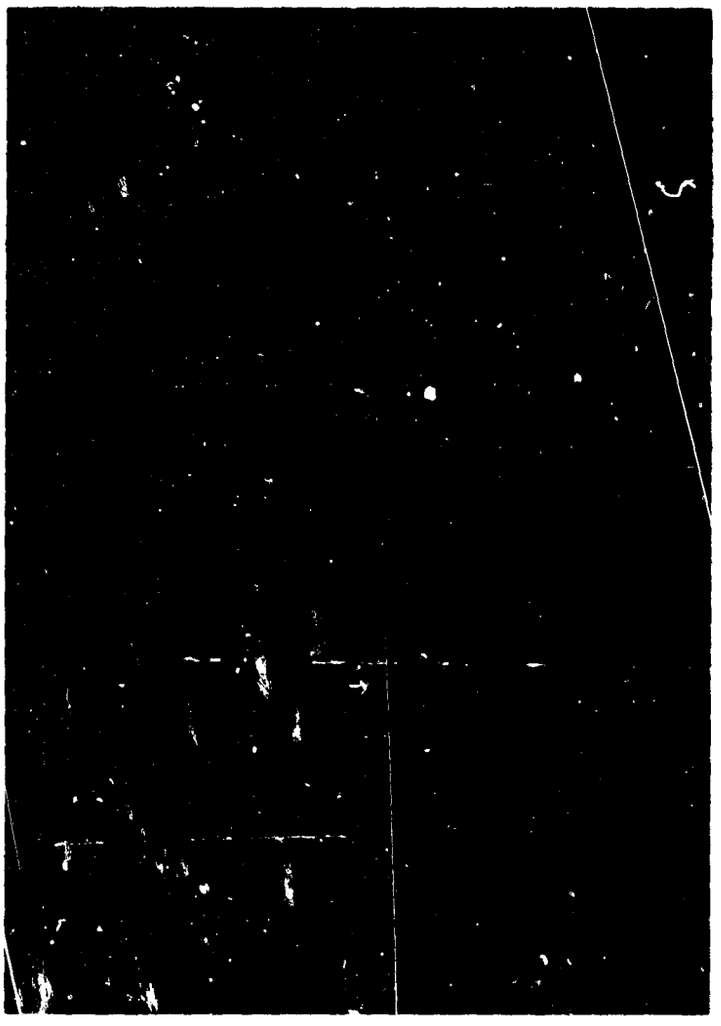

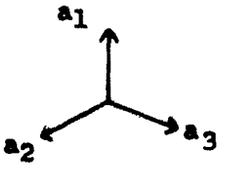

Figure 25. Photograph of Flux Ruby Plate, Orientation of a Axes Shown Above, 7 x

Figure 26. X-ray Topograph of Flux Ruby Plate, Diffraction from (1120), 7 x

Crystal Quality (Continued)

tiny defects could be attributed to surface marks but others are apparently dislocations running from the front surface to the back. It is interesting that at the exact point of attachment of the small crystallite, there is only a slight defect on the topograph and it is similar to other surface damage. A possible small angle grain boundary runs vertically from the bottom of the photograph to join a boundary along the a_1 axis. The included angle of the two is very close to 150°. Similar boundaries run along the top of the photograph and upper right-hand corner with no evident relation to the crystal axes. Within each area there is a profuse band structure. The bands in the left grain are parallel to the a_1 axis while those in the center grain all run perpendicular to the a_1 axis. The lighter areas of the topograph are from portions of the crystal which were not in diffracting position during the exposure.

In order to determine whether a strain was introduced from the mounting procedure, the crystal was removed and remounted in an entirely different manner. At the same time the crystal was rotated 30° in a clockwise direction from Figure 26 and the topograph was taken from the (0330) planes. Figure 27 gives the results and now shows the band structure of the central grain of Figure 26 to be horizontal. A portion of the same grain boundary is also in view. The scan length of the crystal was limited to about 2 mm for Figure 27. The remainder of the crystal was out of diffracting position. Further rotations and remounting of the crystals were made at 60°, 90°, and 120° in a clockwise direction to Figure 26. Topographs were recorded from (11$\bar{2}$0) and (03$\bar{3}$0) planes alternately. In all cases the same general features of the banding were obtained. For (11$\bar{2}$0) planes the complete area of the crystal could be recorded on the topographs. For (03$\bar{3}$0) planes only only 2 mm of the crystal could be scanned under the same experimental conditions. This may arise from a slight bend about the a axis plus the differences in Bragg angles for (11$\bar{2}$0) and (03$\bar{3}$0) planes.

A compilation of the principal dislocation systems in corundum has been given by Scheuplein and Gibbs.[21] Under the conditions of flux growth the temperatures do not exceed 1200-1300°C. The most likely dislocation system is basal slip with (0001) as the slip plane and Burgers vector equal to 1/3 [11$\bar{2}$0]. The prismatic slip system is apparently only activated at temperatures greater than 1600°C. A special study of flux grown rubies has been made by Janowski, Stofel, and Chase.[22] They gave etching evidence of the effects of entrapped flux and twin boundaries. The latter are 180° rotation type twins about [0001]. The most frequent composition plane is (11$\bar{2}$0) with (10$\bar{1}$0) as an alternative. From the preceeding data we can arrive at a tentative explanation of the banding observed on Figure 26 and Figure 27. The general absence of birefringence suggests that large strain fields and their association with twin boundaries are unlikely. Back reflection x-ray photographs also provide no evidence of extensive twin boundaries. The fact that the bands are parallel to the natural growth

Figure 27. X-ray Topograph of Ruby Plate, Diffraction from (0330), Crystal Rotated 30° Clockwise from Fig. 26, 7 x

Crystal Quality (Continued)

faces is possibly because of impurity precipitation and microstrain. The likely impurities are either PbF_2 flux or Cr_2O_3 although both must be on a scale not readily observable at 250 x microscopically. The resultant strains must also be slight and not evident with crossed polarizers. The more powerful x-ray method readily records such defects.

In order to gain more information of the cause of the banding, the crystal plate was annealed in a platinum container for 70 hours at 1400°C. At this point the container was removed from the furnace and allowed to cool to room temperature. A new x-ray topograph (Fig. 28) was then taken utilizing diffraction from $(11\bar{2}0)$ planes. The orientation of the crystal was exactly the same as Figure 26. The striking disappearance of all banding is immediately noticeable. In place of the bands a fine particle structure covers the entire crystal. A faint but noticeable outline of major grain boundaries has persisted. Many of the particles appear to be dislocation lines with their directions parallel to the $(11\bar{2}0)$ planes. Figure 29 is a topograph of the same crystal rotated 30° clockwise with diffraction from $(03\bar{3}0)$ planes. The same defects are present and again the majority run in a direction parallel to the diffracting planes. In both x-ray topographs there is similarity to effects noticed microscopically on decorated crystals. Dislocations in Al_2O_3 have been decorated by means of ZrO_2[23] and many straight segments of dislocation lines have been found parallel to $\langle 11\bar{2}0 \rangle$. There is no reason why PbF_2 or PbO could not act in a similar manner. Ultramicroscopic techniques were not used on the annealed crystal to confirm this reasoning.

The next crystal to be examined was a cut from a large flux grown ruby. This crystal had the plate morphology but measured about 5 mm along [0001]. The $(01\bar{1}2)$ and $(10\bar{1}4)$ planes were highly developed. A cut was made parallel to [0001] and perpendicular to $[2\bar{1}\bar{3}0]$. The large faces were planes of $\{11\bar{2}0\}$ type. The thickness of the crystal after mechanical and chemical polishing was 0.4 mm. A photograph of the crystal is given in Figure 30. Figure 31 shows the x-ray topograph of the crystal taken from $(03\bar{3}0)$ planes which are now vertical. One again notices the banding with the lines almost exactly parallel to $(01\bar{1}2)$ planes. At the bottom of the topograph they intersect the (0001) surface but near the top they meet some dislocations or boundaries which run horizontally across the crystal. The crystal was now rotated in its own plane to get diffraction from $(01\bar{1}2)$ planes. The resulting topograph is given in Figure 32 where the $(01\bar{1}2)$ planes are oriented vertically. The same banding appears with lines now in a vertical direction. However a new feature is prominent across the top right area of the topograph. These are a few wide Pendellosung fringes which show a slight bending in the neighborhood of intersecting line defects. The fringes arose from a natural beveling of the crystal in that region during the chemical polishing. The angle of the bevel was approximately 30°. Figure 33 is a topograph of the same crystal after a net counter-clockwise rotation of about 92° to bring the $(10\bar{1}4)$ planes into diffracting position. The latter

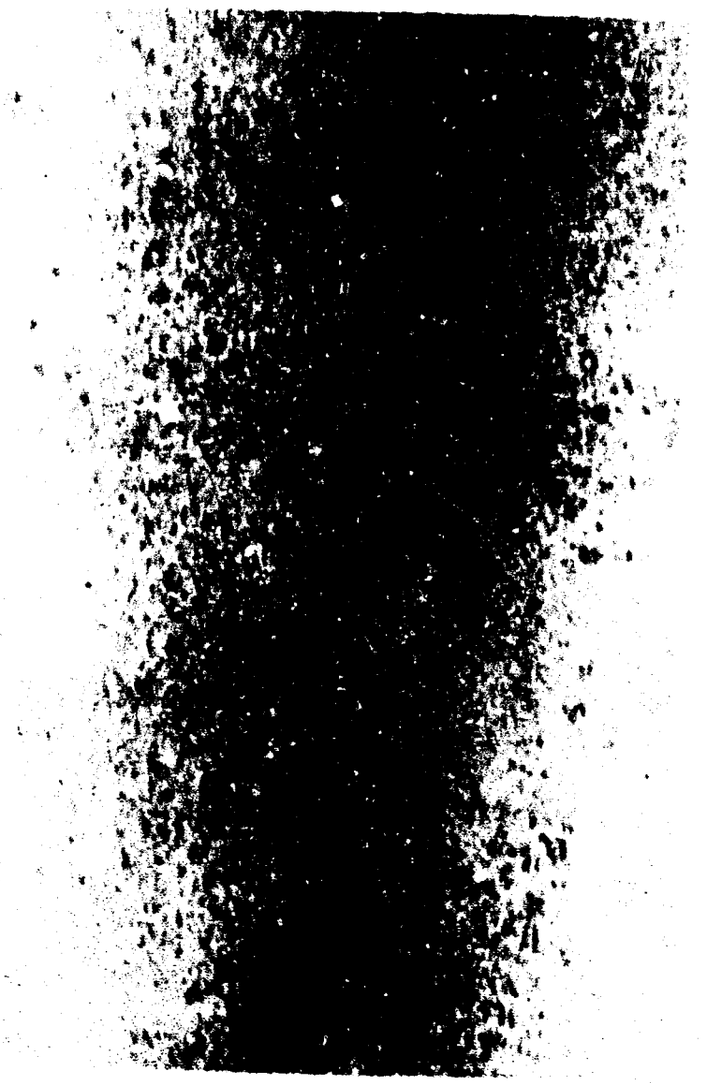

Figure 28. X-ray Topograph of Annealed Ruby Plate Diffraction from (1120), Same Orientation as Fig. 26. Compare. 25 x

Figure 29. X-ray Topograph of Annealed Ruby Plate, Diffraction from (0330). Same Orientation as Fig. 27. Compare. 25 x

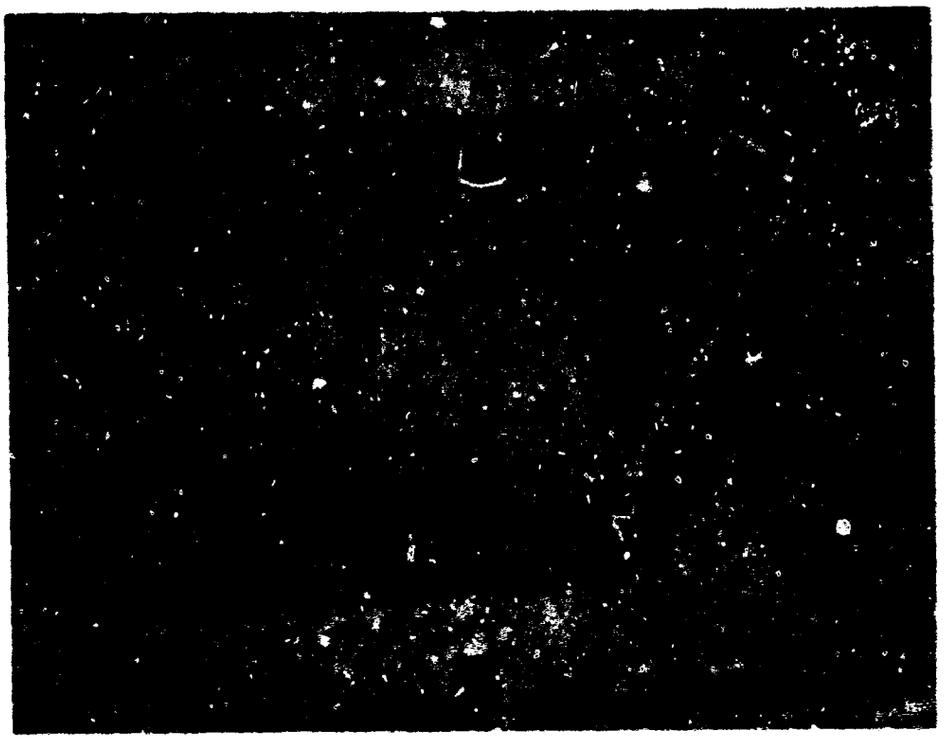

Figure 30. Photograph of Cut Crystal from 5 mm Thick Flux Ruby Plate. One a Axis is Perpendicular to the Plane of the Page. 14 x

Figure 31. X-ray Topograph of Crystal from Fig. 30, Diffraction from (0330), 14 x

Figure 32. X-ray Topograph of Crystal from Fig. 30, Diffraction from $(01\bar{1}2)$, 14 x

Figure 33. X-ray Topograph of Crystal from Fig. 30, Diffraction from (1014), Rotated 92° Counterclockwise from Fig. 32. 10 x

Crystal Quality (Continued)

planes are vertical in the photograph. It may be noticed that the area which contained the banded structure in Figure 32 now shows the same area completely free of any defects. At least six Pendellösung fringes are visible on the left side. All of them bend sharply around a major linear defect. The change of contrast for the banded area in Figure 32 after the rotation, must have been caused by a change in orientation of the Burgers vector b of the defect with respect to the diffracting planes. Maximum contrast (Figure 32) is usually obtained when b is normal to the diffracting planes. Little or no contrast (Figure 33) is seen when b is parallel to the diffracting planes. With this criteria in mind we see that Burgers vector of the banded defect may closely parallel the $(10\bar{1}4)$ planes. Such a Burgers vector has apparently not been observed or reported yet.

It is significant from Figure 32 that the crystal contains some defects which do not intersect the basal planes. This may partially explain the fact that etchants used only on the basal planes consistently show very low (<10) dislocation contents for flux grown ruby.

8.3.2 Flux Ruby and Sapphire Topography

Several crystals of flux ruby were obtained which had a visible gradient of doping level. These crystals had a lath-like habit and were colorless at the outer edges with deeper shadings of pink towards the nucleation center. It was believed that an x-ray topographic scan of the crystal ought to show some correlation with the color. Figure 34 is the actual Lang transmission topograph of a 0.45 mm thick flux ruby plate. The colorless portion of the crystal occurred near the left and bottom of the photograph. The most heavily banded and flux included area near the center corresponded to large and sharp color changes. The x-ray topograph was taken by diffraction from $(11\bar{2}0)$ planes which are vertical on the figure. The c-axis is perpendicular to the plane of the page. In all topographs the parallel bands were primarily found to occur along the morphological growth faces. However, some precipitates were found in random directions.

The preceding results were quite encouraging and offered some direct confirmation that chromium must be the dominating source of banded imperfections. To further substantiate the data it was necessary to examine some samples of sapphire. This material which is free from any added chromium was also grown from PbF_2-PbO flux. It has the same growth morphology as the ruby. Figure 35 is again an x-ray transmission topograph of a 0.75 mm thick sapphire plate crystal. The $(11\bar{2}0)$ planes were used for diffraction. The top of the photograph shows a heavily defective region consisting of many intersecting dislocation lines. This region was probably attached to the wall of the container or to another crystal. Near the center of the topograph are three parallel hooked lines. These as well as the defects under them

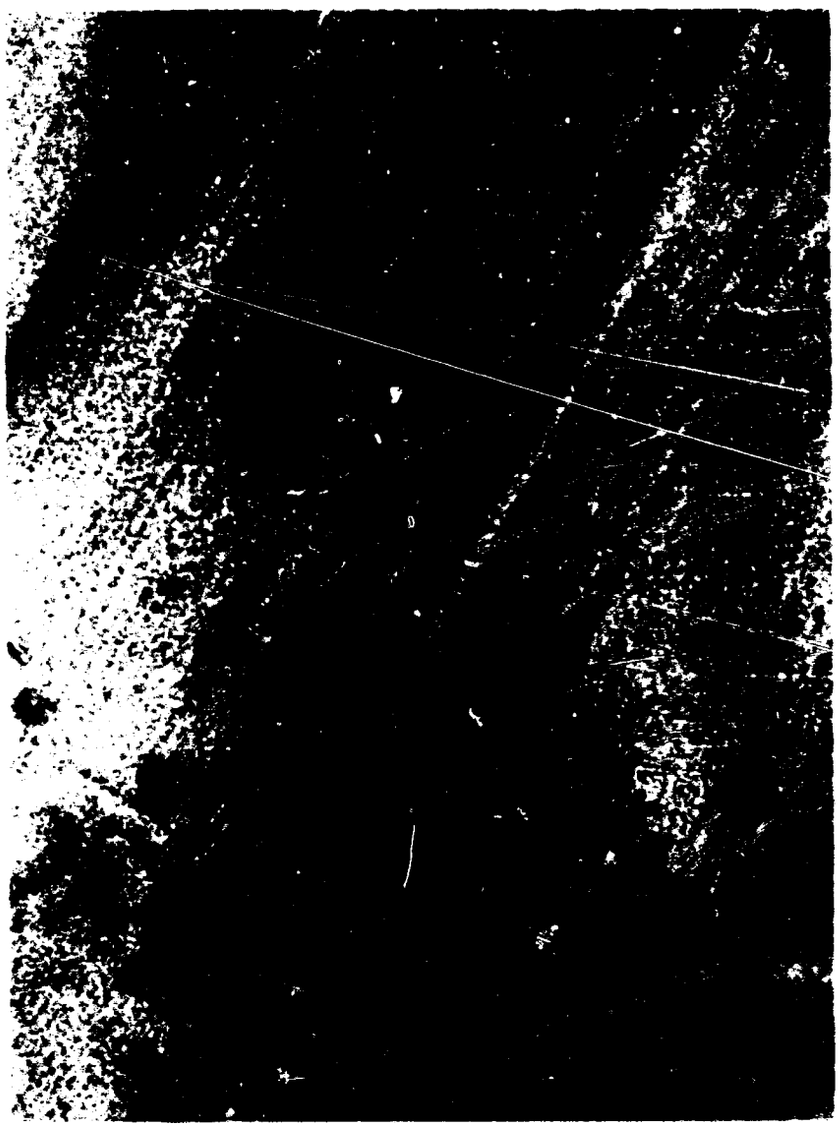

Figure 34. X-ray Topograph of Flux Grown Ruby Plate

Figure 35. X-ray Topograph of Flux Grown Sapphire Plate

Crystal Quality (Continued)

arose from visible lines of included flux. Only a few extended lines are evident as defects and these came from growth steps on the (0001) faces. Some were as thick as 25 μ. It may be noticed that there is a decided absence of parallel bands as found in the case of ruby. Figure 36 is a topograph of the same crystal after a net rotation of 30° in a clockwise direction. The (0330) planes were now used for diffraction and are vertical. The vertical lines at the left are from growth ridges on the exit side of the crystal and x-ray beam. Again the darker lines in the center are from visible thin lines of included flux. It is remarkable that no dislocation lines or fractures emanate from this flux! The top of the crystal shows some inclusions and dislocation lines. No evidence was found for those defects which are characteristic of ruby.

Several other crystals of sapphire were examined in order to confirm the above results. The thickness of the crystal along the c axis is sometimes indicative of the quality. Thus an equidimensional crystal more often was one which contained fewer bands in the case of ruby. Since the same situation may hold for sapphire, a very thin and a very thick crystal were taken in turn. Figure 37 is the transmission x-ray topograph from a 0.2 mm flux grown sapphire plate. The total area of the plate on the (0001) face was about 3 cm^2. The photograph shows only a portion of this area near the center of the sample but the remainder of the crystal was typically the same. The only defects present were tiny precipitates, one small angle grain boundary, and numerous point-like defects. The latter are probably sites of nucleation for other growing crystallites which never attained a measurable volume. An ordinary flux growth of sapphire contains many branched and interleafed plates difficult to separate without fracturing. An area of 3 cm^2 for a thickness of 0.2 mm is not commonly found. It can be noticed that the crystal is completely free of any banded substructure. This was true of the total area of the plate.

A sample of sapphire was now chosen to be relatively thick. By thick is meant a sample where it is still possible to use the Lang transmission method. Ideally the value of μt should be equal to unity for extinction contrast (μ = linear absorption coefficient for x-rays, t = sample thickness). For sapphire using MoK_α radiation, the value of μ is 13.4 cm^{-1} and t should be close to 0.75 mm. Values of t greater than this can be utilized if the perfection of the crystal is very good. For our present "thick" crystal the c axis dimension was 1.75 mm and μt had a value of 2.35. Figure 38 is the resulting x-ray topograph obtained by diffraction from (1120). Some wide bands are evident which in this case must be atributed to crystal strain introduced by the flux alone. It must be added that the crystal was optically very perfect and free of visible internal defects. The (0001) surface contained a few growth ridges but these were also visible in addition to the wider bands. The latter may have been caused by flux inclusions or strain which was confined to a limited volume. They seem to bear no relation to a principle growth direction of the crystal.

Figure 36. X-ray Topograph of Same Crystal of Sapphire, Diffraction from (0330), 30 x

Figure 37. X-ray [illegible]graph of 0.2 mm Sapphire Crystal

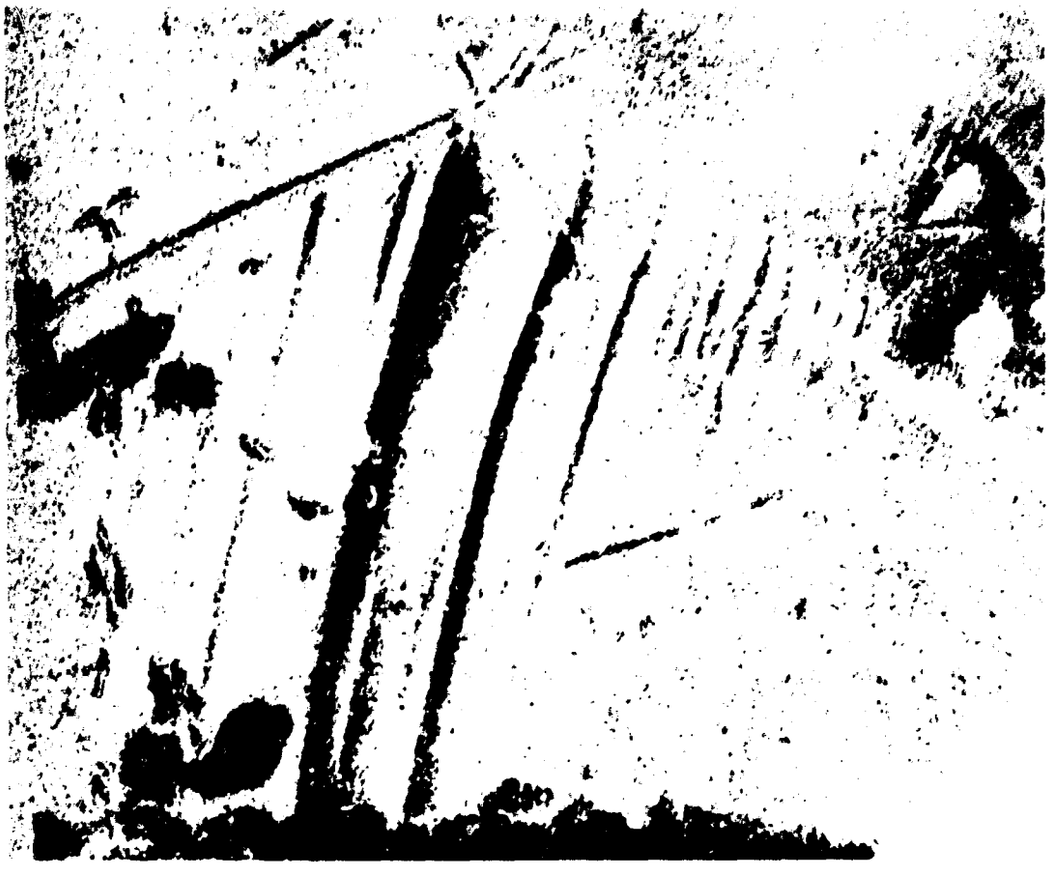

Figure 38. X-ray Topograph of 1.75 mm Sapphire Crystal

Crystal Quality (Continued)

The crystal thickness was at least 5-10 times that of other sapphire and ruby crystals examined in this laboratory. Undoubtedly the width of the defective areas was governed by the exact angle between the diffracting planes and principal growth directions. To illustrate this the crystal of Figure 36 was rotated 30° clockwise to obtain diffraction for (03$\bar{3}$0) planes. The bands are now very diffuse as illustrated in Figure 39. From the x-ray topographic results it may be inferred that the sapphire crystals are approaching the ideally perfect crystal. In no case can we detect many dislocation lines except where the crystal has obviously been damaged.

8.3.3 Hydrothermally Grown Ruby

Initially the growth of hydrothermal ruby was performed on flame fusion seeds. It was soon apparent that flux grown ruby would provide a higher quality seed material. While the size of flux ruby was not too large, a sufficient quantity could be made without any flux inclusions. Many of the preliminary hydrothermal runs gave crystals with severe cracking, inclusions, bubbles, and other visible defects. It was useless to examine these by the Lang method. Some runs did provide an overgrowth on the seed covering an area of 1-2 cm^2 with a thickness of 1-3 mm. The general freedom of visible defects in these crystals suggested that they would be worthwhile to examine by x-ray topographic methods. The morphology of the hydrothermal crystals followed that of the flux seed very closely. Thus the major faces of the crystals were (0001) and the bounding planes were of (01$\bar{1}$2), (11$\bar{2}$0) and (10$\bar{1}$4) type. All of these did not grow at the same rate and even differences were noted in the growth rates along [0001] and [000$\bar{1}$].

Figure 40 is an x-ray topograph of a ruby crystal which was cut parallel to the c axis and parallel to an a axis. In the figure the c axis is vertical and the a axis is horizontal. The dimensions were 12 mm along a and 2 mm along c. The thickness was 0.27 mm. The crystal was oriented to diffract from (11$\bar{2}$0) planes which are also vertical. The topograph shows only diffraction from the hydrothermally grown portion. The seed crystal was entirely out of diffracting position. Obviously the growth was not strictly expitaxial on a micro scale. A partial rotation of the overgrowth about (0001) must have occurred in the early stages of growth. The angle of rotation was not measured but could be as small as 2 to 3 minutes. The presence of many dislocation lines was indicated near the surface of the seed. It can also be noticed that the density of these defects becomes less as the crystal grows in thickness. Probably many of the dislocations have grown out of the crystal after a poor initial fit.

Figure 41 is the topograph of the same crystal. A net rotation of 30° counterclockwise was made in the plane of the crystal. The diffracting planes were (11$\bar{2}$3) and they run vertically. Again the dislocation content seems to be high at the seed-overgrowth interface.

Figure 39. X-ray Topograph of 1.75 cm Sapphire Crystal

Figure 40. X-ray Topograph of Hydrothermal Growth of Ruby on a Flux Seed, Diffraction from $(11\bar{2}0)$, 4 x

Figure 41. X-ray Topograph of Same Crystal in Fig. 40, Rotated 30° Counterclockwise, Diffraction from (1123), 14 x

Crystal Quality (Continued)

A progressive diminishing of defects occurs through the hydrothermally grown material. A comparison of similar areas of Figure 40 and Figure 41 also shows a change of contrast in many of the dislocation lines. In both topographs the defects in the hydrothermal portion run parallel to [0001]. These may be dislocations of a screw type. The extent of growth along [0001] and [000$\bar{1}$] is seen to be unequal. Figure 42 is a topograph taken after rotating the crystal 42° counterclockwise from Figure 40. The diffracting planes were (11$\bar{2}$6). No new features were found.

Another hydrothermally grown ruby was obtained which had growth over a total area of about 10 cm^2 on (0001). Furthermore, the growth along [0001] and [000$\bar{1}$] was 4 mm in each direction. Although the seed and the overgrowth contained several cracks, most of these had not propagated through the entire crystal. A large section could be cut and mechanically polished without complete fracture into many small pieces. The crystal was cut with the major faces parallel to the a and c axes. The (11$\bar{2}$0) planes were used for recording the topographs. For this crystal it was impossible to utilize any final chemical polishing because the high temperatures required would certainly fragment both the seed and the hydrothermally grown areas. Fortunately the few polishing surface scratches which remain can be readily distinguished from bulk defects in the crystal.

Figure 43 is a photomicrograph of the crystal taken by means of transmitted light. The bottom portion of the photograph shows two cracks. The one on the left is contained in both the seed and the hydrothermal overgrowth. It was not possible to tell where the crack initiated. The crack at the bottom right is only in the hydrothermally grown material. The outline of the seed is clearly visible and it also contains a crack running horizontally across the figure. The top half of the crystal is completely free of cracks and shows only some damage close to the surface. A few polishing marks were also visible on the crystal but do not show up clearly on the print.

Figure 44 is a composite of the x-ray topographs of the same areas. It is remarkable that the topograph could be obtained from areas on both sides of a crack. The reason must lie in the fact that the two halves across the crack are still in near perfect registry. Any estimate of the misorientation must be less than about 20 seconds of arc. The area between the two major cracks was free of visible cracks but so severely strained and of such high x-ray contrast that the topograph was completely black. The same thing is true at the cracks themselves. The strain and dislocation content drop off rapidly as you proceed away from the cracks. The top half of the crystal (Figure 43) is completely free of visible cracks. However, on the topograph (Figure 44, top) we see areas of very great strain and high dislocation content similar to those in the local vicinity of cracks. We must be viewing a situation immediately prior to the onset of visible fracture. It is also of interest

Figure 42. X-ray Topograph of Crystal from Fig. 40, Rotated 42° Counterclockwise, Diffraction from (1126), 25 x

Figure 43. Composite Photomicrograph

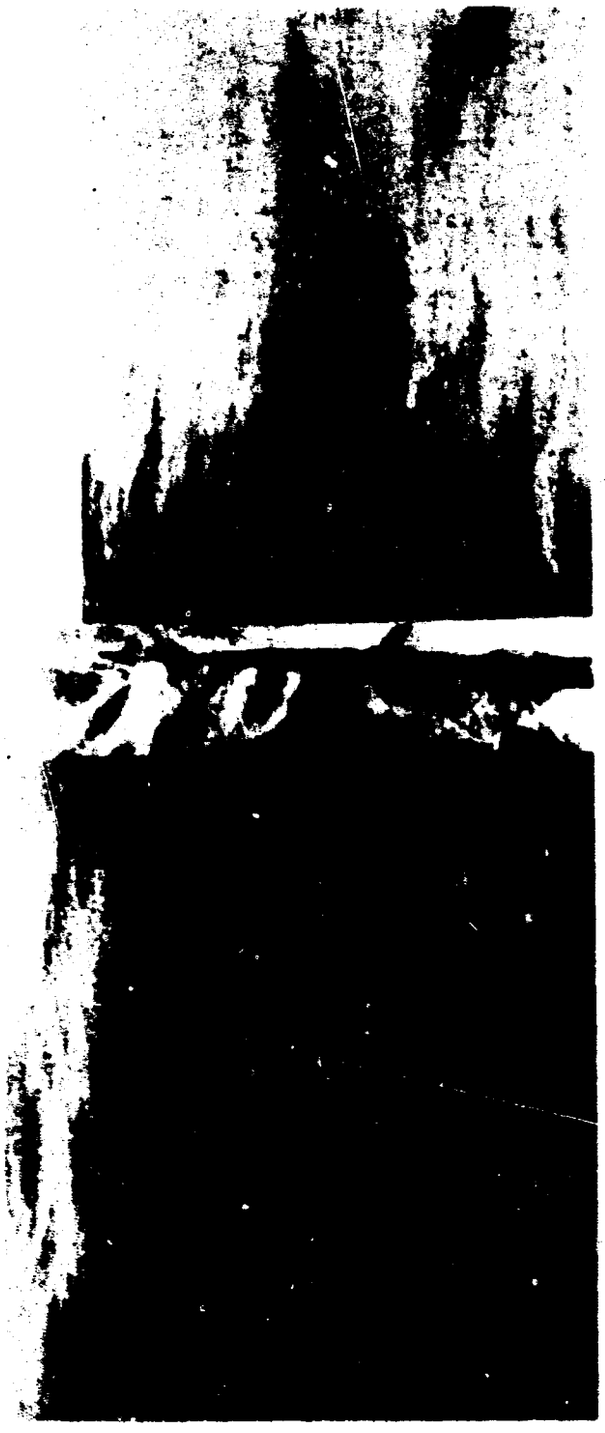

Figure 44. X-ray Topograph of Same Area Shown in Fig. 43

Crystal Quality (Continued)

that a large number of dislocations propagate from the surface of the seed. Again it was found that these seem to grow fewer in number as hydrothermal growth continues. No conclusive evidence has been found that shows dislocations emanating from the seed and continuing into the overgrown crystal.

8.3.4 Line Widths

Measurements were performed on various thicknesses of flux grown sapphire and ruby. The hydrothermal ruby was a crystal which was cut perpendicular to (0001). The (0001) and (000$\bar{1}$) natura faces were examined with no essential difference in perfection. Table XLII is a summary of results. Under the experimental conditions the flux ruby and sapphire are reflecting as almost perfect crystals with no angular misorientations. Since this was found on many different samples of quite random growth runs, the evidence is certainly conclusive. Birks[15] reported data on one flux ruby and under his conditions the misorientation was estimated to be as high as 10 seconds of arc for a local area. No information was given in relation to the source of the crystal and the growth conditions. Turning now to our hydrothermal ruby it is estimated that after correcting for dispersion due to the unequal spacings of the silicon and ruby crystals, a total misorientation of 8-10 seconds is present. A similar result was found for Czochralski ruby in an early report.[14] The data of Birks[15] indicate that his Czochralski ruby was perfect.

Our current work complements and substantiates all of our previous Lang x-ray topographic results. Both flux ruby and sapphire are almost completely free of any dislocations. They still retain some small impurities that segregate along faster growing planes. The (00·12) are the slowest growing and therefore may contain the least strain of all. This leads to the almost perfect crystals when these planes are examined. Both the Lang and line width data indicate that hydrothermal ruby must be growing under conditions where small residual strains are readily incorporated into the crystal. At the present time it is doubtful that the strain arises from a thermal origin or a propagation of defects from the seed crystal. The strain can apparently "grow out" as crystal growth proceeds along [0001]. However the residual misorientation found in crystals may indicate that the diminution of strain was not complete. The results may point to an impurity incorporated in the growing crystal in addition to the Cr^{+3} substituted in the Al_2O_3 lattice.

8.3.5 Infrared Topography

The presence of hydrogen bonded OH^- in hydrothermally grown quartz has been detected and studied in recent years.[24,25,26] These observations have prompted a preliminary study of hydrothermal ruby by means of infrared absorption spectra and x-ray topography.

TABLE XLII

Double Crystal Spectrometer Line Widths

Sample	Thickness along [0001] in mm	Width,[a] W, in sec.	Width,[b] W, in sec.
Flux Ruby	0.6	6.1	-
Flux Ruby	1.1	6.5	-
Flux Ruby	4.9	5.4	9.6
Flux Sapphire	0.2	8.6	-
Flux Sapphire	1.7	5.5	7.0
Flux Sapphire	3.0	-	10.0
Hydrothermal Ruby	3.0	-	16.4

a - 1 mm x 2 mm aperture plus 10 mm x .1 mm aperture
b - 1 mm x 1 mm aperture in front of crystal 2

Crystal Quality (Continued)

Figure 45A is an infrared scan of a 5.0 mm thick piece of flux grown ruby. The scan was obtained on a Perkin-Elmer Model 337 Grating Spectrophotometer. The spectrum covers the 1500-4000 cm^{-1} region. Flux grown ruby was chosen because it was normally the seed material for subsequent hydrothermal growth. It can easily be recognized that ruby is highly transparent to infrared radiation from 1700 to 4000 cm^{-1}. The very high absorbance commencing near 1700 cm^{-1} is due to the Al-O stretching frequency and lattice absorption.

Figure 45B is an identically recorded scan of a clear piece of hydrothermally grown ruby, (Al_2O_3:0.03 wt. % Cr). The thickness of the sample was 2.1 mm. This sample was grown in K_2CO_3 solution at 450°C and 1330 atm pressure. The sample was of very high quality and free of all cracks and microscopic inclusions. The presence of several absorption bands in the 3100-2600 cm-1 region is immediately noticeable. The region from 2940-3660 cm^{-1} is generally characteristic of O-H stretching frequencies. Bands which fall in this region may be attributed to the presence of water in the free absorbed or combined state (as OH^-). A compilation of the principal infrared bands of various aluminas has been presented by Newsome.[27] A recent study of Dorsey[28] was also helpful. Table XLIII presents a summary from these sources. From the spectra of Figure 45 there appears to be a definite mixture of bands of the trihydrate and monohydrate type in the hydrothermal ruby. No single phase as an impurity was capable of giving the observed spectrum. The estimated impurity content was 10-1000 ppm. It was also significant that bands characteristic of the diaspore phase were absent. This phase is one in equilibrium with Al_2O_3 at slightly lower temperatures and pressures than were used in the growth runs. One may also inquire about possible incorporation of $CO_3^=$ into the crystal. The principal absorption bands[29] of $CO_3^=$ are located at 1410-1450 cm^{-1} and 850-880 cm^{-1}. While there is no question of overlap with OH stretch bands, the strong Al-O stretch at 750 cm^{-1} and the onset of lattice absorption near 1500 cm^{-1} prevents a ready answer. Likewise the C-H bending vibrations in the 975-1150 cm^{-1} region were not observed for these thick crystals.

In the case of hydrothermally grown quartz it was possible to lower the H_2O content significantly by using $LiNO_2$ as a dopant.[5] Such a run was also made by adding $LiNO_2$ in hydrothermally grown ruby. The H_2O content was not eliminated although it did appear to be lower. The absorption spectrum of the 4.5 mm thick crystal is given in Figure 45C. While the same bands appeared in this crystal, it was found that the relative intensities changed slightly. Different thicknesses of crystals were used in both cases and independent quantitative measurements of hydrate contents were not made. However, it is very unlikely that the same impurity (Li^+) behaves similarly in two different growth systems. The preferential absorption of an impurity is highly dependent on structural details. Al_2O_3 and quartz are quite different in structure type and should not respond identically. Nevertheless, the principle is general and some impurity absorption could

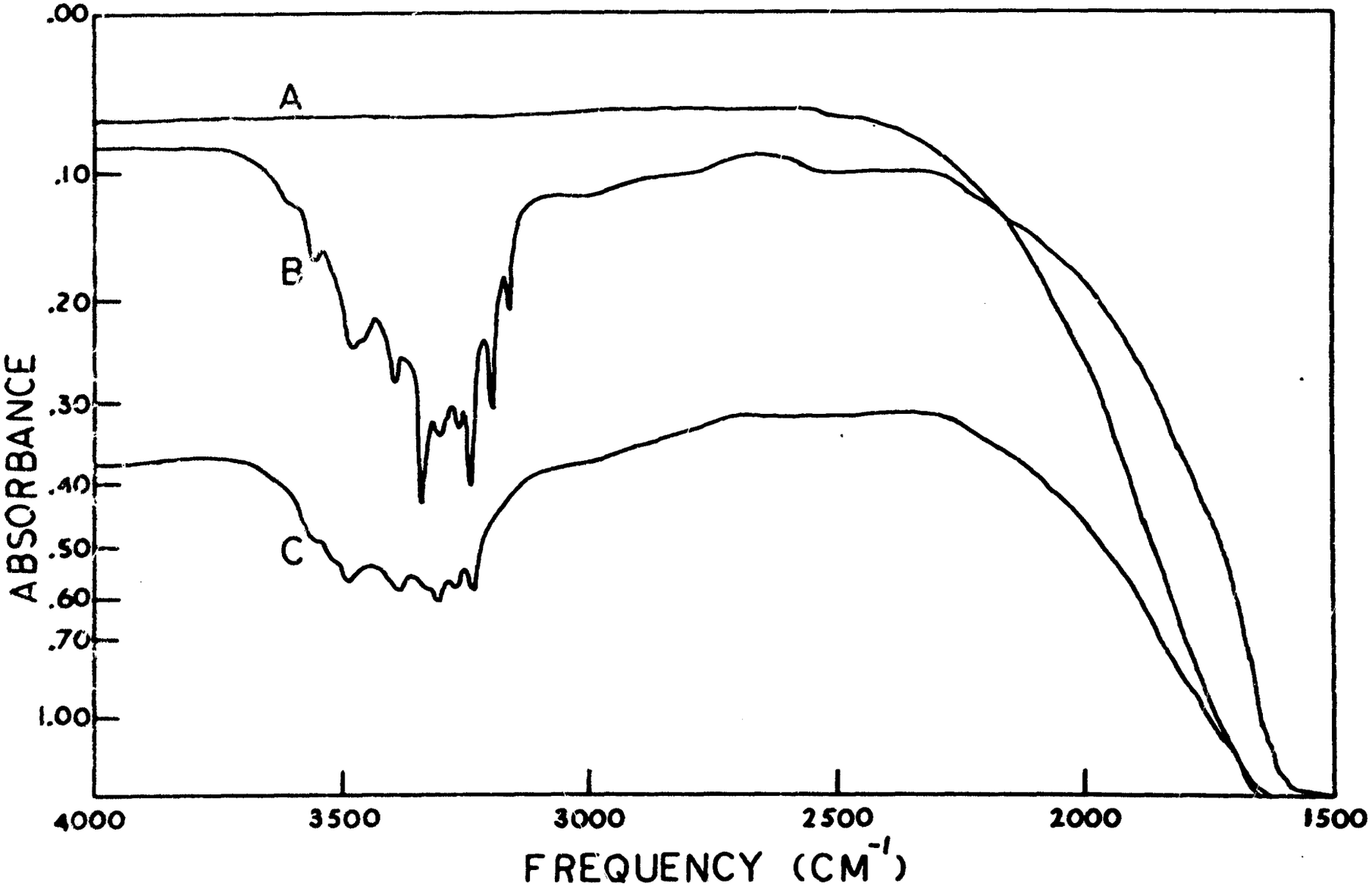

Figure 45. Infrared spectra of ruby samples, beam directed along [0001]. (A)5.0 mm flux ruby. (B)2.1 mm hydrothermal ruby, K_2CO_3. (C)4.5 mm hydrothermal ruby, K_2CO_3 and $LiNO_2$

TABLE XLIII

Infrared OH Stretch Data for Hydrated Aluminas

Phase	Wave Number (cm^{-1}) and Relative Intensity[a]
Alpha Trihydrate (Hydrargillite, Gibbsite)	3617(m), 3514(s), 3428(vs), 3378(m), 3361(s)
Beta Trihydrate (Bayerite)	3536(m), 3519(m), 3454(m), 3400(m)
Alpha Monohydrate (Boehmite)	3263(s), 3080(s)
Beta Monohydrate (Diaspore)	2924(vs), 2342(m), 2114(m), 1984(m)
Tohdite ($5Al_2O_3 \cdot H_2O$)	3240(s)

[a] vs, very strong; s, strong; m, medium

Crystal Quality (Continued)

also force the rejection of hydrated species in Al_2O_3.

An x-ray topograph of a piece of hydrothermally grown ruby is given in Figure 46. This topograph was obtained by transmission via the Lang technique.[19] The surface damage caused by cutting and polishing operations was removed by a chemical polish in a PbO-PbF_2 eutectic. The crystal thickness was 0.6 mm and the image was recorded on an Ilford Nuclear Plate with MoK_α radiation. Diffraction was from $(11\bar{2}0)$ planes which run vertical in the figure. The growth was directed along [0001] which is also vertical and proceeded from bottom to top. The first horizontal line at A is the seed growth interface. A flux grown ruby was the seed and its perfection was such that defects were almost completely absent. The propagation of dislocations from the seed was consequently hindered and this was confirmed by the topograph. Between A and B the defects were rather few and random even though they were microscopically visible inclusions. Between regions B and C several horizontal lines of intense blackening were found. From region B many dislocations emanate and are found in nearly parallel groups along or at a slight angle to (0001). Between regions D and B a much more defective horizontal band occurs. Groups of dislocations were again found to progress towards the surface. In regions E and F several light horizontal lines were evident and near the surface none were observed. While it was highly probable that the defects were located on the slowest growing basal planes, there was no obvious correlation with Cr^{+3} fluctuations. The most likely cause of the horizontal bands of defects is a temperature excursion. The growth rate along [0001] was 0.13 mm/day. The wide band between D and E covers a period of four days growth. A daily record of temperature showed no large deviations from isothermal conditions. Thus some propagation of defects probably occurs after initiation through temperature deviations of a short time duration.

In order to determine whether the most defective regions of the crystal were associated with any of the hydrated Al_2O_3 species, further infrared data were obtained. A highly polished slice of ruby adjacent to that used for the topograph was examined over selected areas with an infrared beam condenser. The size of the infrared beam was 1 mm x 4 mm in area. The 1 mm width of the beam was directed along the 4 mm width of the crystal. The latter corresponded to the vertical direction in Figure 46. Seven overlapping infrared scans were taken in the 3000-4000 cm^{-1} region. The results are presented in Figure 47A-G. Spectrum 47A was taken from the seed area and was completely free of hydrated impurities. Spectra 47B and 47C were from lightly defective areas of Figure 46. Both types of hydrates were present since most of the bands of Table XLIII occur. Spectrum 47D was from the area of Figure 46 which partially included the widest defective growth. Some intensity changes have occurred but the same infrared bands were found. Spectrum 47E was from the portion of the crystal containing the most defects. The very intense bands are now at 3180 cm^{-1} and 3230 cm^{-1}. These bands are characteristic of a monohydrate species. The trihydrate

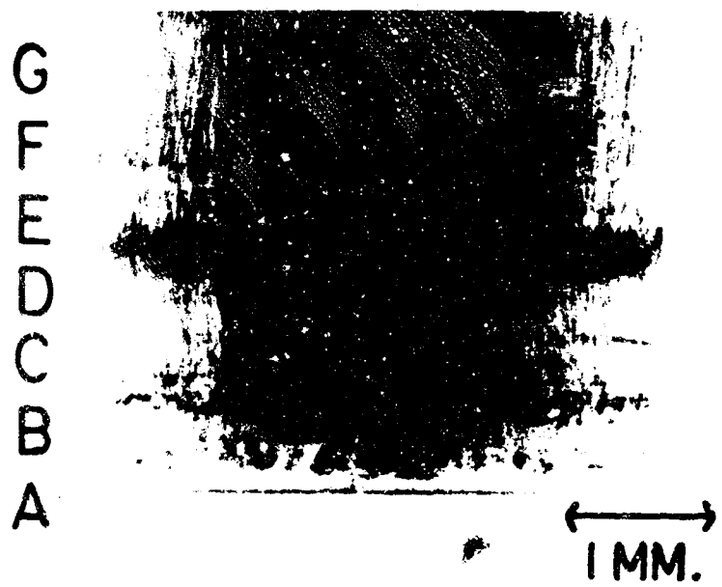

Figure 46. Lang x-ray transmission topograph of hydrothermal ruby, [0001] vertical, diffraction from (1120)

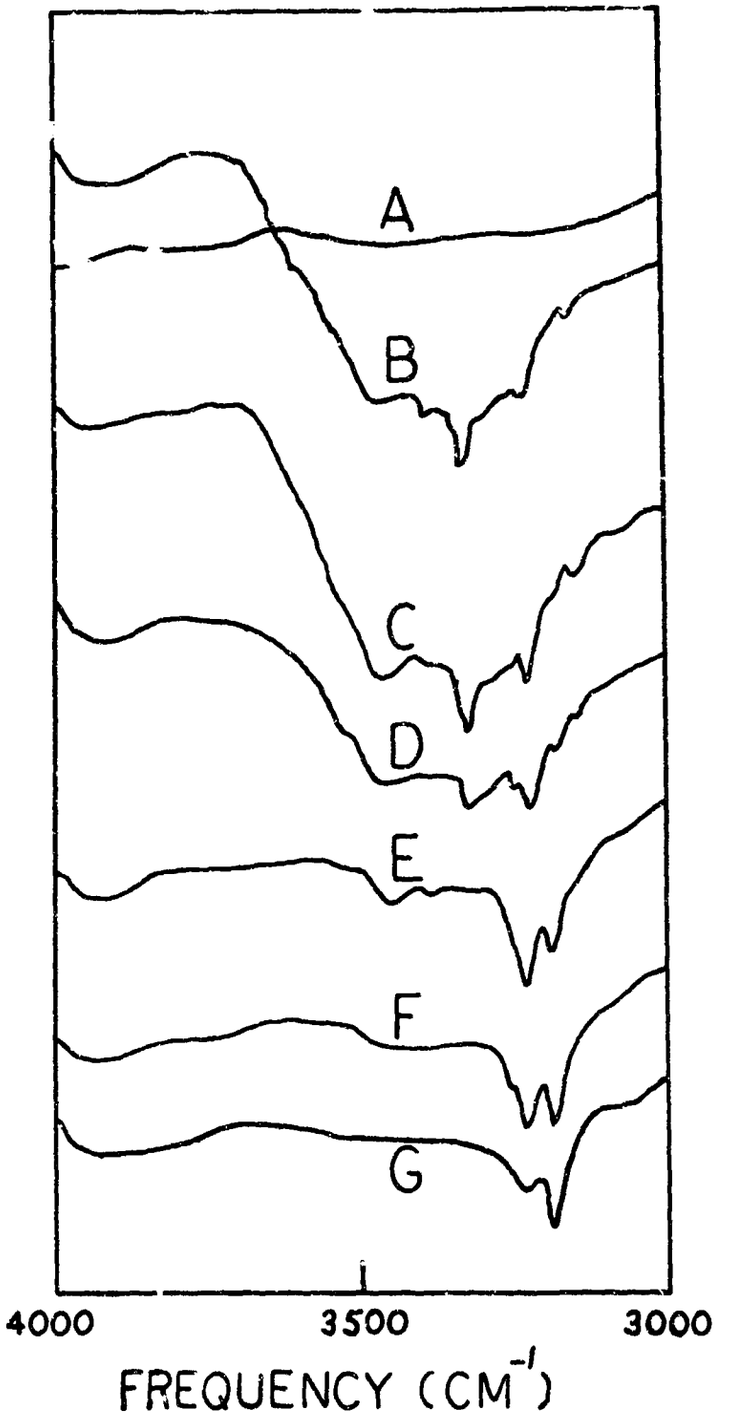

Figure 47. Infrared spectra of the regions A to G indicated on Fig. 46, beam directed along $[\bar{1}100]$, 0.6 mm thick. The spectra were shifted along the ordinate for clarity.

Crystal Quality (Continued)

type bands found at 3340-3600 cm^{-1} were drastically reduced in intensity. Spectra 47F and 47G were obtained from lightly defective areas near the end of growth. The bands at 3180 and 3230 cm^{-1} are now the only ones of strong intensity. The region from 3260 to 3600 cm^{-1} was nearly free of any significant absorption. These initial results indicated that extensive changes in the type or amount of hydrated impurity can be associated with grown-in defects of hydrothermal ruby.

The presence of hydrated Al_2O_3 and crystal defects may have some relation to the ease of fracture of hydrothermal ruby. Stress concentrations can be produced from either a Griffith crack or a piled up group of dislocations.[30] The former may be connected with the visible microscopic inclusions observed in some cases. The barriers necessary for a piled group may be formed by defects at the horizontal bands on the topograph. Dislocations both end and start at these regions. Observations by other workers are also pertinent. Wachtman and Maxwell[31] found that the modulus of rupture of sapphire was at a minimum in the temperature range 400-600°C. The value for bent 0° rods was also the lowest. Hydrothermal ruby is grown around 450°C and the basal planes are the large area faces. Charles[32] has studied the effects of the test atmosphere on the strength of bent sapphire rods. At 240°C the failure stress in tension was measured. When saturated water vapor was used the stresses were about half those when dry nitrogen was used as the surrounding atmosphere. Since surface water may lead to flaw growth, internal hydrates could act in a similar manner. The presence of hydrates may also affect other mechanical measurements on hydrothermal ruby such as internal friction, hardness, and impurity associated properties.

9.0 CONCLUSIONS

New autoclaves with a 3 inch internal diameter were designed by Airtron and fabricated by Autoclave Engineers. The performance of these autoclaves was good throughout the contract period. With the longer autoclaves the seal temperature was effectively reduced. Some difficulties resulted from heat losses out of the top section. A non uniform temperature distribution was found and large amounts of spontaneously nucleated crystals grew in the cooler part of the silver can.

Shorter autoclaves with the seal at higher temperatures were the best systems for ruby growth. Stringent requirements were placed on the seal preparation and assembly. However a good technique was developed for sealing short autoclaves. Any stress or corrosion cracking was eliminated by proper seals and efficient leak testing of the silver cans.

Several alternate nutrients were acquired and tested as substitutes for scrap flame fusion ruby. The most suitable form was a sintered pellet of Al_2O_3 with the required amount of Cr_2O_3. The introduction of additional impurities during manufacture was a persistent problem. Proper care and quality control can overcome this deficiency. Commercial suppliers were located.

Ruby crystals have been grown large enough to extract 1/4 inch diameter x 3 inch long rods. The best seed crystals were those obtained from ruby grown via the flux method. These seeds were almost free of any defects which may propagate to the hydrothermal ruby. Some of the hydrothermally grown crystals weighed approximately one pound. The best experimental conditions for moderate growth rates were 475 - 500°C, an average pressure of 27×10^3 psi, a gradient of 20-40°C, and a 1.75 molal K_2CO_3 solvent. Over growth periods of 20-30 days, the average rates were 10-20 mils/day along the c-axis.

All hydrothermally grown crystals were subject to certain growth flaws called veils. Different runs possessed these in either small or large densities. The principal cause of veiling was thought to arise from the actual growth conditions in the autoclave. The form of the nutrient, slight amounts of impurities, and seed quality had no large influence on the density of veils.

Infrared examination of hydrothermal ruby has revealed the presence of hydroxyl ions or water chemically bonded to the aluminum. X-ray topography has been utilized to associate physical defects with chemical changes of structure. No direct evidence was obtained to associate these changes with the presence or initiation of veiling. It is believed that certain ions may inhibit the amount of water impurity in the crystals.

Both x-ray line widths and x-ray topography have proved that hydrothermal ruby can be grown very perfectly. The residual defects were veils, dislocations, and areas of severe strain. The latter

Conclusions (Continued)

were generally associated with visible cracks or fracture. The estimated dislocation density in good areas of crystal was 10^2-$10^4/cm^2$. Misorientations as low as 8 seconds of arc were measured in several crystals. This quality is comparable to Czochralski grown ruby and much better than Verneuil.

10.0 RECOMMENDATIONS

From the knowledge and experience obtained during this phase of the contract, the hydrothermal growth of large perfect ruby crystals was shown to be feasible. Several difficult problem areas remained. The following recommendations are presented to assist in future plans to manufacture crystals.

1. The many problems arising from the use of large diameter cans and autoclaves should be investigated and eliminated. Vessels of 1.5 inch diameter should be the maximum size for meaningful preliminary experiments.

2. Methods should be developed to monitor the temperatures inside the silver can. If this is too difficult then temperatures should be monitored in the annular space between the silver can and the vessel.

3. The causes of veiling and their elimination in hydrothermal ruby should be a primary concern. Mineralizers other than K_2CO_3 and specific additives should be tried. The nature of the transporting species should be determined by chemical and physical means.

4. A detailed process should be developed for producing a suitable synthetic nutrient of high purity in large amounts. The assistance of commercial suppliers should be utilized under an incentive plan.

5. The performance of hydrothermally grown ruby as a laser crystal should be investigated more thoroughly. A test program should be undertaken to compare optical properties of ruby crystals obtained by the different growth methods.

6. The technology developed under the program should be applied to crystals which cannot be grown by other methods.

11.0 REFERENCES

1. R. R. Monchamp, R. C. Puttbach, and J. W. Nielsen, "Hydrothermal Growth of Large Ruby Single Crystals - Phase I", Final Technical Report AFML-TR-65-369, October, 1965.

2. K. R. Janowski, B. J. Stofel and A. B. Chase, Report No. TDR-469(9250-01)-1, Contract No. AF04(695)-469, August 28, 1964.

3. R. R. Monchamp, R. C. Puttbach, and J. W. Nielsen, J. Electrochem. Soc. 113, 1233 (1966).

4. Robert C. Linares, J. Phys. Chem. Solids 26, 1817 (1965).

5. A. A. Ballman and R. A. Laudise, Appl. Phys. Letters 8, 53 (1966).

6. E. S. Dana, A Textbook of Mineralogy, (John Wiley and Sons, Inc., New York, 1932) 4th Edition, p. 481.

7. R. L. Barns, Proceedings of Technical Conference on Metallurgy of Advanced Electronic Materials, G. E. Brock, Editor, (Interscience, New York, 1962).

8. G. W. Dueker, C. M. Kellington, M. Katzmann, and J. G. Atwood, Appl. Optics 4, 109 (1965).

9. K. R. Janowski and H. Conrad, Trans. Metall. Soc. A.I.M.E. 230, 717 (1964).

10. J. P. Remeika, J. Am. Chem. Soc. 78, 4259 (1956). R. C. Linares, J. Appl. Phys. 33, 1747 (1962).

11. "Czochralski Ruby", Contract No. Nonr-4132(00), Union Carbide Corp., Linde Division, July 8, 1964.

12. A. E. Paladino and B. D. Roiter, J. Am. Ceram. Soc. 47, 465 (1964); R. A. Laudise and A. A. Ballman, J. Am. Ceram. Soc. 80, 2655 (1958).

13. D. F. Nelson and J. P. Remeika, J. Appl. Phys. 35, 322 (1964).

14. "Czochralski Ruby", Contract NONR 4132(00), Linde Division, Union Carbide Corp., January 22, 1965.

15. L. S. Birks, J. W. Hurley, and W. E. Sweeney, J. Appl. Phys. 36, 3562 (1965).

References (Continued)

16. A. H. Compton and S. K. Allison, X-rays in Theory and Experiment, (D. Van Nostrand Co., Inc., Princeton, N. J., 1935), p. 711.

17. M. L. Kronberg, Acta Metall. 5, 507 (1957).

18. National Bureau of Standards Circular 539, 9, 3 (1960).

19. A. R. Lang, Acta Cryst. 12, 249 (1959); J. Appl. Phys. 30, 1748 (1959).

20. D. L. Stephens and W. J. Alford, J. Am. Ceram. Soc. 47, 81 (1964).

21. R. Scheuplein and P. Gibbs, J. Am. Ceram. Soc. 43, 458 (1960).

22. K. R. Janowski, E. J. Stofel, and A. B. Chase, Trans. Metall. Soc. A.I.M.E. 233, 2087 (1965).

23. H. E. Bond and K. B. Harvey, J. Appl. Phys. 34, 440 (1963).

24. J C. King, D. L. Wood, D. M. Dodd, Phys. Rev. Letters 4, 10 (1960).

25. A. Kats, Philips Res. Rep. 17, 133 (1962).

26. D. M. Dodd and D. B. Fraser, J. Phys. Chem. Solids 26, 673 (1965).

27. J. W. Newsome et al., Editors, Alumina Properties, Technical Paper No. 10 (Aluminum Company of America, 1960), p. 33.

28. G. A. Dorsey, Jr., J. Electrochem. Soc. 113, 169 (1966).

29. J. Lecompte, Handbook of Physics, S. Fluegg, Ed. (Springer Verlag, Berlin, 1958), p. 811.

30. J. Friedel, Dislocations (Pergamon, New York, 1964), pp. 326-330.

31. J. B. Wachtman, Jr., and L. H. Maxwell, J. Am. Ceram. Soc. 42, 432 (1959).

32. R. J. Charles, Fracture, B. L. Averbach, Ed (J. Wiley & Sons, New York, 1959), p. 225.

Unclassified

Security Classification

AMD PP90 13152

DOCUMENT CONTROL DATA - R&D

(Security classification of title, body of abstract and indexing annotation must be entered when the overall report is classified)

1. ORIGINATING ACTIVITY (Corporate author)
Airtron Division
Litton Precision Products, Inc.
200 E. Hanover Avenue
Morris Plains, New Jersey

2a. REPORT SECURITY CLASSIFICATION
Unclassified

2b. GROUP

3. REPORT TITLE

Final Report on Hydrothermal Growth of Large Ruby Crystals - Phase II

4. DESCRIPTIVE NOTES (Type of report and inclusive dates)
Final - 2 June 1965 to 31 December 1966

5. AUTHOR(S) (Last name, first name, initial)
Puttbach, Richard C.
Belt, Roger F.
Monchamp, Roch R.

6. REPORT DATE	7a. TOTAL NO. OF PAGES	7b. NO. OF REFS
July 1968	157	32

8a. CONTRACT OR GRANT NO.	9a. ORIGINATOR'S REPORT NUMBER(S)
AF33(615)-3160	R-11-535
b. PROJECT NO. 8-132	
c.	9b. OTHER REPORT NO(S) (Any other numbers that may be assigned this report)
d.	

10. AVAILABILITY/LIMITATION NOTICES
This document is subject to special export controls and each transmittal to foreign governments or foreign nationals may be made only with prior approval of the Manufacturing Technology Division (MAT), Air Force Materials Laboratory, Wright-Patterson Air Force Base, Ohio 45433.

11. SUPPLEMENTARY NOTES	12. SPONSORING MILITARY ACTIVITY
	Air Force Materials Laboratory Manufacturing Technology Division (MATE) Wright-Patterson AFB, Ohio 45433

13. ABSTRACT

Techniques for the growth of pink ruby by the hydrothermal method have been studied. The principal objectives of this project were to grow crystals measuring several cm to control optical properties and internal quality, and to provide manufacturing data for laser crystal production. A comprehensive investigation was performed on autoclave design, fabrication, and operation. The nutrient preparation, actual crystal growth, and physical examination of quality were also studies in detail. Autoclaves of 1.5-3.0" internal diameter were designed and fabricated for ruby growth. These autoclaves performed as well or better than commercially available ones. Special sealing problems, operational procedures and can extraction methods were investigated. The maximum temperature of operation approached 550°C with pressures up to 3 x 104 psi. Growth periods as long as 36 days were attempted. Most common solvent was K_2CO_3. Significant advances in autoclave technology were made. The nutrient for crystal growth was generally scrap flame fusion ruby. An arc fused Al_2O_3 or sintered pellets of Al_2O_3 with added Cr_2O_3 was under development. The residual problems were proper purity and adequate densification. These can be overcome by exacting preparative methods and were mostly a matter of economical availability. Crystals of ruby were grown as large as 2 x 8 x 10 cm. During this time the growth rate along the c-axis averaged about 1-20 mils/day. Many of the crystals grown hydrothermally contained visible flaws called veils. The principal causes of veils were thought to be associated with high growth rates, temperature or pressure fluctuations, and possibly chemical or physical impurities ad defects. The quality of seed crystals and hydrothermally grown clear ruby crystals was determined with X-ray procedures. Residual misorientations approached 10" of arc, dislocation density was less than 10^3/cm². Few dislocations propagated from the seed crystals. Veils were connected with severely strained areas of crystal and high dislocation densities. Small amounts of hydrated alumina were found in the hydrothermally grown ruby. Growth conditions directly influenced the dislocation content and the nature of the chemical impurities. (continued)

DD FORM 1473

Unclassified

Security Classification

Unclassified

Security Classification

14. KEY WORDS	LINK A		LINK B		LINK C	
	ROLE	WT	ROLE	WT	ROLE	WT
Crystals Ruby Hydrothermal Crystal Growth Technique						

INSTRUCTIONS

1. **ORIGINATING ACTIVITY:** Enter the name and address of the contractor, subcontractor, grantee, Department of Defense activity or other organization *(corporate author)* issuing the report.

2a. **REPORT SECURITY CLASSIFICATION:** Enter the overall security classification of the report. Indicate whether "Restricted Data" is included. Marking is to be in accordance with appropriate security regulations.

2b. GROUP: Automatic downgrading is specified in DoD Directive 5200.10 and Armed Forces Industrial Manual. Enter the group number. Also, when applicable, show that optional markings have been used for Group 3 and Group 4 as authorized.

3. REPORT TITLE: Enter the complete report title in all capital letters. Titles in all cases should be unclassified. If a meaningful title cannot be selected without classification, show title classification in all capitals in parenthesis immediately following the title.

4. DESCRIPTIVE NOTES: If appropriate, enter the type of report, e.g., interim, progress, summary, annual, or final. Give the inclusive dates when a specific reporting period is covered.

5. AUTHOR(S): Enter the name(s) of author(s) as shown on or in the report. Enter last name, first name, middle initial. If military, show rank and branch of service. The name of the principal author is an absolute minimum requirement.

6. REPORT DATE: Enter the date of the report as day, month, year, or month, year. If more than one date appears on the report, use date of publication.

7a. TOTAL NUMBER OF PAGES: The total page count should follow normal pagination procedures, i.e., enter the number of pages containing information.

7b. NUMBER OF REFERENCES: Enter the total number of references cited in the report.

8a. CONTRACT OR GRANT NUMBER: If appropriate, enter the applicable number of the contract or grant under which the report was written.

8b, 8c, & 8d. PROJECT NUMBER: Enter the appropriate military department identification, such as project number, subproject number, system numbers, task number, etc.

9a. ORIGINATOR'S REPORT NUMBER(S): Enter the official report number by which the document will be identified and controlled by the originating activity. This number must be unique to this report.

9b. OTHER REPORT NUMBER(S): If the report has been assigned any other report numbers *(either by the originator or by the sponsor)*, also enter this number(s).

10. AVAILABILITY LIMITATION NOTICES: Enter any limitations on further dissemination of the report, other than those imposed by security classification, using standard statements such as:

(1) "Qualified requesters may obtain copies of this report from DDC."

(2) "Foreign announcement and dissemination of this report by DDC is not authorized."

(3) "U. S. Government agencies may obtain copies of this report directly from DDC. Other qualified DDC users shall request through _____."

(4) "U. S. military agencies may obtain copies of this report directly from DDC. Other qualified users shall request through _____."

(5) "All distribution of this report is controlled. Qualified DDC users shall request through _____."

If the report has been furnished to the Office of Technical Services, Department of Commerce, for sale to the public, indicate this fact and enter the price, if known.

11. SUPPLEMENTARY NOTES: Use for additional explanatory notes.

12. SPONSORING MILITARY ACTIVITY: Enter the name of the departmental project office or laboratory sponsoring *(paying for)* the research and development. Include address.

13. ABSTRACT: Enter an abstract giving a brief and factual summary of the document indicative of the report, even though it may also appear elsewhere in the body of the technical report. If additional space is required, a continuation sheet shall be attached.

It is highly desirable that the abstract of classified reports be unclassified. Each paragraph of the abstract shall end with an indication of the military security classification of the information in the paragraph, represented as *(TS)*, *(S)*, *(C)*, or *(U)*.

There is no limitation on the length of the abstract. However, the suggested length is from 150 to 225 words.

14. KEY WORDS: Key words are technically meaningful terms or short phrases that characterize a report and may be used as index entries for cataloging the report. Key words must be selected so that no security classification is required. Identifiers, such as equipment model designation, trade name, military project code name, geographic location, may be used as key words but will be followed by an indication of technical context. The assignment of links, rules, and weights is optional.

DD Form 1473 continuation sheet of Item 13.

13. ABSTRACT (continuation)

This abstract is subject to special export controls and each transmittal to foreign governments or foreign nationals may be made only with prior approval of the Manufacturing Technology Division (MAT), Air Force Materials Laboratory, Wright-Patterson Air Force Base, Ohio 45433. The distribution of this report is limited because it contains technology identifiable with items on the strategic embargo lists excluded from export or re-export under U.S. Export Control Act of 1948 (63 STAT 7) as amended (50 U.S.C. Appn. 2020-2031), as implemented by AFR 400-10, AFR 310-2, and AFSCR 80-20.